Kapitola 1

Changes in surface temperature and humidity parameters resulting from spruce forests decay in the centre of the Šumava National Park

Hais M.

1. Introduction

All types of land cover have their typical temperature and humidity characteristics. In warmer periods of the year and mainly in summer (except periods of extreme precipitations or temperature differences), the temperature and humidity distribution in the latitude of the Czech Republic is as follows: water and forest ecosystems in summer months express relatively low temperature and the highest humidity values, while barren land, build-up areas and agricultural land are characterized by the highest temperature and the lowest humidity. Such characteristics can be used to assess landscape changes as well as landscape functions. In this connection the landscape functions means the fluxes of energy, water and matter in the specific part of catchment area depending on the condition of vegetation (Zichová, 2000). Driving factors of changes in surface temperature and humidity may be numerous. The physical principle is the change of proportion of sun radiance reflection, evapotranspiration and sensible heat (Pokorný, 2001).

The objective of the paper is to study the impact of deforestation on changes in the surface temperature and humidity and subsequent modification of landscape functions. Changes in surface temperature and humidity distribution could have consequences for the microclimate and energy balance of the area (Ripl, 1992; Ripl et al., 1996) as well as for the water outflow regime and matter losses, which reflects the ability of landscape retention and microclimate conditions.

Remote sensing is an excellent tool for assessment of changes in landscape. Unlike point measuring methods, remote sensing collects data representing whole areas, which enables us to make a better picture of temperature and humidity values distribution in the studied area. Older satellite scenes (e.g. Landsat TM4 and TM5) also allow us to analyze conditions more than twenty years ago, assess situations prior to the bark beetle calamity, and to compare results with the current state.

The aim of this study is to describe changes of temperature-humidity parameters of the landscape surface in consequence of the mountain spruce forest decay in the central part of Šumava Mountains through the comparison of the multispectral satellite analyses of scenes from years 1987 and 2002. The purpose of the study comes out some basic assumptions and hypothesis. The basic presumption of the hypothesis is the fact, that the mountain spruce forest decay caused by bark beetle will cause that the spruce forests will stop to serve as a vegetation, which appear as a decrease of water accumulation, evaporation, and

subsequently by the change of Bowen ratio in favour of sensible heat. The analysis of Landsat satellite scenes was used to verify this hypothesis. The area of interest is scanned by the satellite every 16 days, always at 9:18 a. m. of the local time (i.e. 10:18 of the summer time), when the vegetation cover surface starts to differentiate according to temperature and moisture. The size of the smallest picture segment (called pixel) varies according to the scanner type (TM, ETM+) and spectral cannel from 30 x 30 m (all cannels except the 6^{th} thermal), through 60 x 60 m (6^{th} cannel ETM+), to 120 x 120 m (6^{th} cannel TM). Thereby it is possible to notice also the differences in the landscape structures: living forest, decayed forest and clear cut areas.

2. Locality

The study focuses on central Šumava Mountains, particularly on the forest stands affected by bark beetle outbreak. The area is delimited by Velká and Malá Mokrůvka in the east, and Roklan in the west. The northern frontier copies the line connecting Medvědí (1224 m) – Studená (1298 m) hill and the southern end of the area follows the state border and extends into Germany (0.5 – 1 km). The altitude level varies between 1100 – 1200 m and the highest peaks in the Czech part are Velká Mokrůvka (1370 m) and Špičník (1351 m) while the German area is dominated by Luzný (1373 m) and Roklan (1453 m). In hydrological terms, the whole study area is located in catchment of Roklanský and Modravský streams (96 km^2). The geological subsoil is made of moldanubicum and the whole area is mostly located at the geological site knows as Královský hvozd (Royal Forest) (gneiss) characterized by magma bodies rising to the surface – e.g. in the central moldanubic plutonic rocks in the Vydra river massif (biotic granite, adamellites, granodiorites) (Kočárek, 2003). In terms of meteorology, the area shows the high total precipitation and Březník is thought to be the place of the highest precipitation (1550 mm annually) (Strnad, 2003). The area is mostly covered by spruce forests, peats (Rokytská, Rybárenská, Roklanská fens and others), and mountainous meadows. The high percentage of peat and wetland results from relatively high precipitations. In the past, there were certain efforts to drain the area and to transform it into production spruce monoculture forests (Hais, 2003).

2.1 Spruce Forests Decay Caused by bark beetle

The most radical change, affecting the mountain spruce forests of the Šumava Mountains and Bavarian Forest National Parks in 20th century, was the bark beetle outbreak that started in 1980s. As is stated in Skuhravý (2002), its origins could be traced back to 1983 when 173 ha of the Bavarian Forest National Park were damaged by a hurricane. At that time, 88 ha were left without any treatment, which resulted in spread of eight-toothed spruce bark beetle (*Ips typographus*) that in 1986 attacked also other trees due to lack of damaged fallen trees. Despite further hurricanes in 1990 (Vivian and Veibke), the calamity seemed to have diminished in 1988 – 1992 . However, in 1993, affected areas started to spread again, particularly towards the northwest from Luzný in the direction to Velký and Malý Špičník and further northwards and eastwards. Czech air photos of the area delimited by Špičník and Blatný hill in the direction towards Roklan, taken in 1992, show individual affected trees and 12 larger pest focus sites (15 – 20 trees). In later stages, the area was affected by bark beetle leading to creation of many new focus sites in surrounding areas. In 1995 the Šumava National Park administration declared the non-intervention zone. It was enlarged to the southwards from the road between Roklanská lodge and Březník and reaches the total area of 1450 ha in 1997. The bark beetle attack reached its peak in 1996 when it involved 80 % of the non-intervention zone. Outside the zone, the Šumava NP administration adopted measures to clean affected wood and stop calamity progress. Ten percent of cleaned trees were unbarked and left in their original place. Since 1996, new trees have been planted in clear cut areas, mainly spruce, but also rowan, beech, fir, and sycamore. To return future forest generations to the original state it's important to mix spruce with other species (Zatloukal et. al., 2001). The results of overall calamity in 2002 are specified in Table 1.

Table 1 Decayed forest and clear cut areas values in the Bavarian Forest and Šumava National Parks (*Kůrovec a jeho kalamity*, Skuhravý, 2002 – Bark Beetle Calamities)

National Park	Decayed forest (ha)	Clear cut areas (ha)	Scope in mil. m^3
Bavarian Forest	3650	270	1.5 – 1.7
Šumava Mts.	1450	1150	1.1 – 1.3
Total	5100	1420	2.6 – 3.0

3. Methods

To assess surface temperature and humidity, the multispectral remote sensing data were analyzed, specifically Landsat 5 TM and Landsat 7 ETM+ satellite scenes. Thereby it is possible to work with data from the time before the bark beetle outbreak in Šumava Mountains. Satellite scenes taken on July 11, 1987 and July 28, 2002 were transformed geometrically into the JTSK coordinate system according to ortorectified Satellite map *(ČR*© 2002 ARCDATA PRAHA, s.r.o). To enhance geometrical accuracy in central Šumava, the existing grid of ground control points was completed by points taken from aerial ortofotomaps provided by the Šumava National Park administration for the purposes of the project. Data were resampled by applying the nearest neighbour method to preserve original radiometric data for subsequent data processing. Satellite images were subject to atmospheric corrections applying the ATCOR module to eliminate unwanted marks of water vapour in the atmosphere.

To calculate the surface temperature, I used the 6^{th} thermal channel TM and ETM+ comprising records in the electromagnetic radiation interval of 10.4 – 12.5μm (Campbell, 2002). DN values were transformed to temperature values by applying ATCOR2_T (Geomatica Algorithm Reference, 2003) and recalculating radiometric values of surface radiation to temperature of an ideal black body. To enhance accuracy, the ATCOR2_T model was completed by supplementary calibration data: geographic location, medium height above the sea level, Sun zenith angle at the time of image taking (calculated in the SUN software), the visibility range (data provided by the CHMI), and the season. The output comprises maps of the surface temperature absolute values. For the comparability reason, the Satellite data from different periods can be used only after transforming temperature values into relative values.

Soil water content (Šúri et al., 1994) or surface relative humidity values can be determined by using spectral indexes. Most methods apply the Wetness index that forms part of the Tasseled Cup linear transformation (Kauth & Thomas, 1976). With respect to Landsat TM or ETM+ satellite data, the Tasseled Cup transformation processes 6 spectral bands (1 – 5, and 7) applying a method based on the Principle components analysis. For comparability reasons, the values were again transformed into relative categories. In this case, I used the equiareal method. The histogram of satellite images was divided so that each interval contained ideally the same number of values. Reducing the span of discrete

class histogram, we acquired deviations in numbers of values between individual intervals. When the difference of summary values within individual intervals is too big, it is necessary to choose a different numbers of intervals. Nevertheless, the number of intervals is limited by the maximum number of values of one class as specified below:

$$In \leq \frac{\sum c}{L_{\max}}$$

where I_n is the maximum number of equiareal intervals, $\sum c$ is the sum of values of all classes, and L_{max} is the class with the highest number of values. The equiareal distribution is characterized by marginal intervals comprising under normal conditions many classes, which leads to extremes averaging. On the other hand, this distribution method provides a good picture of the values distribution in space.

Temporal comparison of relative data (temperature, the Wetness index) was performed on the basis of a matrix analysis (Geomatica Algorithm Reference, 2003). It resulted in a visual record where the pixel value represented the combination of coinciding classes, mutually corresponding in terms of their location, as specified bellow:

COINCIDENCE MATRIX:

	1	2	3	4	5	6	7	Channel B
1	**1**	2	3	4	5	6	**7**	
2	8	**9**	10	11	12	13	14	
3	15	16	**17**	18	19	20	21	
4	22	23	24	**25**	26	27	28	
5	29	30	31	32	**33**	34	35	
6	36	37	38	39	40	**41**	42	
7	**43**	44	45	46	47	48	**49**	

Channel A

The chart shows values applicable to all combinations of corresponding classes coincidence. When class 1 of channel A corresponds to class 7 of channel B, the resulting value of the pixel is 7. This represents the maximum possible change (e.g. increase in temperature). The same applies to the resulting pixel value of 43, but the change is in the opposite direction (e.g. decrease in temperature). With respect to diagonally distributed

Scennes: 11.7.1987 28.7.2002

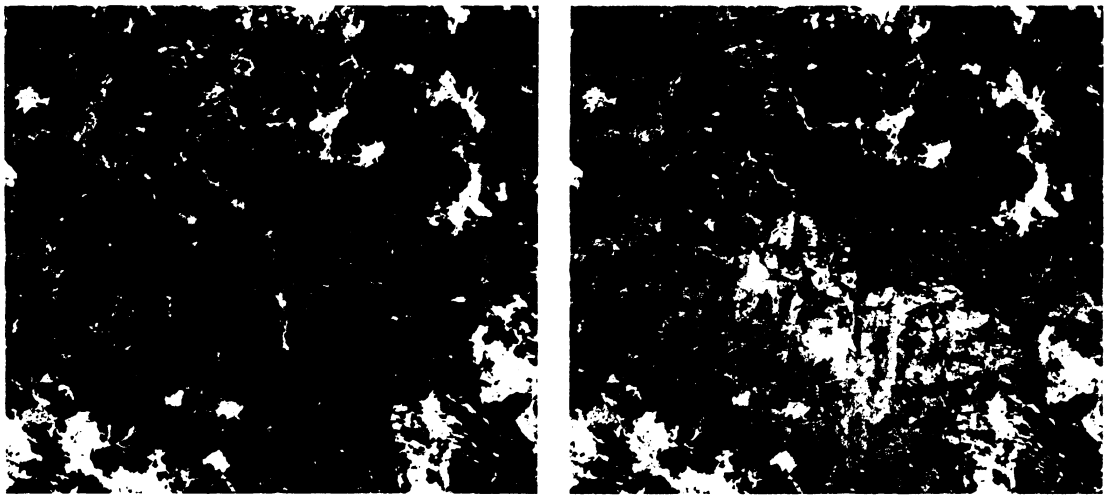

Fig. 1a Landsat 5 TM Landsat 7 ETM+

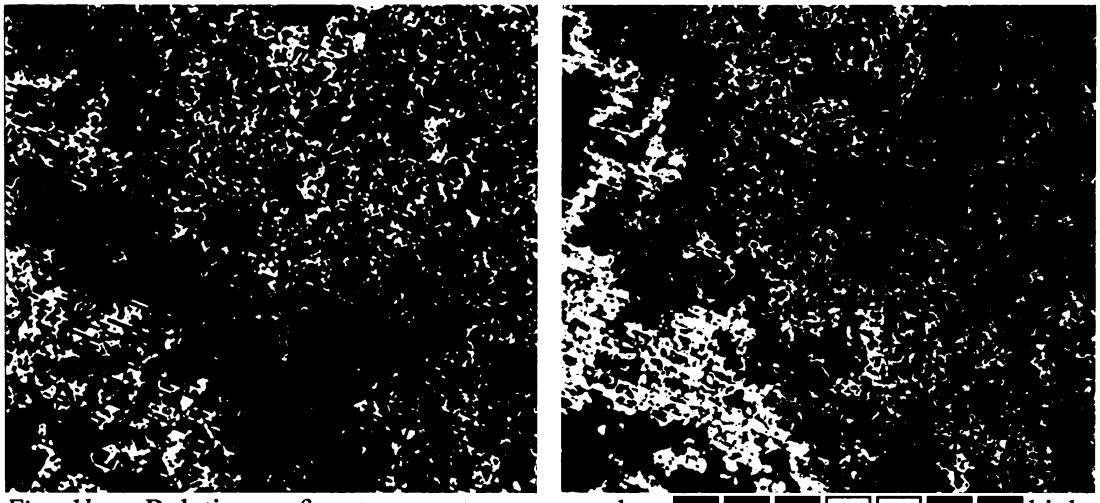

Fig. 1b Relative surface temperatures low high

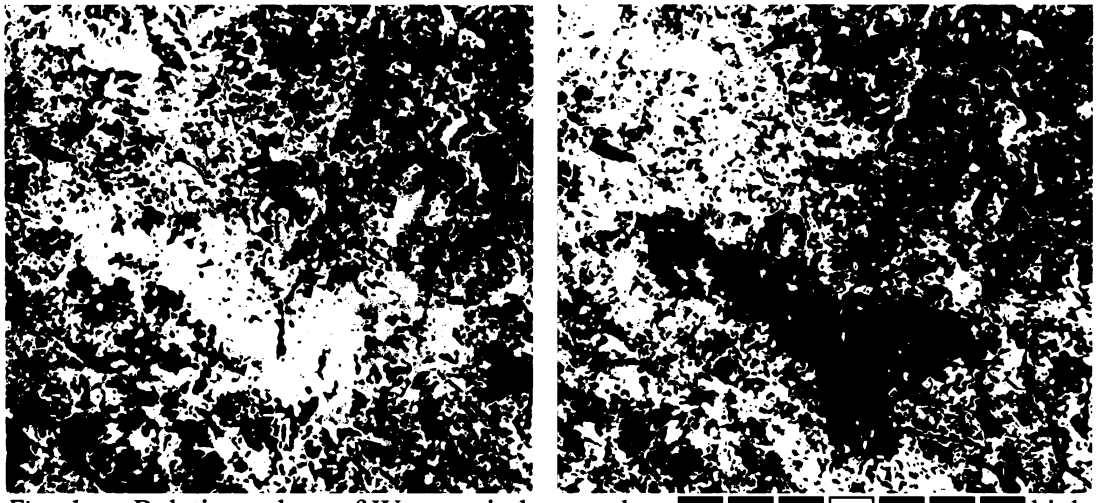

Fig. 1c Relative values of Wetness index low high

values (1, 9, 17... 49), classes of both compared visual records mutually correspond and the result therefore equals zero, i.e. no change (e.g. stable temperature). Based on the matrix analysis, we also made a table of a percentage coincidence of all combinations of selected intervals.

4. Results

The comparison of scenes from 1987 and 2002 in 453 RGB (Red, green, blue) compositions clearly showed lighter zones in the 2002 image (turquoise) around the Luzenský stream extend in the east through Mokrůvka further to Germany and towards Roklan in the west (Fig. 1a). Such zones represent decayed spruce forests and newly formed clear cut areas. Colour differences between clear cut areas and decayed forests in the no-intervention zone aren't very clear (clear cut areas are marked by a lighter shade). Fig. 1b shows the same areas in both monitored years as Fig. 1a, but the coloured scale represents surface temperature values transferred into a relative equiareal (quantile) scale for comparability purposes. The Figure clearly shows an increase in surface temperature that in many cases rose from the lowest to the highest values on the relative scale. This phenomenon is documented by Fig. 2. It shows the matrix analysis results where pixel values are represented on the basis of overlapping classes combination. The biggest change of relative temperature, in other words a shift from the lowest surface temperature class in 1987 to the highest surface temperature class in 2002, was detected in the western slope of Mokrůvka hills, on the whole Špičník border ridge, on Blatný hill, in the Roklanský forest, and clear cut areas eastwards from Medvědí hill. Significant movements from the first (the coldest) class to the sixth or fifth class apply to the whole area affected by the bark beetle calamity. Mountain meadows and wetland in Luzenské valley, around Modrava, at Filipova Huť, Kvilda and Horská Kvilda are free of any temperature changes. Some locations (e.g. Nová slať) were affected by opposite developments, i.e. temperature dropped from the highest to the lowest class.

Fig. 1c indicates the Wetness index values distribution on a seven-grade relative scale. Comparison of both scenes shows a decrease in the Wetness index values between 1987 and 2002. The Wetness index results were also compared by applying the matrix analysis and the outcome is shown in Fig. 2b. Class changes are found mainly in the areas of decayed spruce forests and newly formed clear cut areas. Decrease in the Wetness index

values implies a relative reduction of the surface humidity. However, in this case changes mostly involve shifts from medium to the lowest values.

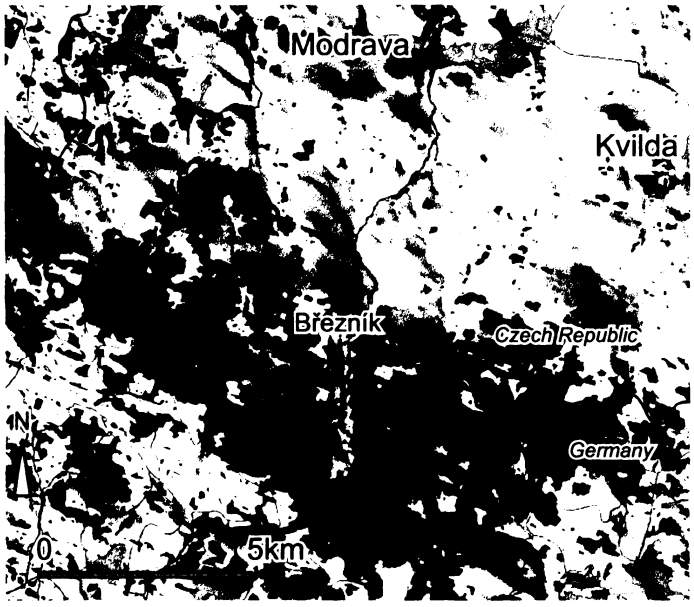

Fig. 2a The difference of surface temperature between the years 1987 and 2002.

Increase by 5-7 classes

Increase by 3-4 classes

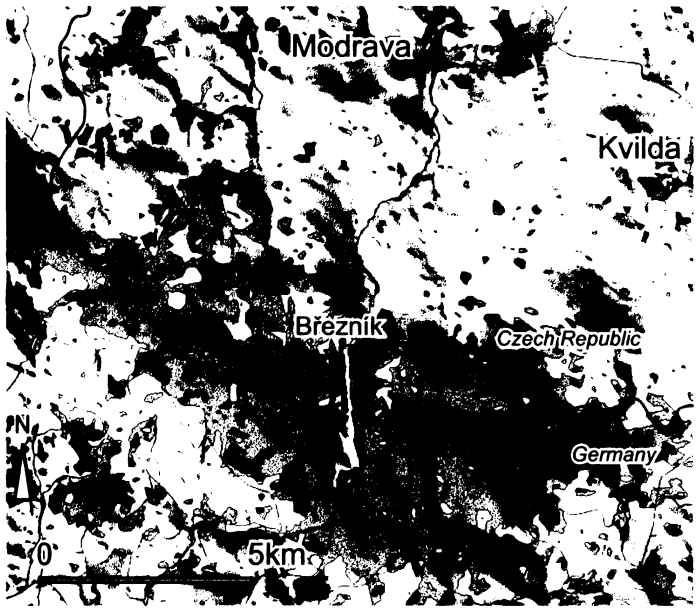

Fig. 2b The difference of Wetness index between the years 1987 and 2002.

Decrease by 5-7 classes

Decrease by 3-4 classes

5. Discussion and Conclusions

The study confirms the assumption that decay and clear cutting of mountain spruce forests in central Šumava Mountains leads to changes in surface temperatures, specifically to a significant warming. Such changes are supported by the fact that the relative seven-grade temperature scale mostly showed shifts from the first (the coldest) class to the

seventh class (the warmest) in the bark beetle calamity areas. Links between beetle bark calamities and temperature changes are mentioned by Aldrich (1979) who, however, indicated only 1°C average differences measured on specific trees. Direct relation between the temperature rise in spruce forests infested by bark beetle and decrease of soil humidity was indicated by Swift et al. (2002). The Wetness index values declined significantly also during the bark beetle calamity in the Březník area. Increase in surface temperature and decrease in the Wetness index values in central Šumava Mountains imply significant environmental changes that may lead to changes in the energy-substance balance of the area, or to formation of hydrological runoff in the river basin. Potential impact of mountain spruce forests decay on runoff conditions was confirmed by Křovák & Kuřík (2001) who studied three experimental river basins in central part of Šumava Mountains.

The dividing of the both temperature and Wetness index values was made by dividing the interval into so-called equiareal classes. This dividing was used by Šíma to compare changes of the landscape surface temperatures in the area of "Podkrušnohorská" soil heaps (Pokorný et al., 2002). Some limitation of this method is given by the fact, that the fewer relative classes we have, the more the marginal extremes are hidden in the Gauss histogram of values. However, the equiareal distribution of classes gives better knowledge about the distribution of temperatures in the landscape than for example equidistant distribution.

According to this study it is possible to state, that the hypothesis of the increasing relative surface temperature and decreasing the Wetness index values in the bark beetle outbreak area was confirmed. It would be necessary to use data with higher resolution for more detail study of particular landscape components.

Acknowledgements

I thank to RNDr. Jan Pokorný for valuable advice, comments and support. My thanks belong also to RNDr Jakub Langhammer, Phd., who provided me both the expert and technical help. I thank also to RNDr. Martin Šíma for the expert consultations in the field of Remote Sensing.

References:

Aldrich, R. C. (1979): Remote sensing of wildland resources: A state-of-the-art review. USDA For. Serv. Gen. Tech. Rep. RM-71, 56 p. Rocky Mt. For. and Range Exp. Stn., Fort Collins, Colo.

Campbell, J. B., (2002): Introduction to Remote Sensing. The Guildford Press. New York

Geomatica Algorithm Reference, (2003): PCI Geomatics.50 West Wilmot Street, Richmond Hill,Ontario, Canada,L4B 1M5

Hais, M., (2003): Vliv odvodnění na funkce krajiny v oblasti Národního parku Šumava. Sborník příspěvků studentů DSP z konference s mezinárodní účastí. Zemědělská fakulta, Jihočeská Universita. 11-15.

Kauth, R. J., Thomas, G.S. (1976): Tasseled Cap – a graphic description of the spectral-temporal development of agricultural crops as seen by Landsat. Proceeding from Remotely Sensed Data Symposium, Purdue University, West Lafayette, Indiana, USA. P. 4b41-4b51.

Kočárek, E., (2003): Geologie a petrologie Šumavy. In: Šumava, příroda, historie, život. Nakladatelství Miloš Uhlíř – Baset. 123 – 130.

Křovák, F., Kuřík, p., (2001): Vliv lesních ekosystémů na odtokové poměry krajiny. *Aktuality šumavského výzkumu.* 75 - 79.

Pokorný, J., (2001): Dissipation of solar energy in landscape-controlled by management of water and vegetation. *Renewable energy.* 24, 641 – 645.

Pokorný, J., Pecharová, E., Sixta, J., Šíma, M., (2002): Obnova a funkce krajiny narušené povrchovou těžbou. Část: Mostecká pánev. Program: Biosféra – SE. Projekt VaV 640/3/00. DÚ 04, Diagnóza krajiny. 98 – 135.

Ripl, W. (1992): Management of water cycle and energy flow for ecosystem control – the Energy – Transport – Reaction (ETR) model. *Ecological Modelling.* 78, 61 – 76.

Ripl, W., Pokorný, J., Eiseltová, M. a Ridgill, S. (1996): Holistický přístup ke struktuře a funkci mokřadů a jejich degradaci. In: Eiseltová, M. (ed.) Obnova jezerních ekosystémů H – holistický p Gístup. *Wetlands International publ.* 32, 16 –35.

Skuhravý, V., (2002): Lýkožrout smrkový (Ips typographus L.) a jeho kalamity. Der Buchdrucker und seine Kalamitäten. Agrospoj, Praha.

Strnad, E., (2003): Podnebí Šumavy. In: Šumava, příroda, historie, život. Nakladatelství Miloš Uhlíř – Baset. 35 - 44.

Šúri, M., Feranec, J., Cebecauer, T., (1994): Determination of soil water content using spectral indices computed from Landsat TM data. *Geografický časopis. Časopis*. 46, 3.

Swift, C. E., Jacobi, W. R., Schomaker, M., Leatherman, D. A. (2002): Environmental Disorders of Woody Plants. Colorado State University Cooperative Extension.

Zatloukal, V., Kadera, J., Černá, j., Přílepková, S., (2001): Předběžné vyhodnocení stavu a vývoje přirozené obnovy v NP Šumava v prostoru Mokrůvka – Špičník – Březnická hájenka. *Aktuality šumavského výzkumu*. 110-115.

Zichová, D., (2000): Hodnocení ekologické stability krajiny na vybraných katastrech okresu Praha – západ. Ústav pro životní prostředí, Přírodovědecká fakulta UK Praha. Diplomová práce.

Kapitola 2

Vliv odlesnění a odumírání horských smrčin na teploty krajinného krytu a možné důsledky pro formování odtoku v oblasti centrální Šumavy

Hais M.

1. Úvod

Využití území je jedním ze zásadních faktorů ovlivňujících odtokové poměry v lokálním, regionálním i globálním měřítku. Změny ve využití území na velkých plochách se mohou odrážet v krátkodobém i dlouhodobém vlivu na zvyšující se rizika extrémních průtoků, případně v dlouhodobém poklesu zásob hladiny podzemní vody (Bhaduri et al., 2000). Vliv změn využití území na rozsáhlých plochách regionálního až globálního charakteru na odtokové poměry popisuje Lu (2004). V této práci je naopak kladen důraz na změny využití území v lokálním měřítku.

Jednou z významných změn krajinného krytu je odlesnění. Odlesnění může odtokové poměry ovlivňovat přímo a nepřímo. Přímým vlivem je snižování retenční schopnosti krajiny. Vliv odlesnění na odtokové poměry zkoumal například Badoux et al., (2006). Výsledky tohoto výzkumu potvrzují předpoklad dlouhodobě vyššího odtoku na plochách s poškozenými lesními porosty vlivem vichřic, který je navíc umocněn sekundárními odvodňovacími kanály. I na Šumavě byl zkoumán vliv odlesnění na snížení retenční kapacity a následný vznik povodní. Na základě historických záznamů povodňových událostí popisuje Šonka (2004) významné zvýšení frekvence povodní na Otavě v 19. století, které dává do souvislosti s intenzívním využíváním lesů. Vliv odlesnění na odtokové poměry a kvalitu vody byl hodnocen i experimentálně na třech šumavských subpovodích s rozdílnými typy vegetačního krytu (zdravý les, rozpadlé horské smrčiny, holá seč). Výsledky této studie dokládají vliv zdravého lesního porostu na vyrovnanost odtokových poměrů (Křovák a kol., 2004). Kromě již popsaného přímého vlivu odlesnění na změnu odtokových poměrů je možné uvažovat ještě vliv nepřímý. Podstatou tohoto vlivu je, že odlesněním nebo v obecné rovině odstraněním vegetačního krytu může docházet na takových plochách během letních, slunečních dnů k přehřívání povrchů. Přehřívání povrchů krajiny může měnit ve svém důsledku místní klima a se zvyšující se velikostí ploch i mezoklima a má rovněž vliv na hydrologický cyklus. Při bezvětrném počasí tak dochází i k značnému ohřívání vzduchu, který je schopen pojmout větší objem vody v podobě páry. Při náhlém ochlazení může dojít k lokálnímu maximu srážek v podobě přívalových dešťů se všemi negativními důsledky včetně povodní (Trenberth, 1999).

Cílem této práce bylo navržení metodického přístupu pro hodnocení kvalitativních i kvantitativních změn krajinného krytu pomocí metod DPZ v termální oblasti spektra a

výsledky diskutovat v širším kontextu srážko-odtokových změn. Práce vychází z toho, že teploty povrchu krajinných struktur jsou integrální veličinou, která vypovídá jednak o fyzikálně-chemických vlastnostech daného materiálu (tepelná kapacita, tepelná vodivost, odrazivost, chemické složení, obsah vody a jiné) a funkci vegetačního krytu (zejm. transpirace, případně snížení dopadajícího slunečního záření na povrch půdy) ale zároveň termální projev přispívá k utváření klimatických a srážko-odtokových podmínek daného území. Pokud tedy dojde vlivem změny krajinného krytu i ke změnám termálního projevu, je možné očekávat i změny ve srážko-odtokovém režimu.

Navržený metodický přístup je ověřován na případě dvou typů odlesnění, kterými jsou: rozpadlé horské smrčiny vlivem přemnožení lýkožrouta smrkového a plochy s asananovanými lesními porosty. Nárůst teplot krajinného krytu vlivem odlesnění byl již popsán v mnoha studiích (Weber, 1971; Yoshino, 1975; Schmid, 1976; Hashimoto & Suzuki 2004). Stejné výsledky již byly publikovány z oblasti centrální Šumavy (Hais, 2003; Hais a Pokorný, 2004; Hojdová et al., 2005), která je zájmovým územím i v případě této studie. Základním předpokladem v této studii je, že teplotní podmínky asanovaných lesních porostů (holých sečí) a rozpadlých horských smrčin se budou lišit. K ověření tohoto předpokladu byly srovnány hodnoty teplot krajinného krytu z družicových scén (Landsat TM a ETM+) pořízených před expanzí kůrovce v oblasti centrální Šumavy a po zásadních změnách vyvolaných touto kalamitou.

2. Materiál a metody

2. 1 Zájmové území

Zájmovým územím této studie je oblast centrální Šumavy (viz obr. 1 a 2A), přičemž hlavní pozornost je věnována lokalitě s významným rozpadem horských smrčin (*Picea abies* [L.] Karst.) vlivem přemnožení lýkožrouta smrkového (*Ips typographus L.*), která vrcholila přelomu 20. a 21. století.

Obr. 1 Rozpadlé smrkové porosty vlivem Lýkožrouta smrkového v okolí Luzenského údolí na Šumavě. Letecký snímek (*foto M. Hais*).

Skuhravý (2002) uvádí, že první větší ohniska napadení smrčin lýkožroutem na české straně byla zaznamenána leteckým snímkováním v roce 1992. K výrazné akceleraci napadení smrčin lýkožroutem pak došlo v letech 1995 a 1996, kdy byla zasažena téměř celá oblast na které došlo k rozpadu smrčin k roku 2000. K tomuto roku připadá celková plocha odlesnění vlivem lýkožrouta smrkového (včetně asanovaných smrčin) na 2600 ha. Území postižené kalamitním přemnožením lýkožrouta smrkového v okolí Březníku je na východě ohraničené Velkou a Malou Mokrůvkou, na západě zasahuje až k Roklanu. Severní hranici tvoří přibližně linie Medvědí – Studená hora a na jihu je studovaná oblast vymezena státní hranicí s mírným přesahem do Německa asi 0,5 – 1 km. Nadmořská výška se zde pohybuje v průměru okolo 1100 – 1200 m.n.m. Nejvyšší vrcholy na české straně představují Velká Mokrůvka 1370 m.n.m a Špičník 1351 m.n.m. Na německé straně pak dominuje vrchol Luzného 1373 m.n.m. a Roklan 1453 m.n.m. Hydrologicky spadá oblast do subpovodí Roklanského a Modravského potoka (96 km^2), které je součástí povodí Otavy. Geologické podloží je tvořeno moldanubikem, přičemž na většině území se uplatňuje geologická jednotka Královského hvozdu (ruly, pararuly), místy vystupují magmatická tělesa, jako je tomu v případě centrálního moldanubického plutónu v masivu

Vydry (biotitická žula, adamellity, granodiority) (Kočárek, 2003). Z hlediska klimatických charakteristik vykazuje tato oblast i v rámci Šumavy nejvyšší srážkové úhrny, přičemž Březník je označován jako nejdeštivější místo na Šumavě ročním srážkovým úhrnem až 1552 mm (Strnad, 2003). Hlavním krajinným prvkem jsou zde horské smrčiny, dále připadá významný podíl na rašeliniště (Rokytská, Rybárenská, Roklanská slať a další) a horské louky. Významný podíl rašelinišť a zamokřených půd, který je odrazem relativně vysokých srážek v této oblasti, vedl v minulosti k hydromelioračním odvodňovacím zásahům ve snaze přeměnit tyto plochy na produkční les smrkových monokultur (Hais, 2004).

Lesní porosty jsou v této lokalitě vystaveny řadě extrémních podmínek. Luzenské údolí je považováno za mrazovou kotlinu s častým výskytem mlh. Jejich velký ekologický význam v oblasti centrální Šumavy zdůrazňuje Hruška a kol. (2005), který popisuje až řádově vyšší naměřené koncentrace látek (sírany, dusičnany apod.) v mlžné a oblačné vodě oproti vodě srážkové. Zvýšené depozice oxidů síry a dusíku pak mohou být jedním z více faktorů, které mohly snížit obranyschopnost smrčin vůči invazi kůrovce smrkového. Pro rozvoj kůrovcové kalamity v této oblasti měl význam také fakt že se zde jednalo často o stejnověké monokultury (Skuhravý, 2002).

2.2 Použité metody

Pro hodnocení teplot krajinného krytu byla využita analýza multispektrálních distančních dat. V tomto případě byly zpracovány scény družicového systému Landsat 5 TM a Landsat 7 ETM+. Výhodou družicového systému Landsat TM je, že jeho uvedení do provozu připadá již na rok 1982 (Lillesand *et al.*, 2004, Jensen, 2000). To má velký význam pro temporální vyhodnocení změn a v této studii je tak možné zpracování dat z období ještě před začátkem kůrovcové kalamity na Šumavě. Doba snímání družicí Landsat je v případě zájmové oblasti 10:34 (SELČ). Ke snímání stejného místa na zemském povrchu dochází v pravidelném šestnáctidenním intervalu.

Pro vymezení porovnávaných ploch byla použita digitalizace leteckých orthorektifikovaných snímků z roku 2002. Výřezy družicových scén z 11. 7. 1987 a 28. 7. 2002 byly geometricky a souřadnicově transformovány do souřadnicového systému JTSK podle orthorektifikované Družicové mapy ČR© 2002 ARCDATA PRAHA, s.r.o. Převzorkování dat bylo provedeno metodou Nearest neighbour z důvodu zachování

původních radiometrických hodnot pro následné zpracování dat. Pro výpočet teplot krajinného povrchu byl využit 6. termální kanál TM a ETM+, obsahující záznam v intervalu elektromagnetického záření 10.4 – 12.5 μm (Campbell, 2002). Přepočet digitálních hodnot na teplotu byl proveden pomocí modulu ATCORT 2 (Geomatica Algorithm Reference, 2003). Pro další zpřesnění hodnot byly do modulu ATCORT 2 začleněny i doplňkové kalibrační údaje: geografická poloha, střední nadmořská výška, zenitový úhel Slunce v době snímání (vypočítaný programem SUN), dohlednost (data získaná z ČHMÚ) a roční doba. Výstupem jsou teploty krajinného krytu v absolutních hodnotách (°C). Z důvodu velmi členitého reliéfu (rozdíly v nadmořské výšce, orientaci a sklonu svahu) nelze porovnávat teplotní rozdíly holin a rozpadlých horských smrčin v rámci jedné scény. Například jihovýchodní svahy vykazují v době snímání družicí vyšší teploty, než svahy severozápadní apod. Rozdíly teplot vlivem odlišné nadmořské výšky, orientace a sklonu byly eliminovány použitím temporální per-pixelové analýzy. To znamená, že jsou porovnávány hodnoty odpovídajících si pixelů (nejmenší segmenty obrazu) v čase. Pro vzájemné porovnání družicových dat z různých časových období je však nutné absolutní hodnoty normalizovat jejich převedením do relativní škály. Důvodem je, že aktuální hodnoty teplot jsou ovlivněny povětrnostními podmínkami. Hais (2003) ve své práci uvádí rozdělení hodnot histogramu dle kvantilového rozpětí. Nevýhodou tohoto přístupu je omezený počet intervalových tříd u diskrétních hodnot, což ve výsledku stírá rozdíly uvnitř těchto tříd. Proto je přesnější vyjádřit míru zvýšení teplot krajinného krytu teplot jako rozdíl standardizovaných hodnot teplot dvou družicových scén. Standardizace hodnot je dána jednoduchým vztahem (Hendl, 2004):

$$x' = \frac{x - \bar{x}}{Sx}$$

kde $\bar{x}$ je průměrná hodnota a Sx je směrodatná odchylka. Někdy se průměr nahrazuje mediánem a směrodatná odchylka interkvantilovým rozpětím (Hendl, 2004):

$$x' = \frac{x - \tilde{x}}{Q}$$

Takto standardizované hodnoty umožňují vzájemné srovnání souborů. Proto bylo možné vyjádřit míru změn teplot krajinného krytu na holých sečích a rozpadlých horských smrčinách.

3. Výsledky

Teploty krajinného povrchu vypočtené z obou družicových scén byly standardizovány podle obou výše zmíněných rovnic. Při srovnání jejich histogramů bylo zřejmé, že standardizace využívající medián a interkvantilové rozpětí o něco lépe vystihuje rozložení dat. Takto standardizovaná data byla dále použita pro další operace. Následoval výpočet rozdílu standardizovaných teplot obou družicových scén. Na obrázku 2A je graficky vyjádřená míra rozdílu teplot pro celé zájmové území. Protože se jedná o standardizované hodnoty, nelze velikost tohoto rozdílu kvantifikovat (např. v °C). Je však možné porovnávat rozdíly změn na vybraných plochách. Cílem bylo srovnání, zda na plochách s asanací lesních porostů došlo k vyššímu nárůstu teplot než v rozpadlých horských smrčinách. Tento předpoklad potvrzuje obrázek 2, kde významné relativní zvýšení teplot krajinného povrchu připadá na asanované lesní porosty, zatímco u rozpadlých horských smrčin k výraznému nárůstu teplot došlo jen v některých lokalitách. Jedná se o oblast Roklanu, Špičníku a Mokrůvek. Vzhledem k okolním lesním porostům, kde nedošlo k rozpadu horských smrčin nebo asanaci porostů vykazují obě zkoumané plochy vyšší hodnoty krajinného povrchu.

Předpoklad, že holiny vykazují vyšší teploty krajinného povrchu na holinách bylo zapotřebí ještě testovat. Graf 1 ukazuje srovnání obou zkoumaných ploch z hlediska teplot krajinného povrchu. Dále bylo ještě provedeno statistické hodnocení odlišnosti obou skupin Mann-Whitneyovým testem. Tento test byl použit, neboť se zde jedná o data, která nemají normální rozdělení. Výsledky Mann-Whitneyovým testu potvrzují odlišnost obou souborů ($Z= -37,07$; $p<0,001$).

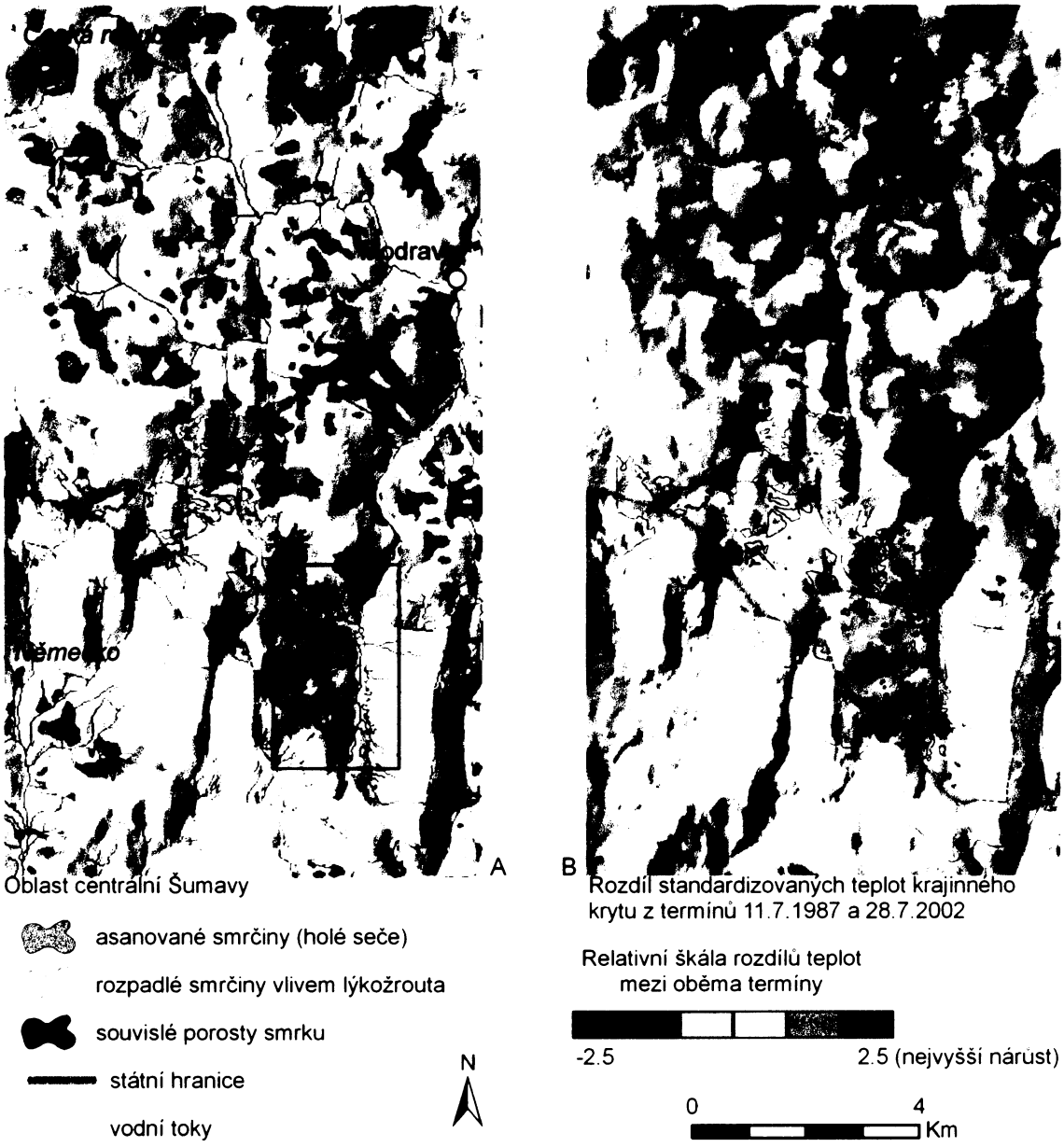

Obr. 2 A) Stav rozpadu horských smrčin a vzniku holích sečí v roce 2002. Obdélníkový rámeček v obrázku (vpravo dole) vyznačuje oblast, která je zachycena na fotografii na obrázku 1. B) Relativní rozdíl standardizovaných teplot krajinného povrchu. Datovým podkladem jsou scény družic Landsat TM z 11. 7. 1987 a ETM+ z 28. 7. 2002.

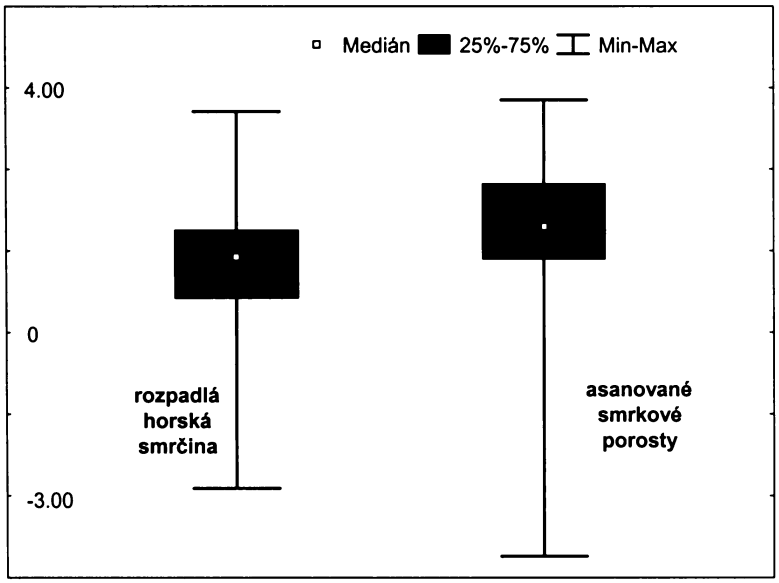

Graf 1 Relativní rozdíl standardizovaných teplot krajinného povrchu.

4. Diskuse

Rozdílný teplotní projev asanovaných lesních porostů (holých sečí) a rozpadlé horské smrčiny popisuje v oblasti centrální Šumavy již Hojdová (2003). Výsledky, ke kterým autorka dospěla byly formulovány na základě bodových terénních měření a mohly by být za určitých okolností ovlivněny stanovištními podmínkami. Průkaznost výsledků byla doložena na základě zpracování teplot krajinného povrchu z družicových dat (Hojdová et al., 2005).

Výsledkem této práce je komplexní hodnocení teplotních rozdílů asanovaných ploch (holých sečí) a rozpadlé horské smrčiny. Výsledky potvrzují předpoklad vyššího přehřívání asanovaných lesních porostů oproti rozpadlým horským smrčinám. Menší nárůst teplot krajinného povrchu v rozpadlých horských smrčinách je možné vysvětlit vyšší členitostí jejich povrchu, což zde vytváří celou řadu lokálně zastíněných ploch, u kterých nedochází k vyššímu zahřívání vlivem solární radiace. Dalším důvodem může být i vyšší odrazivost kmenů odumřelých stromů. Vzhledem k tomu, že relativní rozdíl teplot krajinného povrchu vychází z družicových dat snímaných v obou případech (11. 7. 1987 i 28. 7. 2002) v 10:34 hodin SELČ, dá se předpokládat, že během dopoledne ještě nedošlo k maximálnímu rozrůznění ohřívaných ploch, ke kterému dochází až po poledni. V odpoledních hodinách lze tedy očekávat ještě větší rozdíly mezi zkoumanými povrchy. To se může na plochách asanovaných lesních porostů (holých sečí) projevit extrémními teplotami. To potvrzuje i

práce Hojdové (2003). Odumřelé horské smrčiny tak dávají větší naději na přirozenou obnovu lesa a tím i opětovné zvýšení retenční schopnosti území. Druhým aspektem, který vyplývá z výsledků, je vliv obou sledovaných ploch na mikroklima. Přehřívané plochy asanovaných lesních porostů mohou měnit významně místní klima a zvyšovat i rizika spojenými s extrémními srážko-odtokovými událostmi.

Uvedená metodika pro srovnání relativního nárůstu teplot krajinného krytu na vybraných plochách představuje poměrně nenáročný výpočet teplot ze dvou termínů dat družice Landsat. Tato per-pixelová temporální analýza vychází z předpokladu, že hodnota termálního stupně (lapse rate) se nemění s nadmořskou výškou, což nemusí být vždy zaručeno. Proto je velmi důležitý výběr termínů družicových dat, které by měly být vzájemně co nevíce podobné z hlediska povětrnostních podmínek (teplota, oblačnost, srážky, vítr) v době před a během snímání. Důležitá je i podobnost fenofáze zvolených termínů, zejména při hodnocení vegetačního krytu s výraznou dynamikou. To však není případ hodnocených smrkových porostů, které neprodělávají tak významné změny jako například opadavé stromy. Požadavek na podobnost povětrnostních podmínek (srovnání dat z meteorologické stanice Churáňov) byl splněn. V obou dvou zmíněných termínech lze povětrnostní podmínky definovat jako stabilní anticyklonální počasí bez srážek a téměř bez oblačnosti.

5. Závěr

Výsledky srovnání teplotního projevu holých sečí a rozpadlých horských smrčin z družicových scén jsou v souladu s předpokládanou odlišností obou typů ploch. Na holých sečích došlo k významně vyššímu nárůstu teplot oproti rozpadlým horským smrčinám. Proto je třeba brát ohled na možnost ovlivnění lokálních klimatických podmínek v důsledku odlesnění v případě lesnického hospodaření v produkčních lesích, stejně jako při plánování zásahů v oblastech s určitým statutem ochrany přírody. Další souvislost je možné spatřovat i mezi změnami typu odlesnění a změnou srážko-odtokových poměrů. Termální projev krajiny může být tedy citlivým indikátorem krajinných změn.

6. Summary

The influence of deforestation and decay of spruce forests on the surface temperature and possible consequences for runoff in central part of Šumava Mountains

The aim of this work is to verify a potential of thermal remote sensing to assess quantitative and qualitative changes of land cover/land use and to interpret the results in the context with precipitation-runoff conditions in the landscape. This study is based on a fact, that surface temperature is an integral quantity, which express the physical and chemical characteristics of a given material and the function of vegetation cover. Nevertheless, the surface temperature of land-cover components influences the climatic and precipitation-runoff conditions.

Suggested methodical approach have been used in the cases of two deforestation types: forest decayed because of bark beetle attack and clear cut areas.

The area of interest lies in the central part of Sumava Mountains, surrounding Březník lodge. The main attention was aimed to the locality affected by a significant decay of Norway spruce forests (*Picea abies* [L.] Karst.) due to an outbreak of bark beetle (*Ips typographus L.*), which culminated in the turn of 20th and 21st century. The first larger centres of bark beetle attack on the Czech side of the border had been recorded by an aerial photography in 1992. A significant acceleration of the attack arose in 1995 and 1996, when almost the whole area, where the spruce forests decayed towards 2000, was affected. The total area of the deforestation caused by bark beetle (including the clear cut areas) occupied 2600 ha in this year.

The question was, if the both types of deforestation show different temperature conditions. To verify this hypothesis, the thermal data of Landsat (TM and ETM+) scenes were compared. The first data set was acquired by Landsat TM in July the 11th 1987, when there was no bark beetle outbreak in the central Šumava Mountains yet. The second data set was represented by scene from Landsat ETM+ acquired in July the 28th 2002, when the largest part of spruce forests had been already decayed. The atmospheric conditions differed in the times of the scenes acquisitions, so the data had to be normalized prior the comparison. Regardless of the data normalisation, the similar weather conditions in both terms are really important for the comparison. This precondition was fulfilled, because the

weather had been defined as a stable anticyclonic without precipitation and nearly without clouds. An influence of topoclimatic conditions was eliminated by using a per-pixel change detection analysis.

The result is, that surface temperature increased in both types of deforested areas compared to the state before the bark beetle attack. However, the temperature increasing was significantly higher in case of clear cut areas than in decayed forest. The difference was statistically evaluated by Mann-Whitney test ($Z = -37,07$; $p<0,001$), because the data had no normal distribution.

So the possibility of influence of local climatic condition as a result of deforestation should be considered in management of forest of production as well as of protected forest stands. Different local climatic conditions in two types of deforestation can also result in changes in precipitation-runoff relation in given area.

6. Literatura

Badoux, A., Jeisy, M., Kienholz, H., Lüscher, P., Weingartner, R., Witzig, J., Hegg, Ch. (2006): Influence of storm damage on the runoff generation in two sub-catchments of the Sperbelgraben, Swiss Emmental. *European Journal of Forest Research.* 125, 27–41.

Bhaduri, B., Harbor, j., Engel, B., Grove, M. (2000): Assessing Watershed-Scale, Long-Term Hydrologic Impacts of Land-Use Change Using a GIS-NPS Model, *Environmental Management.* Vol. 26, No. 6, 643–658.

Campbell J. B. (2002): Introduction to Remote Sensing. The Guildford Press. New York. 267 – 271.

Geomatica Algorithm Reference (2003): PCI Geomatics.50 West Wilmot Street, Richmond Hill,Ontario, Canada, L4B 1M5.

Hais, M. (2003): Changes in Land Cover Temperature and Humidity Parameters Resulting from Spruce Forests Decay in the Centre of the Šumava National Park. *Acta Universitatis Carolinae Geographica*, 2, 95 - 105.

Hais, M. (2004): Vliv odvodnění na funkce krajiny v oblasti Národního parku Šumava. Universitas Bohemiae Meridionalis Budovicensis. Collection of Scietific Papers, Faculty of Agriculture in České Budějovice. Agroregion 2004. Vol. 21. 243 – 246.

Hais, M., Pokorný, J. (2004): Změny teplotně-vlhkostních parametrů krajinného krytu jako důsledek rozpadu horských smrčin. – In: Dvořák, L. & Šustr, P., (eds.): Sborník z konference *Aktuality šumavského výzkumu 2*, Srní, 4.-7.10. 2004, 49 - 55.

Hashimoto, S., Suzuki, M. (2004): The impact of forest clear-cutting on soil temperature: a comparison between before and after cutting, and between clear-cut and control sites. *Journal of Forest Ressearch*. 9, 125–132.

Hendl, J. (2004): Přehled statistických metod zpracování dat. Analýza a metaanalýza dat. Portál.

Hojdová, M. (2003): Mikroklima horské smrčiny v různém stádiu rozpadu. Diplomová práce. Přírodovědecká fakulta, UK Praha,

Hojdová, M., Hais, M., Pokorný, J. (2005): Microclimate of a peat bog and of the forest in different states of damage in the Natioanl Park Šumava. *Silva Gabreta*, 11(1), 13 – 24.

Hruška, J., Hofmeister, J., Oulehle, F., Kopáček, J., Vrba, J., Metelka, V., Tesař, M., Šír, M., Máca, P., Beudert, B. (2005): Biogeochemické cykly ekologicky významných prvků v měnících se přírodních podmínkách lesních ekosystémů NP Šumava. Zpráva z projektu VaV/1D/1/29/04.

Jensen, J., R. (2000): Remote Sensing of the Environment: An Earth Resource Perspective, Upper Saddle River: Prentice-Hall.

Kočárek, E. (2003): Geologie a petrologie Šumavy. In: Šumava, příroda, historie, život. Nakladatelství Miloš Uhlíř – Baset. 123 – 130.

Křovák, F., Pánková, E., Doležal, F. (2004): Vliv lesních ekosystémů na hydrický režim krajiny. Influence of forest ecosystems on hydric regime of landscape. – In: Dvořák, L. & Šustr, P., (eds.): Sborník z konference *Aktuality šumavského výzkumu 2*, Srní, 4.-7.10. 2004, 37 – 43.

Lillesand, T. M., Kiefer, R. W., Chipman, J. W. (2004): Remote Sensing and Image Interpretation. John Wiley and Sons. New York.

Lu, X. X. (2004): Vulnerability of water discharge of large Chinese rivers to environmental changes: an overview. *Regional Environment Change*. 4, 182–191.

Skuhravý, V. (2002): Lýkožrout smrkový (Ips typographus L.) a jeho kalamity. Der Buchdrucker und seine Kalamitäten. Agrospoj, Praha. 196 p.

Schmid, J. M. (1976): Temperatures, growth, and fall of needles on Engelmann spruce infested by spruce beetles. USDA For. Serv. Res. Note RM-331, 4 p. Rocky Mt. For. and Range Exp. Stn., Fort Collins, Colo.

Strnad, E. (2003): Podnebí Šumavy. In: Šumava, příroda, historie, život. Nakladatelství Miloš Uhlíř – Baset. 35 - 44.

Šonka, J. (2004): Historické povodně Šumavy a poškození lesů. Historical floods in Bohemian Forest area and disturbance of forest. – In: Dvořák, L. & Šustr, P., (eds.): Sborník z konference *Aktuality šumavského výzkumu 2*, Srní, 4.-7.10, 44 – 48.

Trenberth, K. E. (1999): Conceptual framework for changes of extremes of the hydrological cycle with climate change. *Climatic Change* 42, 327 – 339.

Weber, F. P. (1971): The use of airborne spectrometers and multispectral scanners for previsual detection of ponderosa pine trees under stress from insects and disease. p. 94-104. *In* Monit. for. Iand from high aft. and from space. Annul rep. to Earth Resour. Surv. Prog., Off. Space Sci. and Appl. NASA, Houston, Tex.

Yoshino, M. M. (1975): Climate in a small area. An introduction to local meteorology. Univ. Tokyo Press, Tokyo.

Kapitola 3

The influence of topography on the forest surface temperature received from Landsat TM, ETM+ and ASTER thermal channels

Hais M., Kučera T.

Abstract

The main objective of this study was to assess the influence of topography on the surface temperature of spruce forest in the central part of the Šumava Mountains, Czech Republic. The aim was to design a method for surface temperature normalisation of forest stands in rugged relief. In this study, two Landsat scenes, ETM+ and TM, and one TERRA ASTER scene were used. The different spatial (60 m – 90 m – 120 m) and/or radiometric (8 – 12 bits) resolutions of these scenes enabled the assessment of the influence of these parameters on the accuracy of surface temperature models at the mesoscale landscape context. These models are based on the effect of complex topography (digital elevation model - DEM, and illumination - Hillshade) on surface temperature. Only homogeneous spruce forest stands were used for surface temperature modeling. The influence of topography on surface temperature in spruce forest was confirmed in all types of satellite data used. Three different approaches were used to increase the accuracy of the models. Predictability increased with forest content in the thermal pixel (model 1). The resulting R^2 values (0.47 - 0.49) were similar between all three scenes. Model 2 is based on the weighting of thermal pixels by the forest content (R^2: 0.32 – 0.39). We also assessed the influence of spruce forest edge effect on the accuracy of thermal models. Removing forest buffer zones resulted in greater statistical significance (approximately by 25 – 40 %). The optimal width of forest edge removed was determined to be 90 m. The resulting explained variability (R^2) improved by forest edge removal was 0.57, 0.52, 0.47 in the case of ETM+, ASTER, and TM, respectively. These values correspond with the spatial resolution. However the differences are not significant indicating that all these data are useful for ST modeling of spruce forest. The potential use of ST modeling is to identify temperature anomalies caused by different types of forest disturbance (e.g. harvesting, disease, insect attack) or changes in the condition of stands (e.g. water stress).

Key words: Landsat, ASTER, surface temperature, topography, spruce forest

1. Introduction

Thermal infrared (TIR) remote sensing data can provide important measurements of surface energy fluxes and temperatures, which are integral to understanding landscape processes and response (Quattrochi & Luvall, 1999). Using the Stefan-Boltzmann law it is possible to estimate the kinetic temperature of materials on the land surface:

$$M_r = \varepsilon \sigma T_{kin}^4 \qquad (1)$$

where M_r is the total broadband radiant flux, ϵ is emissivity, σ is the Stefan-Boltzmann constant (5.6697 x 10^{-8} Wm^{-2} K^{-4}, and T_{kin} is the kinetic temperature in degrees Kelvin (Jensen, 2000). The temperature estimated from remote sensed data is generally called surface temperature (ST). In our study this term is used to mean the surface temperature of forest overstory. A more detailed description of surface temperature estimation and emissivity is given by Snyder et al. (1998), Liang (2001) and Dash et al. (2002).

There are many satellites and airborne scanners, which are able to sense thermal infrared radiation (TIR) with different spatial and/or radiometric information (Asrar, 1989; Quattrochi & Luvall, 1999; Jensen, 2000; Campbell 2002; Lillesand et al, 2004). Satellites with middle spatial resolution are used particularly at the regional scale. For these purposes, the Landsat TM/ETM+ and ASTER (Advanced Spaceborne Thermal Emission and Reflection Radiometer) are frequently used, their spatial resolution being 120 m, 60 m and 90 m, respectively (Jensen, 2000; Lillesand et al., 2004). Different accuracy of ST in consequence of varied spatial resolution is closely related to scaling and spatial heterogeneity.

By comparing three types of thermal satellite data (TM, ETM+, ASTER) we assessed the influence of relatively small differences in spatial resolution on modeling accuracy.

Radiometric resolution is another variable, which defines the number of discriminable signal levels, so also data accuracy. For example, the most used 8-bit data have 0-255 levels (e.g. Landsat), but several sensor systems have a 12-bit radiometric resolution with values ranging from 0-4095 (e.g. ASTER) (Jensen, 2000). Nevertheless, there are not big differences in thermal data precision between the Landsat TM/ETM+ and ASTER, which are given as 0.5 °C and 0.3 °C (ERSDAC, 2005), respectivelly. On the other hand, there is a possibility to improve the accuracy of temperature calculation of ASTER using

Temperature/emissivity separation (TES) technique (Gillespie et al., 1998; Kahle & Alley, 1992), where the ST calculation is based on the five channels of ASTER in the thermal region.

Price (1989) mentioned various factors that affect the derivation of surface temperature: evaporation (in the case of vegetation evapotranspiration), moisture in the atmosphere, surface wind speed and surface roughness, the heat-storing capacity, albedo, emissivity and topography.

Topography is an important factor controlling surface temperature (Geiger, 1965; Yoshino; 1975, Geiger et al., 2003). Lookingbill & Urban (2003) suggested a site-specific model for estimating temperature differences across a complex terrain. There are also studies that use satellite-based topoclimatic modeling (Kang et al., 2004). The general factors of local relief are altitude, latitude, and aspect of slope, which are commonly measured in field studies. Altitude and latitude influence the general climatological characteristics, such as annual mean temperature, annual precipitation, temperature minimum in January, and temperature maximum in July. Average temperatures drop by about 6.4 °C per 1000 m, but this differs with region (Bailey, 1996). The local effects of slope and aspect, which influence the potential radiation and heat load are commonly computed in ecological studies (McCune & Keon, 2002), mostly based on DEM (Pierce et al., 2005). In addition to potential radiation and heat load, topographical shading generally has important effects on the energy balance, especially in the case of very complex terrain (Bellasio et al., 2005).

In the present study, we focused on the modeling of the influence of topography on surface temperature (due to the relatively small area we neglected the latitudinal range). The uniqueness of this study lies in modeling ST of a relatively heterogeneous forest surface using remote sensing data. This is almost impossible to do using field measurements. Such modeling contributes to understanding of the influence of topography and Sun position (zenith angle and azimuth) on the thermal character of spruce forest overstory.

2. Material and methods

2.1 Study site

The area of interest (129 km^2) includes the central part of the Šumava Mts., which is located in the south of the Czech Republic and extends into Germany. This locality is created by rugged topography and is almost covered by continuous forest stands. Norway spruce forest (*Picea abies* [L.] Karst.) is the dominant land use unit in this locality. There are also forest stands, which have been affected by a bark beetle outbreak, but these were not used for the analysis in this study. With the exception of the spruce forest, the area is mostly covered by peat (Rokytská, Rybárenská, Roklanská bogs and others) and mountain meadows. The relief of the central Šumava is created by a peneplain with numerous local hills. The elevation ranges from 700 m to 1453 m and the average altitude of the complex relief is 1093 m. Velká Mokrůvka (1370 m) and Špičník (1351 m) are the highest peaks in the Czech part, while the German area is dominated by Lusen (1373 m) and Grosser Rachel (1453 m). The high percentage of peat and wetland areas results from relatively high humidity; precipitation is over 1500 mm annually, especially in the Luzenske valley (Strnad, 2003). In the past there were certain efforts to drain the area and transform it into spruce monoculture forests (Hais, 2004).

2.2 Satellite data

In this project, two Landsat scenes [ETM+ (28 July 2002), TM (10 August 2004)], and one TERRA ASTER scene (15 July 2003) were used. In the case of all three scenes, the spatial resolution of the thermal channels is different (see table 1). From the third column of table 1, it follows that each thermal pixel of the three satellite data is associated with a different number of multispectral pixels of the other channels. This is an important feature for describing models 1 and 2 (see below).

The data acquisition times of the Landsat TM, ETM+ and TERRA ASTER satellites are 9:18 am, 9:48 am, and 10:18 am, respectively, in the case of the area of interest. The orbit for each Landsat and TERRA ASTER satellites result in a 16-day repeat cycle (Jensen, 2000; Campbell, 2002; Lillesand et al., 2004). Ancillary meteorological data from the Czech Hydrometeorological Institute were used to describe the meteorological

Table 1. Spatial resolution of selected spectral channels and their ratio

satellite	***spatial resolution of thermal channel (m)***	***spatial resolution of multispectral channels used for forest classification***	***the number of forest pixels belonging to thermal pixel***
Landsat TM	120	30	16
ASTER	90	15 (VNIR)	36
Landsat ETM+	60	30	4

conditions starting 10 hours before satellite data acquisition. The nearest meteorological station is located on the summit of Churanov hill (approx. 25 km north-east from the centre of the study area, 1122 m above sea level). The following data were used from this station: hourly air temperatures, air pressures, ground visibility and actual weather conditions. The ground visibility value and the air temperature at the time of data acquisition were used in ATCOR2 T (see below) as a calibration values. The other meteorological data were used in order to choose satellite data with similar weather conditions. It is evident from these data that anticyclonic weather, almost without precipitation, preceded all obtained satellite scenes.

The satellite scenes were orthorectified into the S-JTSK coordinate system (Krovak projection, Bessel 1841 elipsoid) according to the Satellite map of the Czech Republic (2002 ArcData Praha, s.r.o.) and a DEM created from contour lines (1:25 000). To enhance the geometrical accuracy in central Šumava, the ground control points (GCPs) were completed by points taken from aerial orthophotos provided by the Šumava National Park administration for the purposes of the project. These data were resampled by applying the nearest neighbour method to preserve the original radiometric values for subsequent data processing.

2.3 Spruce forest classification

The spruce forest thematic layers for all three scenes were obtained by a supervised classification method (Campbell, 2002; Lillesand et al., 2004) using PCI Geomatica software (Geomatica Algorithm Reference, 2003). The classification of spruce forest had to be carried out for all scenes due the land use/cover changes during 2002, 2003 and 2004. For all three scenes the same training fields were used. The trainings fields were chosen

only for non-changed forest (i.e. not harvested) during the years 2002 – 2004. The result of the classification of ETM+ from 2002 was verified using the areal photograph.

The forest edges exhibit different surface temperatures, because they form a microclimatic transition zone to non-forest ecosystems. This is in agreement with the results of Klaassen et al. (2002), who described the increase of heat fluxes near a forest edge. Therefore using progressive masking, the edge zones 30 m (Landsat) or 15 m (ASTER) wide, were successively removed during the following procedure. An example of individual forest buffer zones is shown in figure 1. Forests with minimal areas were also eliminated in the process of edge zone removal.

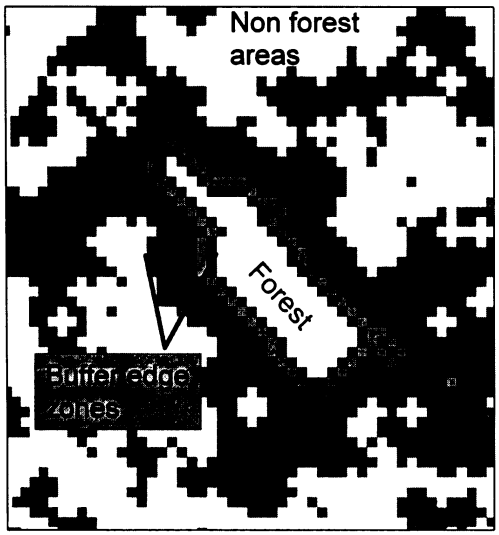

Figure 1. Buffer forest edge zones were subsequently removed using progressive masking in order to increase the accuracy of the models.

2.4 Thermal data

The 6th (10.4 – 12.5 μm) thermal channel of Landsat TM and ETM+ and the 13th (10.25 – 10.95 μm) thermal channel of TERRA ASTER, were used to calculate the surface temperature (Campbell, 2002; Lillesand et al, 2004). DN values were transformed to temperature values by applying ATCOR2_T (Richter, 1990; Richter & Coll, 2002; Geomatica Algorithm Reference, 2003).

The digital number DN in a thermal band is converted into the at-sensor radiance:

$$L = c0 + c1 \times DN \qquad (2)$$

where c0 and c1 are offset and gain of the radiometric calibration for the thermal band. The at-sensor radiance L is converted into a surface radiance L(surface) using the thermal path

radiance Lpath and atmospheric transmittance (tau) for the selected model atmosphere (e.g. midlatitude summer was obtained from the MODTRAN radiative transfer code) and the surface emissivity (eps=0.98):

$$L(surface) = \frac{(L - Lpath)}{(tau \times eps)} = \frac{(c0 + c1 \times DN - Lpath)}{(tau \times eps)} \quad (3)$$

The reflected contribution was neglected because it was insignificant in the case of the high emissivity of needle forest (Snyder et al., 1998). The surface temperature T is obtained from a least squares fit of the calculated table Ls = L(surface) = L(surface,T) for T=270-330 K.

Other calibration parameters were: average elevation, solar zenith angle, ground visibility and date of scene acquisition. The solar zenith angle (Z) for both scenes was calculated using the following formula (Pierce et al., 2005):

$$\cos(Z) = \sin(Lat) \times \sin(Dec) + \cos(Lat) \times \cos(Dec) \times \cos(15(T - 12)) \quad (4)$$

where Lat is latitude, T is the time of day in hours, and the coefficient 15 represents the degrees of longitude the earth rotates each hour. Solar declination (Dec), the angle between the sun and the position directly above the equator at noon, accounts for the tilt of the earth.

Ground visibility values were obtained from the Czech Hydrometeorological Institute. The accuracy of the surface temperature values from the Landsat scene (28 June 2002) was verified by field measurements (Hojdová et al., 2005). For this verification, the surface temperatures were measured using dataloggers: thermometer COMET L0141 (accuracy 0.2 °C; www.cometsystem.cz) in different land use units (meadows, peats) in the central part of the Šumava Mountains.

The spatial resolutions of the thermal channels (e.g. 60 m in the case of ETM+) are integral multiples of other multispectral channels (e.g. 30 m). Nevertheless, the thermal channel has the same pixel size as other multispectral information. This means that the thermal pixel is divided into given number of smaller pixels (table 1). After the geometric correction (resampling), thermal pixels with the same value have different polygon shapes (figure 2).

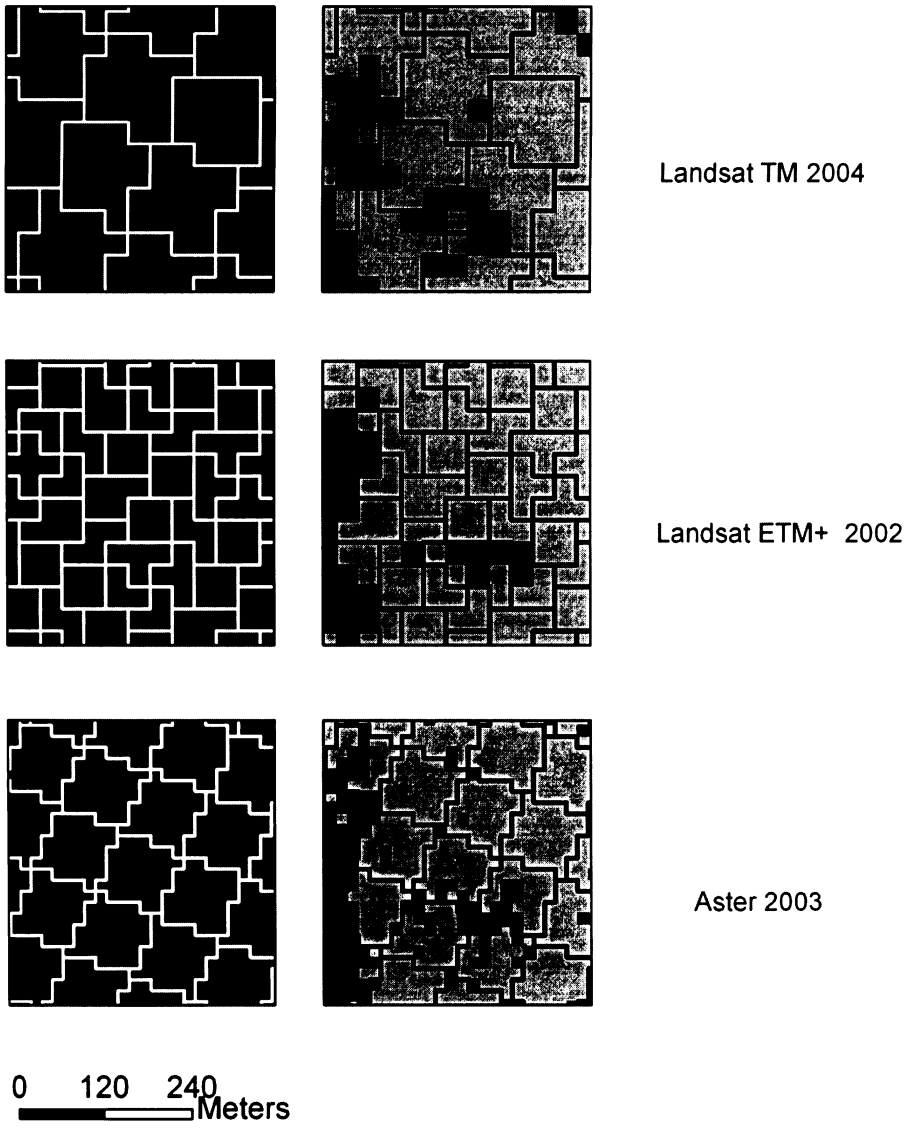

Figure 2. White edges (left) show the characteristic polygon form of thermal pixels after rectification (resampling). This is caused by different pixel size and spatial resolution. The right-hand pictures show the different number of forest pixels belonging to the thermal pixel.

We needed to recalculate the number of forest pixels belonging to these polygons. A higher proportion of forest in the thermal pixel (polygon) results in a higher accuracy for the thermal value. The zonal statistic for the thermal polygons was used to calculate mean values of forest content, Altitude, Hillshade and surface temperature. The proportion of forest content was used as relative weight for the thermal data.

2.5 Topography

To evaluate the influence of Altitude, a digital elevation model (DEM) was calculated with a spatial resolution of 30 m and 15 m in the case of Landsat and ASTER data, respectively. This was done in order to have the same spatial resolution in the DEM and multispectral bands of both satellite systems. In this case, we used the Topo to RASTER module (ArcGIS). Topo to RASTER is an interpolation method specifically designed for the creation of hydrologically correct digital elevation models (DEMs). It is based on the ANUDEM software (Hutchinson, 1993). Topo to RASTER uses knowledge about surfaces and imposes constraints on the interpolation process that results in a connected drainage structure and correct representation of ridges and streams. Contour elevation lines, stream feature class and point elevation data were used for the interpolation. On the basis of the DEM, two parameters (Slope and Aspect) were calculated in degrees using the spatial analyst tool (ArcGIS) (Burrough & McDonell, 1998). Both Aspect and Slope are included in Hillshade (HS), which was calculated on the basis of the DEM (ESRI 1994, Pierce et al. 2005):

$$HS = 255[\cos(90 - Z)\sin(s)\cos(\alpha - A) + \sin(90 - Z)\cos(s)] \quad (5)$$

where Z is the solar zenith, s is the local Slope, A is the solar azimuth and α is the azimuth of the slope facet. The Hillshade gives the hypothetical insolation of a surface by determining illumination values for each cell in a raster. Hence the Hillshade corresponds to differences in the energy balance of areas with different topography. The solar zenith (Z) and solar azimuth (α) in the formula (5) express the sun position in the given time of day and year. Therefore, individual Hillshade values were calculated for each date because of the different terms of satellite data acquisition. Lastly, the relation of the dependency of surface temperature on DEM and Hillshade was calculated. This was carried out for the surface temperatures of all three satellite scenes.

2.6 Surface temperature

The influence of relief on the surface temperature of the spruce forest was calculated using linear regression. There are two main independent variables in this regression, Altitude (DEM) and Hillshade (HS):

$$ST = a + b \times HS + c \times DEM + error \quad (6)$$

The ST (°C) was calculated from the satellite data; the estimation of Hillshade (0 – 255) and DEM (m) is described above. The error term consists of both systematic and random errors. Systematic error is dependent on the homogeneity of the surface in each thermal pixel. Generally, the most homogeneous pixels have the highest explained variability. Therefore, the three different models were used in order to decrease the systematic error in formula 6.

To normalise the thermal data, the first step is to calculate the regression, where the ST values are the thermal satellite data. The resulting coefficients (a,b,c in the formula 6) are used to calculate modeled ST. Then the modeled ST values are subtracted from the ST satellite data. Thus the effect of topography is removed and the deviations from null express the differences in water contend, evapotranspiration etc.

3. Results

The quality of the thermal data largely determines the explained variability of the thermal models. We tested the influence of the increasing proportion of forest content in the thermal pixel in the first model in order to determine the threshold of the forest content. All thermal pixels (of forest) were used in the second model and their values were weighted by forest content. The influence of removing edge buffer zones with different widths was tested in the third model.

1st model: Proportional content of forest in thermal pixel

This model is based on the assumption that the model has greater accuracy when more forest pixels are within one thermal pixel. Thus, the greatest model accuracy will be achieved in the case when the thermal pixels (polygon) include only forest pixels. Figure 3A shows the dependence of the explained variability (R^2) of the three different thermal channels on the proportion of forest pixels. In the case of all three types of satellite data, the R^2 values increased with the number of forest pixels up to 100 %, when there were only forest pixels. It is interesting that the highest R^2 values are almost the same for all three satellite data. However, the R^2 values for fewer forest pixels content are different for all

three satellites (figure 3A). The highest proportion of explained variation is achieved in the Landsat ETM+ data.

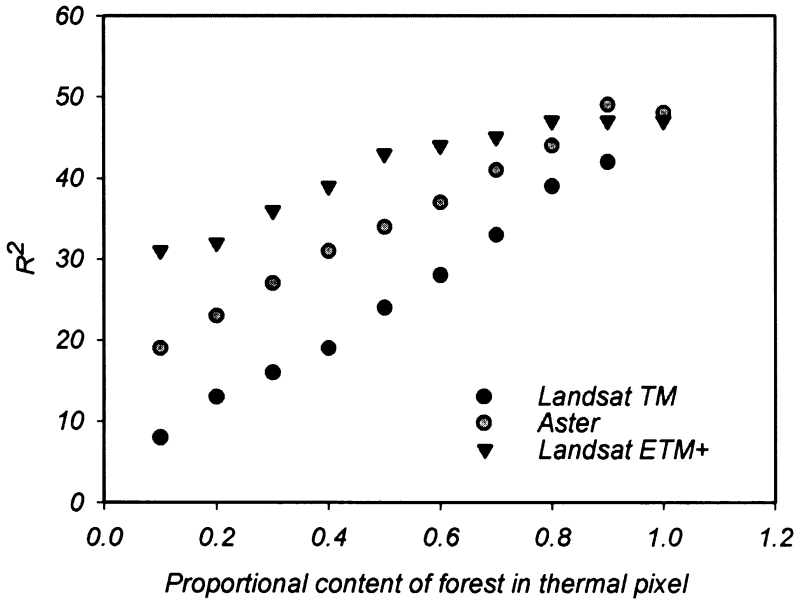

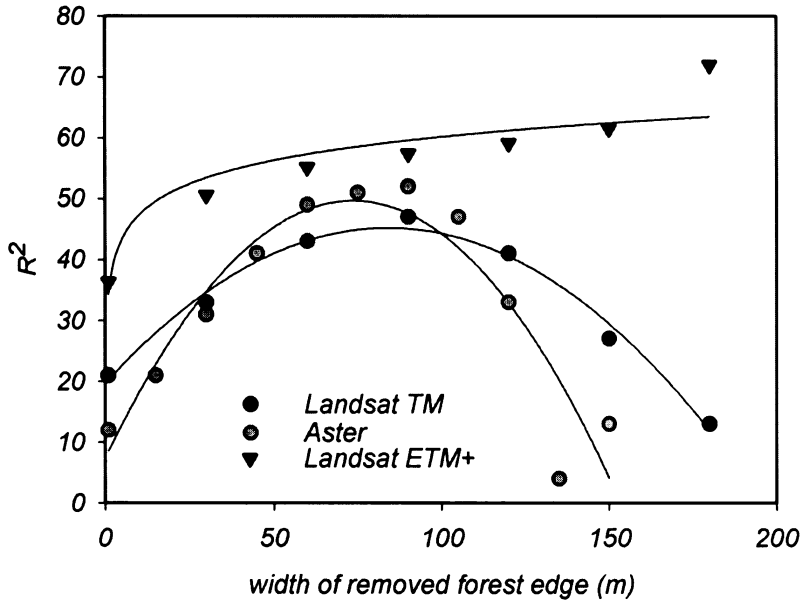

Figure 3. A - The dependence of the explained variability (R^2) on the proportion of forest pixels in the thermal pixel (1st model). B – The dependence of the explained variability (R^2) on the width of removed forest edge (3rd model).

2nd model: Weighting of thermal pixels by the forest content

This model was based on the same principle as the 1st model, but in this case all thermal pixels (polygons), which included at least one forest pixel, were used. The thermal pixels

have a different weight according to the proportion of forest pixels belonging to the thermal pixel (polygon). In this approach, the proportion of explained variation was lower in all three types of satellite data (Table 2).

Table 2. Comparison of explained variability of the models. R^2 is the explained variability, p is the probability value of statistical test

	R^2	F	p
Proportional content of forest in thermal pixel			
Landsat TM	0.49	244.9	0.0000
ASTER	0.48	120.6	0.0000
Landsat ETM+	0.47	1918	0.0000
Weighting of forest pixels by the forest content			
Landsat TM	0.32	447.4	0.0000
ASTER	0.23	525.7	0.0000
Landsat ETM+	0.39	2565	0.0000
Removal of forest edge			
Landsat TM	0.47	2398.6	0.0000
ASTER	0.52	470.7	0.0000
Landsat ETM+	0.57	1402.1	0.0000

3rd model: Removal of forest edge

This model is the most restricted in selecting thermal pixels for regression analysis. The buffer of forest edge zones was stepwise removed and the R^2 values were determined (figure 3B). Figure 3B shows the dependence of the R^2 values on the width of the removed buffer edge zones. In this model, we expected that the R^2 values would increase with the buffering of edge zones up to a certain point and then would be constant. In agreement with this assumption, the R^2 values increased with buffering of the forest edge zones in all three satellite data. However, the R^2 values decreased after reaching a peak value in the Landsat TM and ASTER data. Decreasing R^2 values, when forest edge zones were wider than 90 m, corresponds to the decreasing pixel numbers which were used for analyses. For model comparability the 90 m wide buffer edge zones were used for all three satellites,

although in the case of Landsat ETM+ the R^2 values increased with even wider buffer zones.

Table 2 shows that the highest R^2 values occur in the 3rd model. Therefore, this model was used for calculating the linear regression equations of all three types of satellite data:

ASTER

$$ST = 30.9 + 0.0055 \times HS - 0.0029 \times DEM \quad (7)$$

Landsat TM

$$ST = 25.4 + 0.0054 \times HS - 0.0047 \times DEM \quad (8)$$

Landsat ETM+

$$ST = 25.0 + 0.0101 \times HS - 0.0054 \times DEM \quad (9)$$

It is evident that all of these three equations show some similarities. Firstly, the relationship between ST (°C) and Hillshade (HS) values is directly proportional. This is in agreement with the assumption that the higher illumination of terrain causes the higher ST. Secondly, surface temperatures were lower at higher altitudes. This corresponds to a general trend of decreasing of temperature with increasing of altitude (Geiger, 1965; Yoshino, 1975; Geiger et al., 2003). However, this trend does not always hold true and depends on weather conditions.

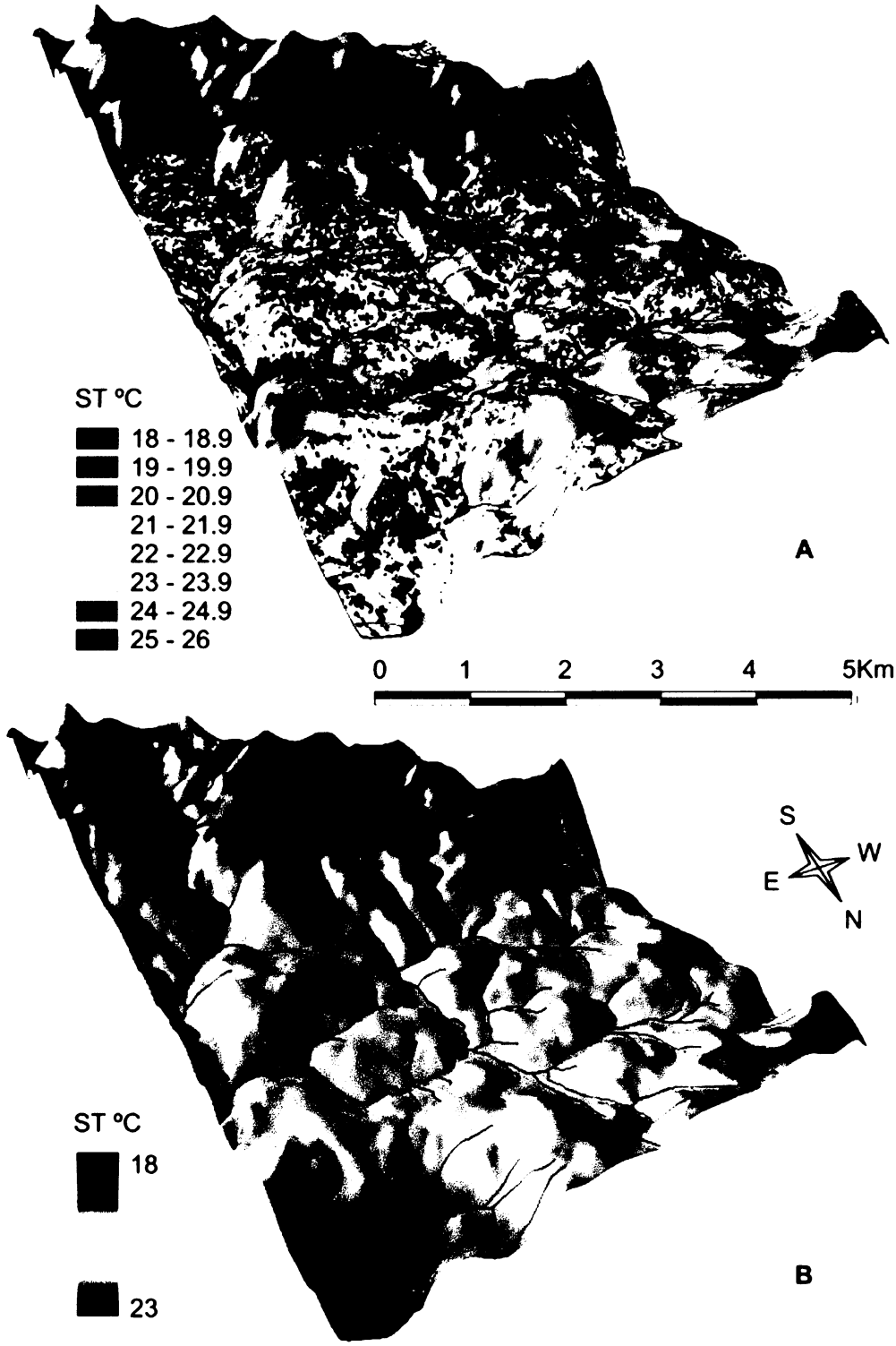

Figure 4. A – Surface temperature (ST) of spruce forest stands from Landsat 7 ETM+ (28 July 2002). Higher temperatures of the small forest areas and also of areas with lower altitude can clearly be seen. B – Estimated surface temperature according to formula 9 (above). The ST was extrapolated for the whole area.

4. Discussion

Thermal infrared remote sensing (TIR) is a unique tool for the assessment of many quantitative and qualitative characteristics of land cover. TIR data are used in many studies, for example, in providing measurements of surface thermal properties of geologic bedrock or land surface thermal energy fluxes for forest, agricultural, or other landscape attributes (Quattrochi & Luvall, 2004). Comparing thermal remote sensed data with different spatial and/or radiometric resolutions is important, because of evaluation of explaining variability of the data in landscape ecology studies. The relevance of such comparisons can be seen in connection with the construction of new thermal remote sensing systems, particularly The Landsat Data Continuity Mission (LDCM) (Byrnes, 2001; Irons & Ochs, 2004).

The ST modeling was implemented only for the spruce forest. For this reason, the problem with different emissivities of surface objects was almost eliminated (Price, 1989; Campbell, 2002). In addition, the emissivity value of green needle forest is near to 1 (Snyder et al., 1998). It was assumed that the spruce forest we investigated was a relatively homogenous land use/cover unit for several reasons. First, the age structure, treetop density and height of the trees should not be significantly different in the area of interest. If there is strong variation in the age structure of the forest stands, and therefore also in their height, the infrared and visible reflectance may be significantly influenced (Ahern et al., 1991). This increasing variability is a sign of older stands in many forest types and can be seen in optical imagery as the presence of increasing shadow (Lefsky & Cohen, 2003). This also could cause differences in surface temperature distribution of spruce forest. Second, the canopy cover should not be significant variable, because the changing canopy and background causes variability in reflectance (Lefsky & Cohen, 2003). Therefore, the very strict threshold by forest classification was used. This resulted in a relatively homogenous forest layer without mixed values (mixels). Nevertheless, local heterogeneities of forest stands could increase the rate of error in formula 6.

Assessment of the topography effect on surface temperature in the different approaches was used in order to improve the accuracy of the models. When we compared the models according to the explained variability, the 3rd model (Forest edge zones removal) gave the best results (table 2, figure 4 A, B), even though this model used the minimum number of thermal pixels of the models used in this study. There is a need to determine the threshold

of the minimal rate of thermal pixels for a given model. In this case, we used the 90 m threshold buffer edge zone width, because wider buffer zones caused a significant decrease in the number of thermal pixels. Therefore, the R^2 values beyond this threshold are considered to be unpredictable (figure 3B). The 1st model, based on the proportional content of forest in thermal pixel, results in similar R^2 values (0.47 – 0.49) as in the case of full forest content in thermal pixels. The assumption that the R^2 values will not increase after a certain value of forest content was not fulfilled. The 2nd model shows the lowest R^2 values, because of high number of non-forest pixels in the thermal polygons. This could be resolved by changing the linear weighting to nonlinear.

The highest R^2 value in the 3rd model was achieved with the Landsat ETM+, followed by ASTER and Landsat TM, respectively. Such results correspond with the spatial resolution of the thermal data. However, this holds true only for the 3rd model; in models 1 and 2, the regression of the ASTER data resulted in lower R^2 values than Landsat TM. A possible reason for this could be the smaller differentiation in surface temperature distribution, which is caused by small diurnal amplitudes of temperature and/or precipitation before satellite data acquisition (Humes et al., 2004). This thermal differentiation is smallest in the ASTER data, where the lapse rate is only 0.29 °C. The lapse rates are 0.47 and 0.54 per 100m in Landsat TM and ETM+, respectively. The above-mentioned lapse rate values correspond to the results of Yoshino (1975: 190), who stated that the values differ around 0.5 °C per 100 m because of the influence of water vapour, air temperature and pressure. The actual values of 0.51 and 0.54 per 100 m relate to 800-1000 mb and 10 °C. Generally, the lapse rate is smaller on the lower part of the slope or in low mountains, because of the high frequency of low-level inversion (for more discussion, see Yoshino, 1975).

In addition to the influence of elevation on temperature, relative slope position is also important as an additional potential explanatory variable (Geiger, 1965; Geiger et al., 2003). Wilson and Gallant (2000) noted that surface temperature is a function of latitude, slope, aspect, topographic shading, time of day and year. The influence of these topographic parameters is included in the Hillshade index (Pierce et al., 2005), which was used in this study. The assessed relation between Hillshade and ST was also confirmed.

The potential relevance of our study can be seen in thermal modeling of forest stand overstory. The temperature deviations from the models can indicate forest disturbances (e.g. harvesting, disease, insect attack). This method was applied to compare satellite and

modelled values of ST in the clear cut areas and decayed forest (Hais & Kučera, submitted for publication). Another application could be fire risk area idendification.

5. Conclusion

The influence of topography on surface temperature in spruce forest was confirmed in all types of satellite data. Surface temperature decreased with elevation and increased with higher values of insolation in all assessed satellite scenes (2002, 2003 and 2004). The highest accuracy in the relationship between topography and surface temperature was found when the edge zones of spruce forest were removed, due to their deviations in heat fluxes.

From the results, it follows that the spatial resolution of the thermal channels determines the accuracy of the models. However, the differences in the explained variability (R^2) among the used satellites are not great. It is likely that the adjacent important factors influencing the accuracy of thermal modeling are the size of segment land cover units and their homogeneity, and the influence of edge effect.

Acknowledgements

We are grateful to three anonymous referees for their valuable comments. We thank also to Dr. Rolf Richter for sending of atmospheric correction references; Sarah Wexler and Keith Edwards for language improvement. M.H. was supported by the Institutional research project MSM 6007665806. T.K. was supported by the Institutional research project AV0Z60870520.

References

Ahern, F. J., Erdle, T., Maclean, D. A., Kneppeck, I.D., 1991, Aquantitative relationship between forest growth rates and Thematic Mapper reflectance measurements. *International Journal of Remote Sensing*. 12, pp. 387 - 400

Asrar, G., 1989, Theory and applications of optical remote sensing. A Wiley-Interscience Publications. New York. pp. 743

Bailey R. G., 1996, Ecosystem geography. Springer, New York etc. pp. 1 - 204

Bellasio, R., Maffeis, G., Scire, J. S., Londoni, M.G., Bianconi, R., Quaranta, N., 2005, Algorithms to account for topographic shading effect and surface temperature dependence on terrain elevation in diagnostic meteorological models. *Boundary-Layer Meteorology*. Springer. 114, pp. 595–614

Byrnes, R. A., 2001, Executive summary, Landsat Data Continuity Mission Workshop. *Photogrammetric Engineering & Remote Sensing*. pp. 543 – 544.

Campbell, J.B., 2002, Introduction to Remote Sensing - third edition. Taylor and Francis, London.

Dash, P., Göttsche, F. M., Olesen, F. S., Fischer, H., 2002, Land surface temperature and emissivity estimation from passive sensor data: theory and practice–current trends. *International Journal of Remote Sensing*, 23, pp. 2563–2594

ERSDAC, 2005. ASTER Users Guide, Part 1 General, Version 4, http://www.science.aster.ersdac.or.jp/en/documnts/users_guide/part1/pdf/Part1_4E.pdf, last accessed, August, 2007.

ESRI, ARC/Info 7. 1994, Environmental Systems. Research Institute Inc, Redlands, CA, USA.

Geiger, R., 1965, The climate near the ground. Harvard Univ. Press, Harvard. pp. 611

Geiger, R., Aron, R. H., Todhunter, P., 2003, The climate near the ground. Sixth edition. Rowman & Littlefield Publishers, Inc., Langham etc. pp. 584

Geomatica Algorithm Reference, 2003, PCI Geomatics.50 West Wilmot Street, Richmond Hill,Ontario, Canada,L4B 1M5

Gillespie, A., Rokugawa, S., Matsunaga, T., Cothern, J. S., Hook, S., & Kahle, A. B. 1998, A temperature and emissivity separation algorithm for advanced spaceborne thermal emission and reflection radiometer (ASTER) images. *IEEE Transactions on Geoscience and Remote Sensing*, 36, 1113−1126

Hais, M., 2004, Influence of Drainage on Landscape Functioning in Sumava National Park. In.: Hermann A. (ed.) Extended Abstract – International conference on Hydrology of Mountains Environments. Berchtesgaden, Federal Republic of Germany, 27 September – 1 october 2004. pp. 125

Hais, M., Kučera, T., Submitted for publication, Surface temperature change of spruce forest as a result of bark beetle attack: Remote sensing and GIS approach. *European Journal of Forest Research*.

Hojdová, M., Hais, M., Pokorný, J., 2005, Microclimate of a peat bog and of the forest in different states of damage in the Natioanl Park Šumava. Silva Gabreta, 11, pp. 13 – 24

Humes, K., Hardy, R., Kustas, W, P., Prueger, J., Starks, P., 2004, Estimating environmental variables using thermal remote sensing, in *Thermal Remote Sensing in Land Surface Processes,* J. Luvall and D. Quattrochi, (Eds) CRC Press, pp. 110 – 132

Hutchinson, M. F., 1993, Development of a continent-wide DEM with applications to terrain and climate analysis. In *Environmental Modeling with GIS*, Ed. M. F. Goodchild et al., New York: Oxford University Press pp. 392–399

Irons, J. R., Ochs, W. R., 2004, Status of the Landsat Data Continuity Mission. *Geoscience and Remote Sensing Symposium*. 20-24 Sept. 2004, 2, pp. 1183 – 1185

Jensen, J. R., 2000, Remote Sensing of the Environment: An Earth Resource Perspective, Upper Saddle River: Prentice-Hall, pp. 544

Kang, S., Lee, D., Kimball, J. S., 2004, The effects of spatial aggregation of complex topography on hydroecological process simulations within a rugged forest landscape: development and application of a satellite-based topoclimatic model. *Canadian Journal of Forest Research*, 34, pp. 519-530

Kahle, A. B., Alley, R. E., 1992, Separation of temperature and emittance in remotely sensed radiance measurement. *Remote Sensing of Environment*. 42, pp. 107-11

Klassen, W., van Breugel, P. B., Moors, E. J., Nieveen, J. P., 2002, Increased heat fluxes near a forest edge. *Theoretical and Applied Climatology*, 72, pp. 231 – 243

Lefsky, M. A., and Cohen, W. B., 2003, Selection of remotely sensed data. In *Remote Sensing of Forest Environments: Concepts and Case Studies*. Wulder and Franklin, (Eds) Dordnecht, Kluwer Academic Publishers, pp. 13-46.

Liang, S., 2001, An Optimization Algorithm for Separating Land Surface Temperature and Emissivity from Multispectral Thermal Infrared Imagery. IEEE Transactions on Geoscience and Repote Sensing. 39, pp. 264-274

Lillesand, T. M., Kiefer, R. W., Chipman, J. W., 2004, Remote Sensing and Image Interpretation. John Wiley and Sons. New York, pp. 763

Lookingbill, T. R., Urban, D. L., 2003, Spatial estimation of air temperature differences for landscape-scale studies in montane environments. *Agricultural and Forest Meteorology* 114, pp.141–151

McCune, B., Keon, D., 2002, Equations for potential annual direct incident radiation and heat load. *Journal of Vegetation Science,* 13, pp. 603-606

Pierce, K. B., jun., Lookingbill, T., Urban D., 2005, A simple method for estimating potential relative radiation (PRR) for landscape-scale vegetation analysis. *Landscape Ecology,* 20, pp.137–147.

Price, J. C., 1989, Quantitative aspects of remote sensing in the thermal infrared. In *Theory and Applications of Optical Remote Sensing*, Ed. Asrar, G., pp. 578–603.

Quattrochi, D. A., Luvall, J. C., 1999, Thermal infrared remote sensing for analysis of landscape ecological processes: methods and applications. *Landscape Ecology,* 14, pp. 577–598

Quattrochi, D. A., Luvall, J. C., 2004, Introduction, in *Thermal Remote Sensing in Land Surface Processes,* J. Luvall and D. Quattrochi, (Eds) CRC Press, pp. 1-8

Richter, R., 1990, A fast atmospheric correction algorithm applied to Landsat TM images. *International Journal of Remote Sensing*, 11, pp. 159-166.

Richter, R., Coll, C., 2002, Band-resampling effects for the retrieval of surface emissivity. *Applied optics*, 18, pp. 3523-3529.

Strnad, E., 2003, Climate of Šumava, In *Šumava, Nature, History*, Life, (in czech) pp. 35 – 44

Snyder, W.C., Wan Z., Zhang, Y., Feng, Y.Z., 1998, Classification-based emissivity for land surface temperature, measurement from space. *International Journal of Remote Sensing*, 19, pp. 2753-2774

Yoshino M. M., 1975, Climate in a small area. An introduction to local meteorology. Univ. Tokyo Press, Tokyo, pp. 547

Wilson, J.P., Gallant, J.C., 2000, Secondary topographic attributes. In *Terrain Analysis: Principle and Applications*. Wilson J.P. and Gallant J.C. (Eds), pp. 97–132 (New York :John Wiley).

Kapitola 4

Surface temperature change of spruce forest as a result of bark beetle attack: Remote sensing and GIS approach

Hais M, Kučera T.

Abstract

In the 1990s, a bark beetle (*Ips typographus*) infection caused the decay of spruce forest (*Picea abies*) in the central part of the Šumava Mountains, the Czech Republic, bordering the Bavarian Forest National Park, Germany, where the bark beetle infection started in the late 1980s. Some areas were left without human intervention and, consequently, the trees around these areas were removed in order to stop further bark beetle outbreak. The objective of our study was the assessment of surface temperature (ST) change in spruce forest decayed under bark beetle and following clear-cutting. The change detection of ST is based on the comparison of modelled values and thermal satellite data. For this purpose, Landsat scenes from July 11th, 1987 and July 28th, 2002 were used. The models describe the dependence of ST of living spruce forest on topography. The topography effect is based on the Altitude and Hillshade index, which expresses the influence of Aspect and Slope on the relief insolation. Then the modelled ST values were extrapolated for decayed spruce forest and clear-cut areas. In order to increase model accuracy, the forest edge zones (90 m wide) were removed because of their different energy balance; then explained variability value (R^2) increased from 0.37 to 0.55. The results of comparing modelled values with satellite ST in the decayed spruce forest and clear-cut areas show an average increase of ST by 5.2 °C and 3.5 °C, respectively. The thermal satellite data from 1987 were used for model validation. This showed that the accuracy of ST modelling using topography was sufficient, because the difference between the modelled ST with and without decayed spruce forest and clear-cut areas was at most only 0.4 °C.

Key words: surface temperature, Landsat, spruce forest, topography

1. Introduction

Since the 1990s, Norway spruce (*Picea abies* (L.) Karst.) stands were attacked by bark beetle (*Ips typographus*) in the Šumava Mountains (Czech Republic); this outbreak originated in the neighbouring Bavarian Forest (Germany) (Heurich et al., 2001; Skuhravý, 2002). Two different approaches were applied to the attacked forests in the Šumava National Park: (1) a small portion of the stands in the core zone of the national park was left without intervention, relying upon natural regeneration, and (2) traditional technical measures were adopted, in which attacked trees were felled and removed (Jonášová & Prach, 2004). Jonášová and Prach (2004) found that there was a good regeneration of spruce under the dead canopy of the stands left without intervention, while the numbers of spruce were significantly lower in clear-cut areas. The mentioned areas differ also in microclimatological conditions. From field measurements, the maximum daily temperature amplitude of clear-cut areas, decayed spruce stands and living stands in 2002 were: 27.9 °C, 21.7°C and 17.9 °C, respectively (Hojdová et al., 2005). In our study, we compared the surface temperature (ST) of these same stands.

The use of satellite thermal channels to detect increasing ST as a result of bark beetle attack is also described by Hais (2006). Nevertheless this study was based on the temporal comparison of relative temperature classes, which is not able to quantify changes.

Land surface temperature (LST), which is controlled by the (1) surface energy balance, (2) atmospheric state, (3) thermal properties of the surface, and (4) subsurface media, is an important factor controlling most physical, chemical, and biological processes of the Earth (Becker and Li, 1990; Campbell, 2002).

One of the most important factors influencing surface energy balance is topography (Geiger, 1965; Yoshino, 1975; Geiger et al., 2003). General factors of local relief are altitude, latitude, and aspect of slope, which are commonly measured in field studies. The general influence of Altitude can be expressed as an average temperature drop of about 6.4 °C per 1000 m, but it differs by region (Bailey, 1996). Slope and aspect influence potential radiation and heat load. They are commonly computed in ecological studies (McCune & Keon, 2002), mostly based on digital elevation models (DEM) (Pierce et al., 2005).

Atmospheric state is another factor controlling surface temperature, especially wind, precipitation and cloudiness (Campbell & Norman, 1998). Because of the very complicated influence of wind and decreasing differentiation of ST due to precipitation and

cloudiness, we used terms of stable weather conditions, with negligible wind and without precipitation and cloudiness. General climatological characteristics, such as annual mean temperature, annual precipitation, temperature minimum in January, and temperature maximum in July, cover the macroclimatological effects of latitude.

The thermal properties of the surface and subsurface media are influenced mostly by the albedo, thermal capacity and conductivity (Campbell, 1977). In the case of vegetation, ST is also very important for the ability of vegetation to convert incoming solar radiation to energy for transpiration (Schulze et al., 2005). The physical principle is the change in the proportion of sun radiance reflection, evapotranspiration and sensible heat (Gates, 2003; Pokorný, 2001). Removing vegetation cover may result in increasing surface temperatures (Shin & Lee, 2005; Hais, 2006). Such changes could have consequences for the microclimate and energy balance of the area (Ripl, 1992; Ripl et al., 1994). Furthermore, the ST variability is influenced by the heterogeneity of the land use/cover unit. In the case of forest stands, this means the variability in age structure, treetop density and height of the trees. If there would be strong variance in the age structure of the forest stands, and therefore also in their height, the infrared and visible reflectance would be significantly influenced (Ahern et al., 1991). This could result in differences in the surface temperature distribution within a spruce forest. Therefore, forest stands with low density and edge zones were not used for ST modelling in this study.

The objective of the present study was to assess ST changes due to spruce forest decay and clear-cutting as a consequence of bark beetle attacks. We supposed that ST values will increase in both mentioned areas. Comparing changes in ST values between both areas was also an important aim of the study. For such a temperature comparison, it is important to take into account the factors controlling ST values. Because of the complex topography in the Šumava Mountains, we modelled the influence of this factor on ST values. Temperature changes due to forest clear-cutting (Yoshino, 1975; Hashimoto & Suzuki 2004) and/or by stress from bark beetle attacks (Weber, 1971; Schmid, 1976) has already been described by many authors. Nevertheless, this study is unique, because of the use of satellite data and topography normalisation.

2. Material and methods

2.1 Study site

The area of interest includes the central part of the Šumava National Park, which is located in the south-west of the Czech Republic. The southern part of the area of interest stretches into the Bavarian Forest National Park, Germany. The area partly includes localities where the mountain spruce forest has been affected by a bark beetle epidemic with the adjacent surroundings. Spruce forest stands were mostly damaged during the 1990s. Forest losses in the Šumava National Park and the Bavarian Forest National Park reached more than 5000 ha in the form of damaged spruce groves and more than 1420 ha in the form of cuttings (Skuhravý, 2002).

With the exception of spruce forest, the area is mostly covered by peat (Rokytská, Rybárenská, Roklanská mires and others) and mountain grasslands. The relief of the central Šumava is created by a peneplain with numerous local hills. The average altitude of the complex relief is 1093 m. Velká Mokrůvka (1370 m) and Špičník (1351 m) are the highest peaks in the Czech part, while the German area is dominated by Lusen (1373 m) and Grosser Rachel (1453 m). The lowest positions in the area of interest have an altitude of about 700 m (right upper and left lower corners in Figure 1 A, D. The high percentage of peat and wetland areas results from relatively high precipitation, especially in the Luzenske valley (1500 mm annually) (Strnad, 2003). There were efforts to drain the area in the past and transform it into spruce monoculture forests (Hais, 2004).

2.2 Satellite scenes and their calibration

The spruce forest thematic layer (TM/ETM+ channels: 2, 3, 4, 5, 7) and surface temperature (TM/ETM+ channel: 6) values were the main data inputs. These data were obtained by processing Landsat 5 TM and Landsat 7 ETM+ scenes acquired on July 11th, 1987 and July 28th, 2002, respectively. The spatial resolution of the Landsat satellite system is 30 m (except for thermal bands - see below). The data were obtained at 10:38 AM. The orbit for each Landsat satellite results in a 16-day repeat cycle (Jensen, 2000; Campbell, 2002; Lillesand et al., 2004). The covering of an area by a regular grid of values without the need for interpolation is a great advantage of this type of data. Ancillary meteorological data from the Czech Hydrometeorological Institute were used to describe the meteorological conditions starting 10 days before satellite data acquisition. The nearest

meteorological station is located on the summit of Churanov Hill (approx. 25 km north-east of the centre of the study area). The following data were used from this station: mean daily temperature, air pressure, and actual weather conditions. It is evident from these data that anticyclonic weather, almost without precipitation, preceded both obtained Landsat scenes. Nevertheless, mean daily temperature and air pressure values were higher on July 28th, 2002 than July 11th, 1987. The satellite scenes were rectified into the S-JTSK coordinate system according to the orthorectified Satellite map of the Czech Republic (2002 ArcData Praha, s.r.o.). To enhance the geometrical accuracy in central Šumava, an existing grid of ground control points was completed by points taken from aerial orthophotomaps provided by the Šumava National Park administration for the purposes of the project. Data were resampled by applying the nearest neighbour method to preserve the original radiometric values for subsequent data processing.

2.3 Spruce forest classification

The spruce forest thematic layers for both scenes were obtained by a supervised classification method (Campbell, 2002; Lillesand et al., 2004). The threshold of the classification was chosen so that the resulting mask did not contain any mixels. Mixel values originated from mixed radiometric information of other surfaces (rocks, water, deciduous trees...). Therefore, the area of the spruce forest thematic mask is smaller than in reality. However, there is a higher probability that the thematic mask covers only the spruce forest. Because of land use/cover changes between 1987 and 2002, classification of spruce forest had to be done for both scenes. Because the forest edges form a microclimatically transitional zone to non-forest ecosystems, they exhibit different surface temperatures (Geiger, 1965; Klaassen et al., 2002). Those edge zones, 90 m wide, were removed during the following procedure. Forests with minimal areas (smaller than 5 pixels) were also removed. Therefore, the area of used forest mask was smaller than the original forest layer. Only the thermal values under this mask were used for the ST modelling.

2.4 Surface temperature

The 6th thermal channel of Landsat 5 TM and Landsat 7 ETM+ was used to calculate the surface temperature. This channel contains records in the electromagnetic radiation interval of 10.4 – 12.5μm. The spatial resolution of the 6th channel of Landsat 5 TM and

Landsat 7 ETM+ is 120 x 120 m and 60 x 60 m, respectively (Campbell 2002, Lillesand et al. 2004). The ETM+ data were resampled to 30 m for unification of the spatial resolution in both scenes. DN (digital number) values were transformed to temperature values by applying ATCOR2_T (Geomatica Algorithm Reference, 2003). Additional data were required for the surface temperature equation using ATCOR2_T (Richter, 1990). For better results, the RED, NIR and SWIR bands were specified. Other calibration parameters were: average elevation, solar zenith angle, ground visibility and date of scene acquisition. The solar zenith angle for both scenes was calculated using SunAngle software (http://susdesign.com/sunangle/). Ground visibility values were obtained from the Czech Hydrometeorological Institute.

2.5 DEM and georelief parameters

A digital elevation model (DEM) was calculated to evaluate the influence of Altitude (Hutchinson, 1993). On the basis of the DEM, two parameters (Slope and Aspect) were calculated using a spatial analyst tool (ArcGIS) (Burrough and McDonell, 1998). Both Aspect and Slope are included in the parameter Hillshade, which was calculated on the basis of the DEM (ESRI, 1994; Pierce et al., 2005):

$$\text{Hillshade} = 255\,[\cos(90 - Z)\sin(s)\cos(\alpha - A) + \sin(90 - Z)\cos(s)] \qquad (1)$$

where Z is the solar zenith, s is the local slope, A is the solar azimuth and α is the azimuth of the slope facet. The solar zenith and solar azimuth were calculated using the SunAngle software. The Hillshade function gives the hypothetical insolation of a surface by determining insolation values for each cell in a raster. Individual Hillshade values should be calculated for each date, because of the different dates of satellite data acquisition. Lastly, the dependence of surface temperature on the DEM and Hillshade was calculated by regression analysis.

2.6 Matrix analysis

Next, we explored the dependence of surface temperature on the relief parameters. The resulting regression models of surface temperature were compared with the satellite temperature data, using matrix analysis. This analysis creates a coincidence (intersection) matrix for the classes of two images and an image of the coincidence values (Geomatica

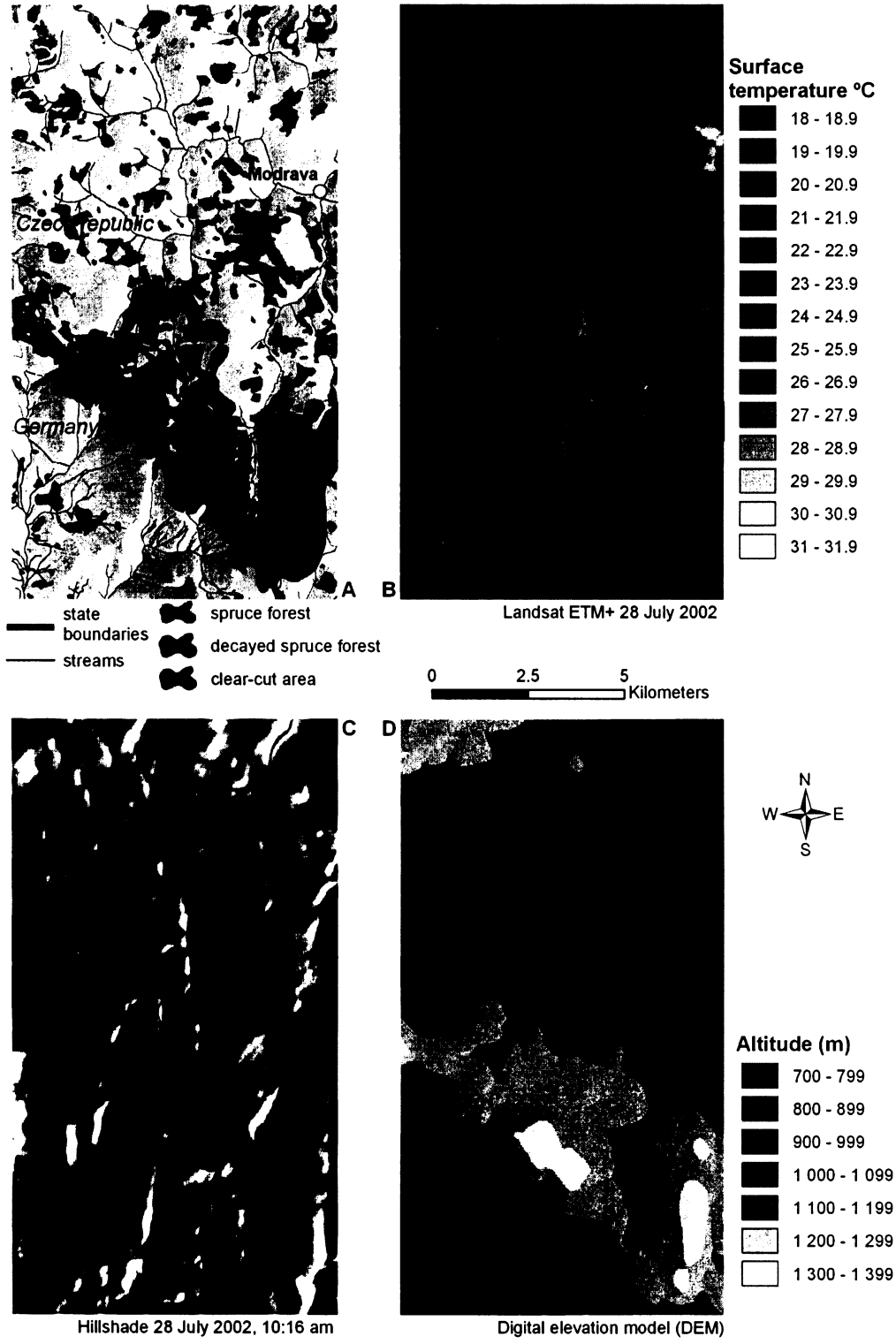

Fig. 1 A- the area of interest: Central part of the Šumava Mountains with marked clear-cut areas and decayed forest in 2002. B – ST from Landsat ETM+ on July 28th, 2002. C- Hillshade, which was estimated based on the actual Sun position of the satellite data acquisition. D – Main intervals of DEM.

Algorithm Reference, 2003). A cell in the (i)th column and (j)th row in the matrix represents the overlap of class i from image 1 and class j from image 2.
The value of the cell in the coincidence matrix is the rate (percentage) of overlap of the matched classes in the whole area (spruce forest).

3. Results

ST change detection in clear-cut areas and decayed forest in 2002

Before detecting the change of ST in the study areas, it was important to describe the influence of topography (Hillshade and Altitude) on ST. A multiple regression was used for this purpose:

$$ST = a + b*Hillshade + c*DEM \quad (2)$$

where ST is surface temperature in °C, which was estimated from the thermal channel, Hillshade is expressed in an 8-bit scale as a spaceless value, and DEM represents the Altitude in metres. The relation was used for ST modelling only of the healthy spruce stands. The resulting regression for July 28th, 2002 was:

$$ST = 24.97 + 0.01013*Hillshade - 0.00538*DEM \quad (3)$$

From the formula, it follows that ST decreases with Altitude (DEM) and increases with Hillshade (insolation) values. Using formula (3), ST was extrapolated for decayed stands and clear-cut areas. The resulting explained variability (R^2) of this model was 0.57. Then we subtracted the modelled ST values from the ST of the thermal channel. The mean difference of the resulting ST model (3) for living spruce forest (2002) from the thermal channel values was 0.004 °C (STD 0.5). The mean increase of ST was 5.2 °C (STD 1.2) in clear-cut areas, while the increase was significantly lower in the decayed stands (3.5 °C, 1.1 STD). The whole scheme of the task sequence is described in Figure 2. The resulting comparison of ST between decayed stands and clear-cut areas is shown in Figure 3 and 4A,B.

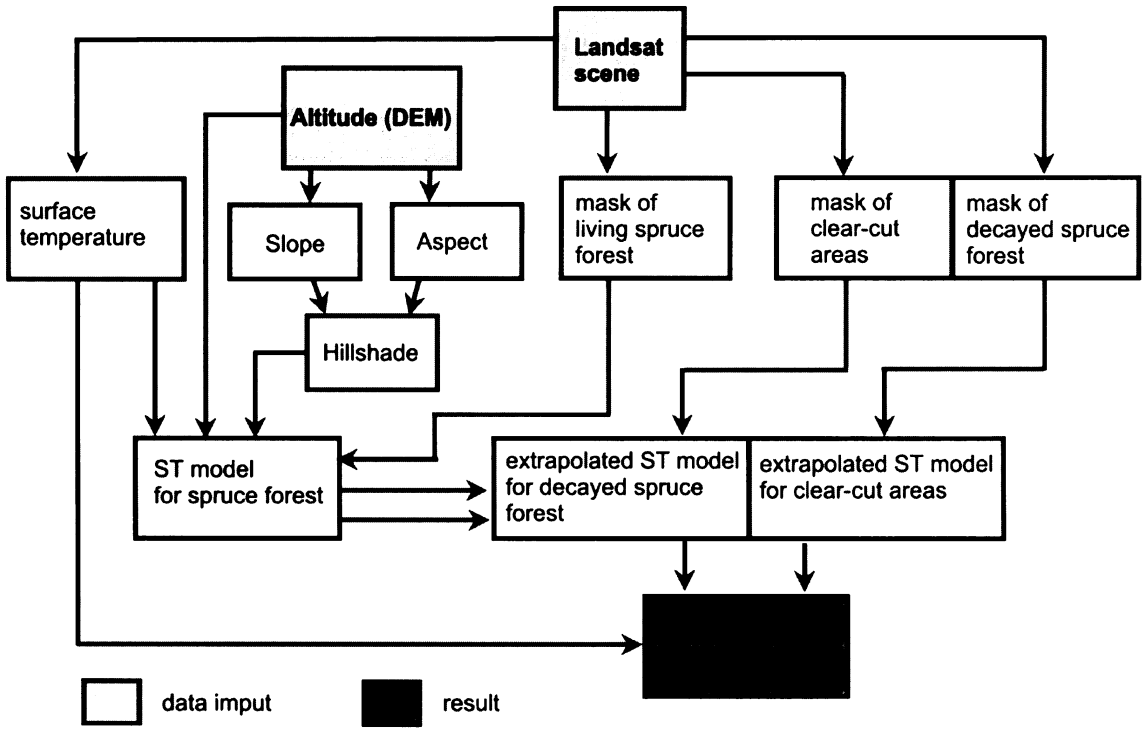

Fig. 2 The scheme of change detection of ST in a clear-cut area and decayed forest in comparison with modelled ST values for a living spruce forest in 2002.

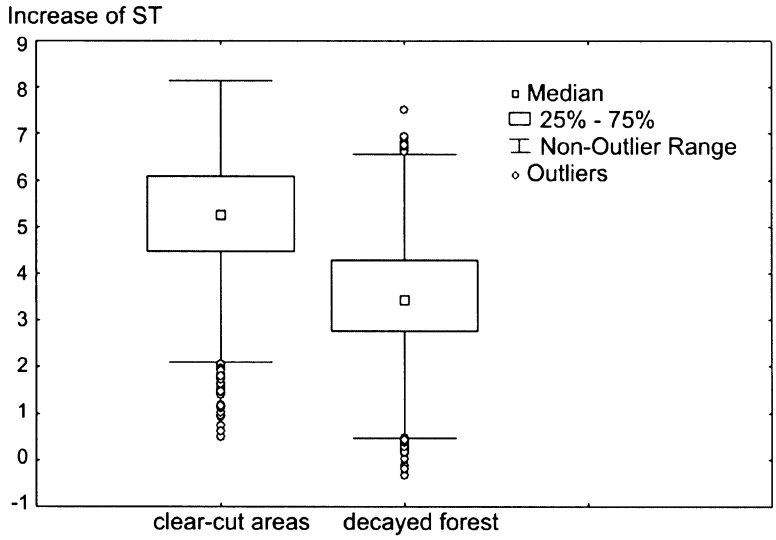

Fig. 3 Differences between the modelled and thermal channel ST values. The higher value means an increase of ST in the given type of area. Thus, the ST of a clear-cut area shows a higher ST than in decayed forest.

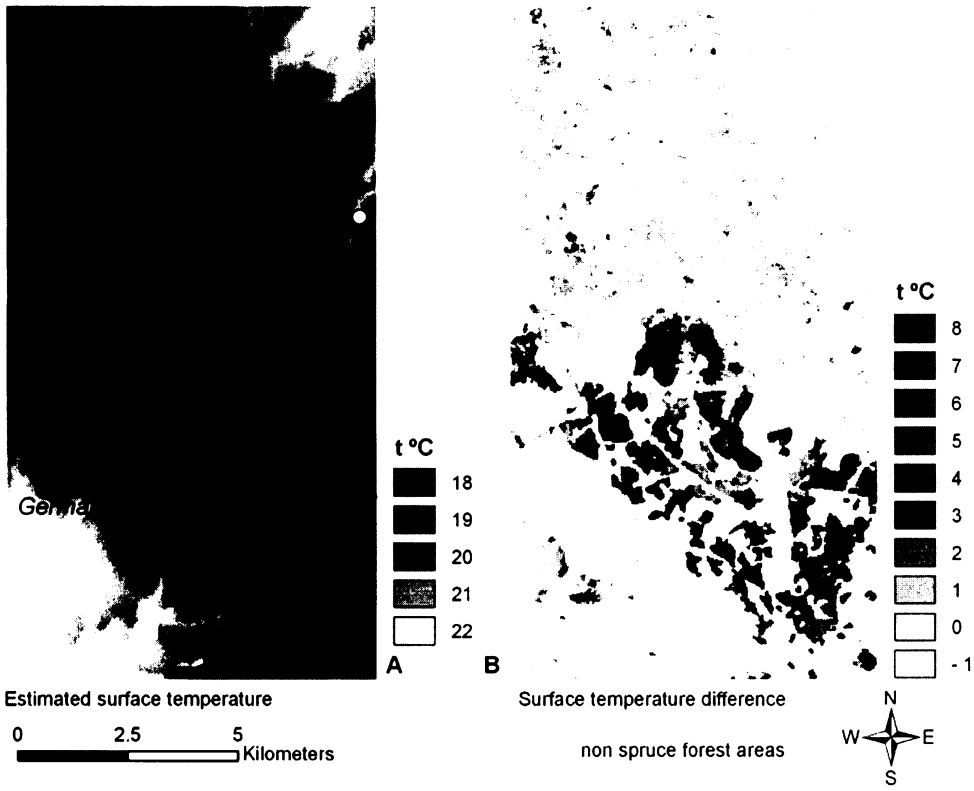

Fig. 4 A – the ST modelled according to formula (3). B – the differences of ST between the clear-cut area and decayed forest in 2002. It is possible to distinguish the increase in ST values in the clear-cut area and decayed forest as distinct from living spruce forest.

Matrix analysis

The estimated surface temperature values from model 3 were compared with the Landsat data from 2002 using matrix analysis. Overlap of the same temperature classes represents 61.5 %, while a maximum difference of 1 °C represented 99.6 %, of the spruce forest area.

Validation of ST model (2002) using the thermal channel from 1987

For validation purposes, the same method of ST modelling was implemented using the thermal satellite data acquired before the bark beetle outbreak (1987). Two regression ST models were calculated also only for spruce forest. In the first model (4), we excluded the area that was subsequently affected by bark beetle outbreak (decay stands and clear-cut areas):

ST = 18.81 + 0.01521*Hillshade –0.00453*DEM (4)

The second ST model included all spruce forest stands:

ST = 19.27 + 0.01711*Hillshade –0.00536*DEM (5)

Both ST models 4 and 5 were compared (Table 1). The reason of such a comparison was to discover if the area affected by bark beetle outbreak significantly changed the slopes of Hillshade and DEM in the model 4. The differences between the models and ST from the thermal channel (July 11th, 1987) were calculated (Fig. 5B,C). Finally, these differences were mutually compared (Fig. 5D). From figure 5D it follows that the difference in deviations of both models is lower than 0.4 °C.

Table 1 Results of the dependence of ST on topography.

Model (regression)	Spruce forest mask	date	R	R^2	p
3	Without decayed stands and clear-cut areas in 2002	28.7.2002	0.76	0.57	>0.001
4	Without decayed stands and clear-cut areas in 2002	11.7.1987	0.70	0.49	>0.001
5	All spruce forest	11.7.1987	0.81	0.66	>0.001

4. Discussion

Thermal infrared (TIR) remote sensing data are widely used in research related to the analysis and modelling of land surface energy fluxes and land surface processes (Quattrochi and Luval, 2000). In the present work, we used surface temperature (ST) as an indicator of quantitative (clear cutting) and/or qualitative (health state) changes of spruce forest due to bark beetle attack. An assessment of the influence of different altitude and insolation was needed for such a comparison. The use of a digital elevation model (DEM) and ST from Landsat TM/ETM+ satellites allowed us to calculate lapse rates values. The resulting lapse rates (5.4 °C/km, 4.5 °C/km, 5.4 °C/km) of models 3,4,5 are similar to the mean lapse rate (4.5 °C/km) in montane environments (Lookingbill & Urban, 2003) and/or

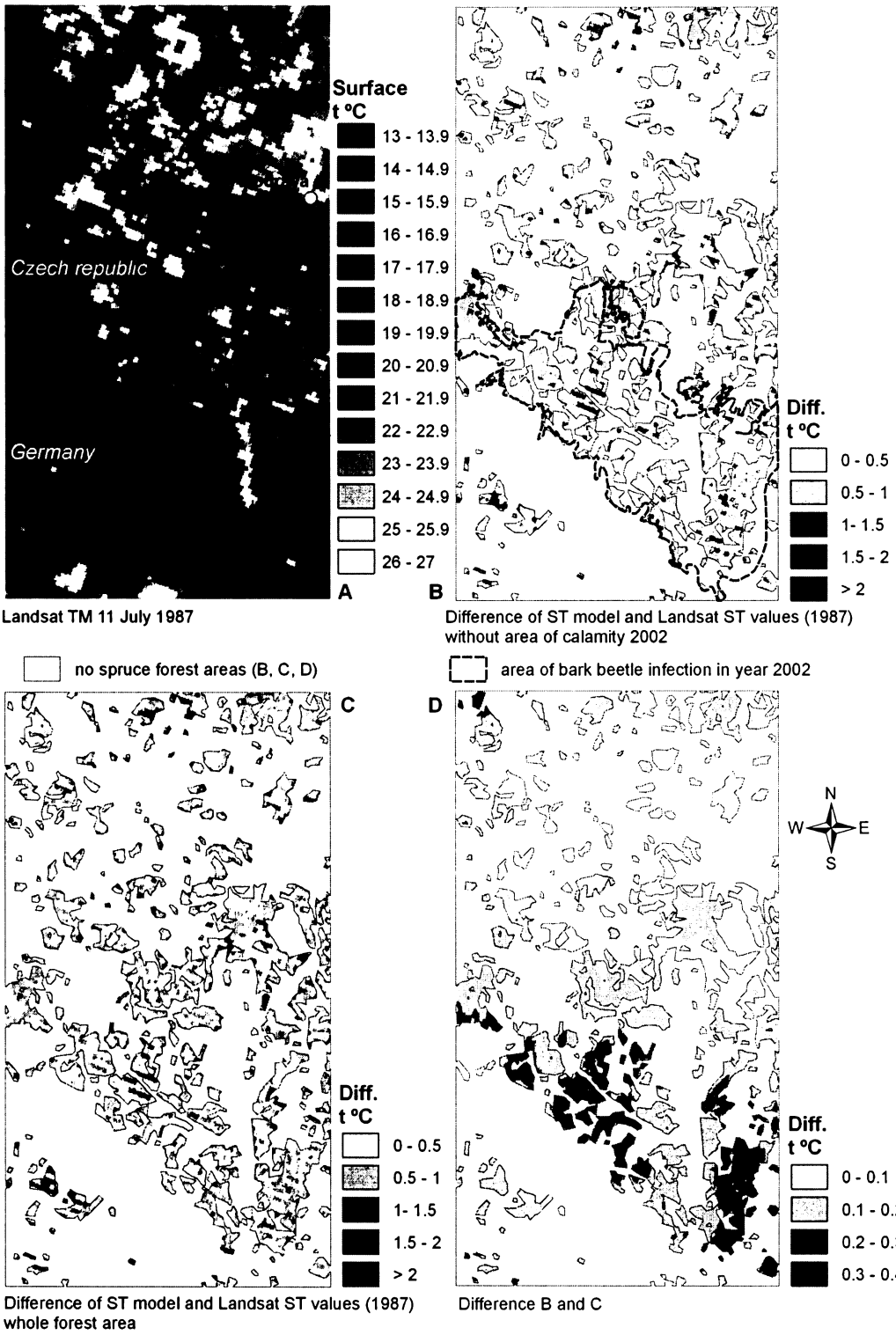

Fig. 5 A – ST from Landsat EM on July 11th, 1987. B - difference of ST between values of the Landsat thermal channel (July 11th, 1987) and modelled values; areas affected by bark beetle in 2002 were excluded. C – the same difference as in B. Nevertheless the ST model was estimated using the whole spruce forest mask. D there is a comparison of results B and C.

the generic environmental lapse rate (6.5 °C/km) (Bailey, 1996). It is noteworthy that when we used areas without the bark beetle infestation, the lapse values were the same (5.4 °C/km) in both terms (July 28th, 2002 and July 11th, 1987). On the contrary, when all spruce forests were used (model 5), the lapse rate was lower (4.5 °C/km). This is probably caused by the fact that the bark beetle infested areas comprised most of the areas at higher altitudes, where the summit effect is present (Barry, 1992). Nevertheless, the comparison of ST models 4 and 5 differed by at most only 0.4 °C.

The effect of Hillshade (insolation) on the ST values was different in both terms.

Although the value was close to 0.010 (model 3) in 2002, in 1987 the Hillshade slope was nearly 0.015 (4), and 0.017 (5). We assume that the main reason for the different influence of Hillshade on surface temperatures results from the different meteorological conditions. The higher value of the Hillshade slope in 1987 is probably caused by a relatively higher diurnal temperature amplitude two days before satellite data acquisition (Fig. 6). This higher amplitude was caused by two cooler nights immediately before satellite data acquisition: the daily maxima, minima and amplitudes correspond to a higher importance of the Hillshade index in 1987. This is correlated with a lower morning temperature minimum on the day of data acquisition and the day before that, and an afternoon maximum 2 days before (Fig. 6). The temperature change between the second and third days before data acquisition also show the time-lag of heat accumulation. This is in agreement with increasing thermal diurnal amplitude, which emphasises the influence of relief on surface temperature distribution. Furthermore, the values of the Hillshade slope differ in equations (3) and (4,5) due to differences in solar zenith and azimuth. However, the influence of these factors should be very small, because July 11th and 28th are only 17 days apart and the difference between the solar zenith and azimuth angle are 2.63 and 2.62 degrees, respectively.

The influence of relief on surface temperatures may be affected by the heterogeneity of vegetation cover. There is a whole range of such heterogeneity sources when working with the forest growth surface. Different tree height is the first source, because it causes local shadows; this effect is greater when the Sun is closer to the horizon. Bosveld et al. (1999) described a definite effect of shading on the observed radiation temperatures, relating the line of sight of the instrument to the solar angle.

Different tree overstory density can be another source of heterogeneity. Cohen and Spies (1992) concluded that tree size and overstory density of conifer forest were well correlated with a number of spectral indices, with R^2 values of 0.78–0.86. Normalized

Difference Vegetation Index (NDVI) is one of the most frequently used spectral indices (Tucker, 1979). Waring and Running (1998) describe the relation between NDVI and surface temperature of forest canopy, where surface temperature decreased with NDVI values. The influence of tree height and overstory density is partly eliminated in similar-aged monocultures, which is the case in the larger part of the area of interest.

Edge effect is another cause of heterogeneity; higher surface temperatures can be expected at forest edges during clear weather in summer (Geiger et al., 2003). Small patches of forest, where the whole growth is formed by edges, can be designated as a special type of edge effect. The influence of those edge zones was eliminated by their filtering, further increasing the predictive ability of the model.

Inaccuracies in data collection and processing will also influence the results. The DEM in this study was created on the basis of contour lines (in the scale 1:25 000), valley lines and a point vector layer of tops. However, inaccuracy of the contour lines layer is a smaller source of error than the limited spatial resolution (60 or 120 m, respectively). This limited resolution can lead to mistakes, because the pixel value is calculated as an average of individual values in the pixel area. If the resulting value is an average of values with extensive variance, then this would be labelled as a mixel (Lillesand et al., 2004). However, the influence of mixels at edges has been eliminated by the filtering of the buffer zones. Differences in moisture levels, caused by local differences in precipitation, and also microclimatic deviations, such as frost pockets, could be natural sources of heterogeneity.

In spite of all of the mentioned causes of inaccuracies, the resulting models were able to describe a large part of the variability of the forest surface temperatures. After computing the models based on the influence of topography on ST, it was possible to compare the ST of areas with different topography.

The resulting mean increase of ST in the clear-cut areas (by 5.2 °C) and decayed spruce forest (by 3.5 °C) corresponds with field measurements of temperature in the same area in 2002 (Hojdová et al., 2005). There can be several reasons for the higher ST in clear-cut areas compared to decayed spruce forest. We suppose the main reason is the higher reflectance of dead trees, in particular without bark, in the decayed forest. The higher reflectance causes a lower absorption of radiance (Jensen, 2000). Furthermore, lying and standing dead trees result in a more complicated microrelief with many shaded places (Siitonen et al., 2000; Zielonka & Piatek, 2004). The second reason is the expected difference of evapotranspiration in both types of areas. The higher density of vegetation in the decayed forest may result in higher transpiration. The sparse vegetation of

Calamagrostis sp. in the clear-cut areas does not effectively protect the soil from drying and overheating.

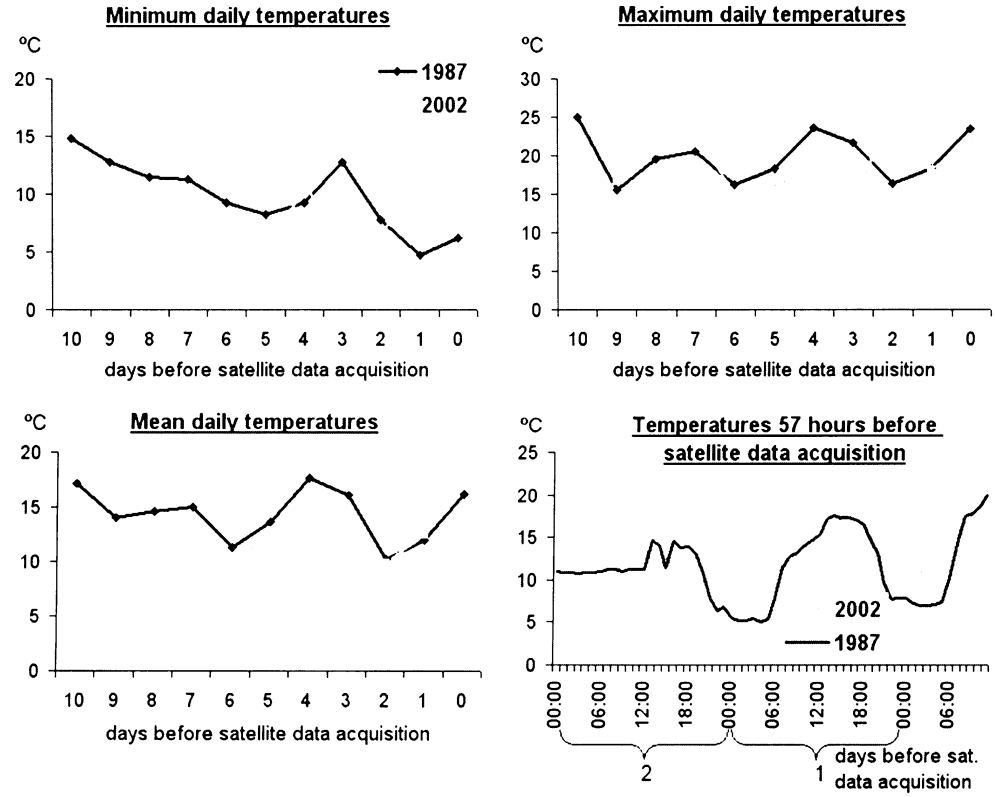

Fig. 6 Comparison of air temperature conditions 10 and 2 days before Landsat satellite data acquisition: July 11th, 1987 and July 28th, 2002. The meteorological conditions during the 2 days before scenes acquisition are most important. The higher temperature amplitudes in 1987 than 2002 are the reason for the higher influence of Hillshade on surface temperatures in 1987.

5. Conclusion

Using thermal remote sensing, we found increasing surface temperature of spruce forest attacked by bark beetle. The mean increase was higher in clear-cut areas (5.2 °C), compared to decayed spruce forest (3.5 °C). A normalisation of ST on the topography was needed in order to compare these areas. The resulting ST models confirmed the influence of topography on surface temperature in a spruce forest. ST decreased with elevation and increased with a higher insolation value (Hillshade) in both assessed satellite scenes (1987, 2002). The accuracy of the models was higher when the edge zones of spruce forest were removed, because of their deviations of heat fluxes.

Acknowledgements

We are grateful to Dr. Keith Edwards for language improvement. M.H. was supported by the Institutional research project MSM 6007665806. T.K. was supported by the Institutional research project AV0Z60870520.

References

Ahern, F. J., Erdle, T., Maclean, D. A., Kneppeck, I. D. (1991): Aquantitative relationship between forest growth rates and Thematic Mapper reflectance measurements. *International Journal of Remote Sensing*. (12) 3, 387 – 400.

Bailey, R.,G. (1996): Ecosystem geography. Springer, New York etc.

Barry, R., G. (1992): Mountain Weather and Climate. 2nd ed. London, New York: Routledge.

Becker, F., Li, Z. L. (1990): Towards a local split window method over land surfaces. *International Journal of Remote Sensing*, 11, 369-393.

Bosfeld, F. C., Holtslag, A. A. M., Van den Hurk, B. J. J. M. (1999): Interpretation of Crown Radiation Temperatures of a Dense Douglas fir Forest with Similarity Theory. *Boundary-Layer Meteorology*. 92, 429–451.

Burrough, P. A., McDonell, R. A. (1998): Principles of Geographical Information Systems. Oxford University Press, New York.

Campbell, J. B. (2002): Introduction to Remote Sensing. The Guildford Press. New York.

Campbell, G. S. (1977): An Introduction to Environmental Biophysic. Springer.

Campbell, G. S., Norman JM (1998): An introduction to environmental biophysics. 2nd ed. Springer.

Cohen, W. B., Spies, T. A. (1992): Estimating structural attributes of Douglas-fir/western hemlock forest stands from LANDSAT and SPOT imagery, *Remote Sensing of Environment*. 41,1-17.

ESRI, ARC/Info 7. (1994): Environmental Systems. Research Institute Inc, Redlands, CA, USA.

Gates, D. M. (2003): Biophysical ecology. Dover Publ. Inc., Mineola, New York.

Geiger, R. (1965): The climate near the ground. Harvard Univ. Press, Harvard.

Geiger, R., Aron, R. H., Todhunter, P. (2003): The climate near the ground. Sixth edition. Rowman & Littlefield Publishers, Inc., Langham etc.

Geomatica Algorithm Reference, (2003): PCI Geomatics.50 West Wilmot Street, Richmond Hill,Ontario, Canada,L4B 1M5

Hais, M. (2003): Changes in Land Cover Temperature and Humidity Parameters Resulting from Spruce Forests Decay in the Centre of the Sumava National Park. *Acta Universitatis Carolinae*. Geographica, 2, 95 – 105.

Hais, M. (2004): Influence of Drainage on Landscape Functioning in Sumava National Park. In.: Hermann A. (ed.) Extended Abstract – International conference on Hydrology of Mountains Environments. Berchtesgaden, Federal Republic of Germany, 27 September – 1 october 2004.

Hashimoto, S., Suzuki, M. (2004): The impact of forest clear-cutting on soil temperature: a comparison between before and after cutting, and between clear-cut and control sites. *Journal of Forest Ressearch*. 9,125–132.

Heurich, M., Reinelt, A., Fahse, L. (2001): Die Buchdruckermassenvermehrung im Nationalpark Bayerischer Wald. 9 – 48 In: Nationalparkverwaltung Bayerischer Wald: Waldentwicklung im Bergwald nach Windwurf und Borkenkäferbefall. Bayerische Staatsforstverwaltung,

Hojdová, M., Hais, M., Pokorný, J. (2005): Microclimate of a peat bog and of the forest in different states of damage in the Natioanl Park Šumava. *Silva Gabreta*, 11(1), 13 – 24.

Hutchinson, M. F. (1993): Development of a continent-wide DEM with applications to terrain and climate analysis. In Environmental Modeling with GIS, ed. M. F. Goodchild et al., New York: Oxford University Press. 392–399

Jensen, J. R. (2000): Remote Sensing of the Environment: An Earth Resource Perspective, Upper Saddle River: Prentice-Hall.

Jonášová, M., Prach, K. (2004): Central-European mountain spruce (*Picea abies* (L.) Karst.) forests: regeneration of tree species after a bark beetle outbreak. *Ecological Engineering*. 23, 15 – 27.

Klassen, W., van Breugel, P. B., Moors, E. J., Nieveen, J. P. (2002): Increased heat fluxes near a forest edge. *Theoretical and Applied Climatology*. 72, 231 – 243.

Lillesand, T. M., Kiefer, R. W., Chipman, J.W. (2004): Remote Sensing and Image Interpretation. John Wiley and Sons. New York.

Lookingbill, T.R., Urban, D.L. (2003): Spatial estimation of air temperature differences for landscape-scale studies in montane environments. *Agricultural and Forest Meteorology*. 114: 141–151

McCune, B., Keon, D. (2002): Equations for potential annual direct incident radiation and heat load. *Journal of Vegetation Science*.13, 603-606.

Pierce, K. B., jun. Lookingbill, T., Urban, D. (2005): A simple method for estimating potential relative radiation (PRR) for landscape-scale vegetation analysis. *Landscape Ecology* 20,137–147.

Pokorný, J. (2001): Dissipation of solar energy in landscape-controlled by management of water and vegetation. *Renewable energy* 24, 641 – 645.

Quattrochi, D. A., Luval, J. C. (2000): Thermal Remote Sensing in Land Surface Processes. CRC PRESS. London.

Richter, R. (1990): A fast atmospheric correction algorithm applied to LANDSAT TM images. *International Journal of Remote Sensing*. 11(1), 159-166.

Ripl, W. (1992): Management of water cycle and energy flow for ecosystem control – the Energy – Transport – Reaction (ETR) model. *Ecological Modelling*. 78, 61 – 76.

Ripl, W., Pokorný, J., Eiseltová, M., Ridgill, S. (1994): A holistic approach to the structure and function of wetlands and their degradation. IWRB Publ. 32, 16–35.

Schmid, J. M. (1976): Temperatures, growth, and fall of needles on Engelmann spruce infested by spruce beetles. USDA For. Serv. Res. Note RM-331, 4 p. Rocky Mt. For. and Range Exp. Stn., Fort Collins, Colo.

Schulze, E. D., Beck, E., Müller-Hohenstejn, K. (2005): Plant ecology. Springer Berlin, Heidelberg.

Shin, D., Le, K. (2005): Use of remote sensing and geographical information systems to estimate green space surface-temperature change as a result of urban expansion. *Landscape and Ecological Engineering*.1, 169–176.

Skuhravý, V. (2002): Lýkožrout smrkový (*Ips typographus L.*) a jeho kalamity. Der Buchdrucker und seine Kalamitäten. Agrospoj, Praha. (in czech)

Strnad, E. (2003): Climate of Šumava, In Šumava, Nature, History, Life, (in czech) 35 – 44.

Siitonen, J., Martikainen, P., Punttila, P., Rauh, J. (2000): Coarse woody debris and stand characteristics in mature managed and old-growth boreal mesic forests in southern Finland. *Forest Ecology and Management*. 128 (3), 211-22.

Tucker, C. J. (1979): Red and photographic infrared linear combinations for monitoring vegetation. *Remote Sensing of the Environment*. 8, 127-150.

Waring, R. H., Running, S. W. (1998): Forest ecosystems: Concept and management. Academic press, San Diego, CA.

Weber, F. P. (1971): The use of airborne spectrometers and multispectral scanners for previsual detection of ponderosa pine trees under stress from insects and disease. p. 94-104. *In* Monit. for. Iand from high aft. and from space. Annul rep. to Earth Resour. Surv. Prog., Off. Space Sci. and Appl. NASA, Houston, Tex.

Yoshino, M. M. (1975): Climate in a small area. An introduction to local meteorology. Univ. Tokyo Press, Tokyo.

Zielonka, T., Piatek, G. (2004): The herb and dwarf shrubs colonization of decaying logs in subalpine forest in the Polish Tatra Mountains. *Plant Ecology*. 172 (1), 63-72.

Kapitola 5

Surface temperature changes of spruce forest stands as a result of bark beetle outbreak

Hais M., Kučera T.

Abstract

The aim of our study was to assess changes in the health of forest stands using thermal satellite data. For this purpose, spruce forest stands in the central part of the Šumava Mountains, Czech Republic were studied. These forest stands were attacked by bark beetles in the beginning of the 1990s. The main assumption was that transpiration of the attacked trees will decrease in summer, resulting in higher surface temperatures. The surface temperatures were taken from Landsat TM/ETM+. The thermal satellite data acquired on July 10, 1995 and 28, 2002 were compared to detect the changes and data from July 11, 1987, which were taken for model validation. Normalisation of surface temperature was needed, because of the complex topography of this area. Therefore, the additional characteristics Altitude, Aspect and Slope were calculated based on the digital elevation model (DEM). Slope and Aspect were combined and expressed as an index of illumination (i.e., Hillshade). Then multiple regressions were calculated relating surface temperature to Hillshade and Altitude. This model was calculated only for non-attacked spruce forest. The higher model accuracy was when the buffer edge zones (90 m) of forest stands and stands with small area were removed. The resulting models confirmed the influence of topography on the surface temperature of spruce forest in the case of all three scenes: 1987 (R^2= 0.49, $p<0.0001$), 1995 (R^2= 0.54, $p<0.0001$) and 2002 (R^2= 0.57, $p<0.0001$). Comparison of the modelled and satellite surface temperatures in the years 1995 and 2002 shows that temperature significantly increases during the process of forest stand death. The maximum increase of normalised surface temperatures was 6.8 °C and 7.5 °C in the models of 1995 and 2002, respectively.

Keywords: Landsat, thermal remote sensing, topography, change detection

1. Introduction

Detection and assessment of forest disturbances using remote sensing include a lot of approaches and use many types of data with different spatial, spectral and radiometric resolutions (Franklin, 2001; Wulder & Franklin, 2007). The first studies were focused on the detection of change in forest stands and are based mostly on the NIR data interpretation (i.e. Leckie & Gougeon, 1981). Since then, many spectral indices were developed. These indices are based mostly on the MIR and NIR spectral bands and are used not only for change detection but also to assess the degree of change (i.e. the change of health state) (Rock et al., 1985; Rosengren & Ekstrand 1987, Lambert et al., 1995; Jin & Sader, 2005). Nevertheless, there is a lack of studies, which employ the long wave spectral region in the case of forest stands. Therefore, we used the thermal infrared (TIR) data for an assessment of spruce forest disturbance. In our study, we used surface temperatures (ST) of three Landsat TM/ETM+ scenes to detect the temporal changes of spruce forest stands attacked by bark beetle.

However, a direct thermal data comparison is not possible, because the ST are strongly dependent on the weather conditions. Therefore, we have applied the ST models extra for each scene. These models fit the weather conditions, include the differences of seasonal insolation during the year, and different topography effect. The main assumption is that if surface temperature modeling under the given atmospheric conditions is successful, then the established differences from real temperature could indicate a change in forest health.

2. Material and Methods

2.1 Locality

The area of interest includes the central part of the Šumava National Park, which is located in the south-west of the Czech Republic. The southern part of the area of interest stretches into the Bavarian Forest National Park, Germany. The area includes localities where the mountains spruce forest (*Picea abies* (L.) Karst.) has been affected by a bark beetle (*Ips typographus*) outbreak and the adjacent surroundings (see Fig. 1). The bark beetle outbreak had its origin in windfallen trees (173 ha) in 1983 after two hurricanes in the western part of the Bavarian Forest NP. In 1984, the managers of the Bavarian Forest

NP decided to retain 86 ha of spruce forest without human intervention. These fallen and heavily damaged trees provided the basis for the start of the outbreak. It was almost finished in 1991, but new attacked areas arose since 1993 (Skuhravý, 2002). The main acceleration of bark beetle dispersion took place between 1995 and 1996. The forest losses in the Šumava NP and the Bavarian Forest NP reached more than 5000 ha in the form of damaged spruce groves and more than 1420 ha in the form of cuttings (Skuhravý, 2002).

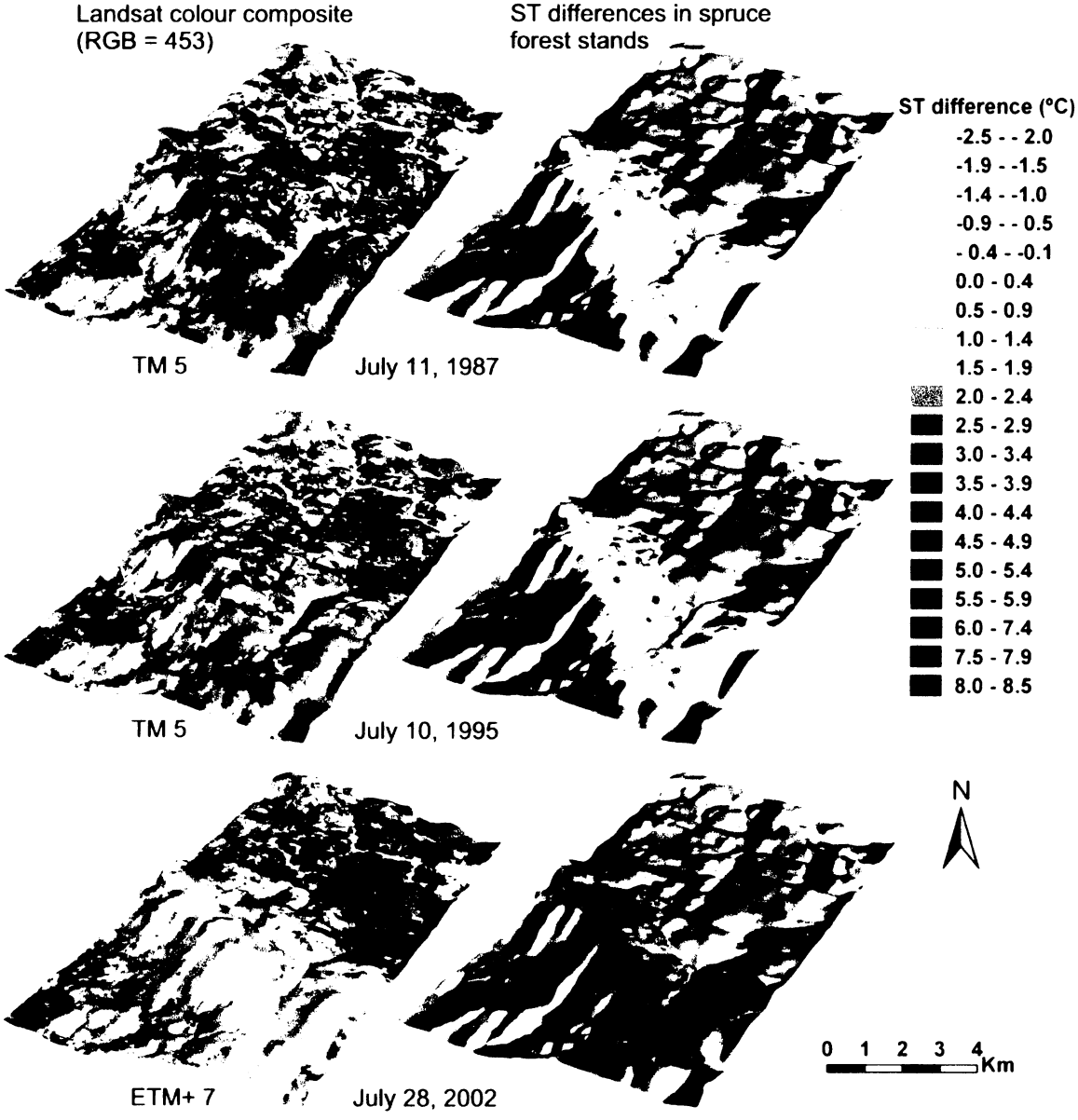

Figure 1. Progress of bark beetle outbreak in the central part of the Šumava Mountains. Pictures on the left side show the gradual decaying of spruce forest. In the right side is the obvious increase of ST in contrast to modelled ST values.

Nevertheless, the clear-cut areas were not assessed in this study. The area of multitemporal comparison was defined as the maximal extent of bark beetle outbreak in 2002. However, the only living spruce stands outside the outbreak area were used for surface temperature modeling. The central part of Šumava Mountains is formed by a complex topography with valleys (i.e. Luzenské valley) and many local hills. The average altitude is 1093 m. Velká Mokrůvka (1370 m) and Špičník (1351 m) are the highest peaks in the Czech part, while the German area is dominated by Lusen (1373 m) and Grosser Rachel (1453 m).

2.2 Preprocessing

The three Landsat TM/ETM+ scenes were selected to represent the following main states of spruce forest disturbance: before the main dispersion of the bark beetle (July 11, 1987), acceleration of bark beetle propagation (July 11, 1995) and the decayed spruce forest (July 28, 2002). Because of possible seasonal differences of weather conditions, only Landsat data acquired in July were used. The satellite scenes were rectified into the S-JTSK coordinate system according to the orthorectified Satellite map of the Czech Republic (2002 ArcData Praha, s.r.o.). DN values of the 6^{th} Landsat channel were transformed to surface temperature (ST) values by applying ATCOR2_T (Geomatica Algorithm Reference, 2003). It was hypothesized that ST in given atmospheric conditions are dependent on altitude, slope and aspect (due to the relatively small area we have neglected the latitudinal range).

The spruce forest thematic layers for both scenes were obtained by a supervised classification method (Campbell, 2002; Lillesand et al., 2004). Because of land use/cover changes during 1987, 1995 and 2002, classification of spruce forest had to be done for all scenes. Because the forest edges form a microclimatically transitional zone to non-forest ecosystems, they exhibit different surface temperatures (Geiger, 1965; Klaassen et al., 2002). Therefore the edge zones were removed in a 90 m buffer using the following procedure.

The GIS layer of forest decayed by bark beetle was obtained from areal orthophotographs taken in 2002.

A digital elevation model (DEM) was calculated to evaluate the influence of Altitude (Hutchinson, 1993). On the basis of the DEM, two parameters (Slope and Aspect) were calculated using a spatial analyst tool (ArcGIS) (Burrough & McDonell, 1998). Both

Aspect and Slope are included in the parameter Hillshade (HS), which was calculated on the basis of the DEM (ESRI, 1994; Pierce *et al.*, 2005):

$$HS = 255\ [\cos(90 - Z)\sin(s)\cos(\alpha - A) + \sin(90 - Z)\cos(s)], \quad (1)$$

where Z is the solar zenith, s is the local slope, A is the solar azimuth and a is the azimuth of the slope facet. The solar zenith and solar azimuth were calculated using the SunAngle software. The Hillshade function gives the hypothetical illumination of a surface by determining illumination values for each cell in a raster. Individual Hillshade values were calculated for each date, because of the different dates of satellite data acquisition. Lastly, the dependence of surface temperature on the DEM and Hillshade was calculated by regression analysis.

Surface temperature modeling

It was important to describe the influence of topography on ST before detecting ST change in the study areas (Hillshade and Altitude). Multiple regression was used for this purpose:

$$ST = a + b*HS + c*DEM, \quad (2)$$

where ST is surface temperature in °C, which was estimated from the thermal channel, HS is Hillshade expressed in an 8-bit scale as a spaceless value, and DEM represents the Altitude in metres. The relation was used for ST modeling only of the healthy spruce stands; the area with decayed forest in 2002 was excluded from the data modeling of all three scenes. The resulting regressions for all three scenes were:

1987

$$ST = 18.81 + 0.01521*HS - 0.00453*DEM \quad (3)$$

1995

$$ST = 29.40 + 0.01287*HS - 0.00449*DEM \quad (4)$$

2002

$$ST = 24.97 + 0.01013*HS - 0.00538*DEM \quad (5)$$

From these formulas it follows, that ST decreases with Altitude (DEM) and increases with Hillshade (illumination) values in all cases. The resulting explained variability (R^2) of this

model is shown in Tab. 1. Using formulas (3, 4, 5), ST were calculated for the area of decayed stands (in 2002). Then the estimated ST were subtracted from the thermal channel satellite ST values (see Figs 1 and 2). It is obvious from Fig. 2 that both the estimated and thermal channel ST are very similar in 1987.

Table 1 Results of the multiple regression of ST on topography.

Regression Model	date	R	R^2	p
3	11.7.1987	0.70	0.49	>0.001
4	10.7.1995	0.73	0.54	>0.001
5	28.7.2002	0.76	0.57	>0.001

However, in 1995, the ST calculated from thermal channels begins to be higher and in 2002 the ST are significantly higher than the modelled values. These results are shown also in Fig. 1 on the left side. The maximal differences between estimated (modelled) ST and ST from thermal data were 6.6 °C, 6.8 °C and 7.5 °C in the models of 1987, 1995 and 2002, respectively. The mean differences between estimated (modelled) ST and ST from thermal data were 0.1 °C, 0.4 °C and 3.5 °C in the models of 1987, 1995 and 2002, respectively.

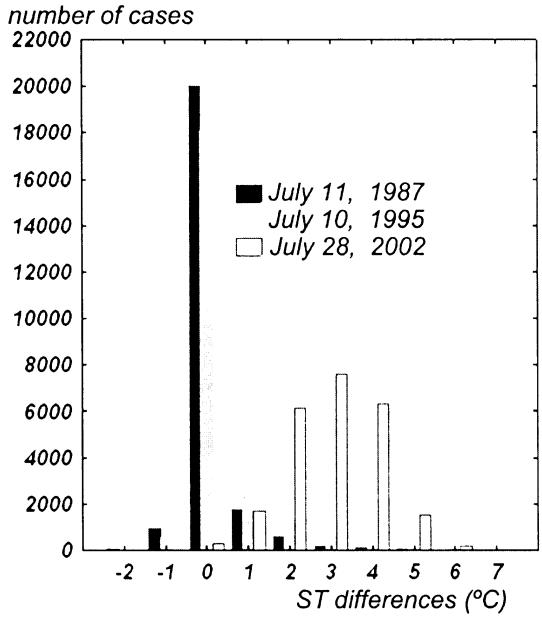

Figure 2. The difference between estimated (modelled) ST and ST from Landsat thermal data. The positive values express the increasing of ST in dependence of decaying spruce forest.

3 Discussion

Surface temperatures are determined by many kinds of weather parameters (solar radiation, cloudiness, precipitation, frontal disturbances etc.), land use and topography. They also provide information about the quantity and/or quality (health state) of vegetation cover. A worsening of the vegetation health, indicated as a surface temperature change, is often connected with decreasing water content (Fitter & Hay, 2002). If it is possible to describe the influence of land use, topography and atmospheric conditions on surface temperature, then the deviation of values caused by disturbances, such as the changing health of vegetation cover, may be obviously distinguished. The influence of topography on surface temperatures may be also affected by the heterogeneity of vegetation cover. There is a whole range of such sources of heterogeneity when working with the forest growth surface. Different tree height is the first source, because it causes local shadows; this effect is greater when the Sun is closer to the horizon. Bosveld et al. (1999) describe a definite effect of shading on observed radiation temperatures, relating the line of sight of the instrument to the solar angle. Different tree overstory density can be another source of heterogeneity. Cohen and Spies (1992) concluded that tree size and overstory density of conifer forest were well correlated with a number of spectral indices, with R^2 values of 0.78–0.86. Normalized Difference Vegetation Index (NDVI) is one of the most frequently used spectral indices (Tucker, 1979). Waring and Running (1998) describe the relation between NDVI and surface temperature of forest canopy, where the surface temperature decreased with NDVI values. The influence of tree height and overstory density is partly eliminated in same-aged monocultures, which is the case in the larger part of the area of interest.

Edge effect is another cause of heterogeneity; higher surface temperatures can be expected at forest edges during clear weather in summer (Geiger et al., 2003). Small patches of forest, where the whole growth is formed by edges, can be designated as a special type of edge effect. The influence of those edge zones was eliminated by their filtering out of our models, which further increased the predicative ability of the models.

In spite of all of the above-mentioned causes of inaccuracies, the resulting models were able to describe a large part of the variability of the forest surface temperatures (see Tab. 1). After computing the models, which are based on the influence of topography on ST, it

was possible to compare the ST of spruce forest with different stages of decay caused by the bark beetle outbreak.

The resulting mean increase of ST in the decayed spruce forest (by 3.5 °C) in 2002 corresponds with field measurements of temperature in the same area (Hojdová et al., 2005). The method of forest stand thermal modeling, which was used in this study, was applied also in order to compare the ST in the areas with different forest management (Hais & Kučera, 2007). The result shows that mean increase was higher in clear-cut areas (5.2 °C), compared to decayed spruce forest (3.5 °C). Another type of application of the above-mentioned method is the possibility to distinguish accurately the different stages of bark beetle attack (green, red and grey attack). Nevertheless, more precise ST models are needed for such modeling, which will describe a larger part of the variability.

4 Conclusion

We found increasing surface temperature of spruce stands using thermal remote sensing in forests attacked by bark beetle. A normalisation of ST on topography was needed in order to compare the ST under different weather conditions. The ST models confirmed the influence of topography on surface temperature in a spruce forest. ST decreases with elevation and increases with a higher insolation value (Hillshade) in all assessed satellite scenes (1987, 1995 and 2002).

Acknowledgements

We are grateful to the reviewers for their remarks to our abstract. We thank Dr. Keith Edwards for language improvement. M.H. was supported by the projects: GA AV KJB600870701 and the Institutional research project MSM 6007665806. T.K. was supported by the Institutional research project AV0Z60870520.

References

Bosfeld, F.C., Holtslag, A. A. M., Van den Hurk, B. J. J. M. (1999): Interpretation of Crown Radiation Temperatures of a Dense Douglas fir Forest with Similarity Theory. *Boundary-Layer Meteorology*. 92, 429–451.

Burrough, P. A., McDonell, R. A. (1998): Principles of Geographical Information Systems. Oxford University Press, New York.

Campbell, J. B. (2002): Introduction to Remote Sensing. The Guildford Press. New York.

Cohen, W. B., Spies, T. A. (1992): Estimating structural attributes of Douglas-fir/western hemlock forest stands from LANDSAT and SPOT imagery, *Remote Sensing of Environment.*, 41, 1-17.

ESRI, ARC/Info 7. (1994): Environmental Systems. Research Institute Inc, Redlands, CA, USA.

Fitter, A. H., Hay, R.K.M. (2002): Environmental physiology of plants. 3d ed. Academic Press, San Diego, Calif. 367.

Franklin, S. E. (2001): Remote Sensing for Sustainable Forest Management, CRC Press (Lewis), Boca Raton, FL, 407p.

Geiger, R. (1965): The climate near the ground. Harvard Univ. Press, Harvard.

Geiger, R., Aron, R. H., Todhunter, P. (2003): The climate near the ground. Sixth edition. Rowman & Littlefield Publishers, Inc., Langham etc.

Geomatica Algorithm Reference. (2003): PCI Geomatics.50 West Wilmot Street, Richmond Hill,Ontario, Canada,L4B 1M5

Hais, M., Kučera, T. (2007): Surface temperature change of spruce forest as a result of bark beetle attack: Remote sensing and GIS approach. *European Journal of Forest Research*. submitted

Hojdová, M., Hais, M., Pokorný, J. (2005): Microclimate of a peat bog and of the forest in different states of damage in the Natioanl Park Šumava. *Silva Gabreta*. 11(1), 13 – 24.

Hutchinson, M. F. (1993): Development of a continent-wide DEM with applications to terrain and climate analysis. In Environmental Modeling with GIS, ed. M. F. Goodchild et al., New York: Oxford University Press. 392–399.

Jin, S., Sader, S.A. (2005): Comparison of time series tasseled cap wetness and the normalized difference moisture index in detecting forest disturbances. *Remote Sensing of Environment*. 94, 364-372.

Klassen, W., van Breugel, P. B., Moors, E. J., Nieveen, J. P. (2002): Increased heat fluxes near a forest edge. *Theoretical and Applied Climatology*. 72, 231 – 243.

Lambert, N. J., Ardö, J., Rock, B. N., and Vogelmann, J. E. (1995): Spectral characterization and regression- based classification of forest damage in Norway

spruce stands in the Czech Republic using Landsat Thematic Mapper data. *International Journal of Remote Sensing*. 16, 1261-1287.

Leckie, D. G., Gougeon, F. A., (1981): Assessment of spruce budworm defoliation using digital airborne MSS data. Proceedings of the Seventh Canadian Symposium on Remote Sensing held in Winipeg, Manitoba, in 1981,190-196.

Lillesand, T. M., Kiefer, R. W., Chipman, J. W. (2004): Remote Sensing and Image Interpretation. John Wiley and Sons. New York.

Pierce, K. B., jun. Lookingbill, T., Urban, D. (2005): A simple method for estimating potential relative radiation (PRR) for landscape-scale vegetation analysis. *Landscape Ecology*. 20, 137–147.

Rock, B. N., Williams, D. L., Vogelmann, J. E. (1985): Field and airborne spectral characterization of suspected acid deposition damade in red spruce (Picea rubens) from Vermont. Pages 71 – 81 in Procedings of the 11th International Symposium on Machine Processing of Remotely Sensed Data. Purdue University, West Layette, IN.

Rosengren, M., Ekstrand, S. (1987): A method aiming at monitoring large area forest decline using satellite imagery. In: Proceedings, Seminar on Remote Sensing and Forest Decline Attributed to Air Pollutands held in Laxenburg, Austria, on 11-12 March 1987.

Skuhravý, V. (2002): Lýkožrout smrkový (Ips typographus L.) a jeho kalamity. Der Buchdrucker und seine Kalamitäten. Agrospoj, Praha. (in czech)

Tucker, C. J. (1979): Red and photographic infrared linear combinations for monitoring vegetation. *Remote Sensing of the Environment*. 8, 127-150.

Waring, R. H., Running, S. W. (1998): Forest ecosystems: Concept and management. Academic press, San Diego, CA.

Wulder, M. A., and S. E. Franklin, (eds.), (2007): Understanding Forest Disturbance andSpatial Pattern: Remote Sensing and GIS Approaches, CRC Press (Taylor and Francis),Boca Raton, FL, 252p.

KAPITOLA 6

The mutitemporal comparison of two types of forest disturbance using Landsat TM/ETM+ and field vegetation data

Hais M., Jonášová M., Langhammer J., Kučera T.

Abstract

Various types of forest disturbances may influence many processes in landscapes, such as changes in microclimate, hydrology, soil erosion etc. Therefore, it is important not only to identify and/or classify the disturbance types, but also to describe the disturbance dynamics. Our study incorporates multitemporal and spectral comparisons of two types of spruce forest *(Picea abies [L.] Karst.)* disturbances. The first disturbance type was the bark beetle (*Ips typographus [L.]*) outbreak during the last 20 years (gradual disturbance – GD). Clear cut areas represent a second type of disturbance (discrete disturbance - DD). The study area is located in the central part of the Bohemian Forest, in the border region between the Czech Republic and Germany. The analyses were conducted at two levels: (1) general trends were described in whole disturbance areas (WDA), and (2) sampled disturbance areas (SDA) were selected to assess the direct influence of field vegetation data on the spectral response.

Thirteen Landsat TM/ETM+ scenes from 1985 to 2007 were used for the multitemporal assessment. From these data, the following spectral indices were estimated: NDMI, Tasseled Cap (Brightness, Greenness, Wetness), DI and DI′. DI', Wetness and Brightness showed the highest sensitivity to forest disturbance in the case of both disturbance types (DD, GD). The temporal development in both disturbance types (DD and GD) can be divided into three main phases according to spectral response: 1) relatively stable forest with an almost invariant spectral response (1985 – 1992), 2) acceleration of forest disturbance resulting in gradation of changes in normalized spectral values (1992 – 2004), and 3) forest regeneration and return of the normalized values to origin state (2004 – 2007). The highest spectral differences between the DD and GD disturbances were found during the second phase (1992 – 2004). DD resulted in a significantly higher spectral difference from the origin forest and occurred as a more discrete event in comparison to GD. The relationship between the spectral indices and field vegetation data was assessed using RDA analysis. The field vegetation data described 60 % of the explained variability of the spectral indices data.

Key words: Landsat, forest disturbance, spectral indices

1. Introduction

1.1. Forest disturbance

Forest disturbances represent an important factor, which significantly influences the character of forest ecosystems (Pickett & White, 1985). The disturbances are very often disscused theme mainly in the natural protected areas. In this connection, the question is whether to actively prevent against disturbances and preserve the forest continuity, or allow the forest to develop naturally. Disturbances are important for biodiversity, age stand heterogeneity and long term forest stability (Waring & Running, 1989). On the other hand, disturbances represent a discontinuity of forest stands.

According to the general definition, a disturbance causes a sudden change in the behavior or properties of a system (Rykiel et al., 1988). However, these relatively sudden events differ in spatio-temporal dynamics (Oliver & Larson, 1996). In the case of forest stands, we suggest to distinguish "discrete disturbances" (DD) resulting from very fast changes (clear-cut harvesting, fire, windstorms) and the "gradual disturbances" (GD), which arise as a progressive deforestation over time and/or space. Typical examples of GD are insect attacks, diseases and forest thinning. Type and severity of the disturbance influences stand dynamics and regeneration success (Linke et al., 2007).

1.2. Spectral response of forest disturbances

Our study is based on multispectral scenes with middle spatial resolution, which are very often used in order to assess forest stand disturbances at the regional scale (Iverson et al., 1989; Cohen et al., 2002; Wulder & Franklin, 2007). We supposed that both types of disturbances would differ in spectral response and dynamics.

In general, the better the contrast in reflectance between disturbed and undisturbed forest, the more easily canopy removal can be measured (Healey et al., 2007). Clear cut areas are, therefore, best identified immediately after harvesting (Wilson & Sader, 2002; Healey et al. 2005). The capability of detecting clear cut areas decreases with regeneration of the herb and tree layers (Wulder et al., 2004).

Different spectral responses can be expected in the case of forest stands attacked by insects. The beginning of such disturbances is often connected with color changes of leafs and needles. For example, a pine beetle attack results in different color stages (green, red and gray attack) of affected pine crowns (Wulder et al., 2006b). For the spectral response

of these types of disturbance it is also typical that the ground story is not eliminated. Many studies have described the disturbances caused by insect attack (Muchoney & Haack, 1994; Wulder et al., 2006a,Wulder et al., 2006b).

Forest disturbances and the following regenerations are often detected and mapped using spectral indices. These indices are mostly based on the SWIR and NIR bands (Horler & Ahern, 1986; Lambert et al., 1995; Toomey & Vierling, 2005). For these purposes, the Tasseled Cap (TC) linear transformation is most often used. TC is composed of three indices: Brightness, Greenness, and Wetness (Crist & Cicone, 1984; Kauth & Thomas, 1976). Of these three components, Wetness (TCW) is often used to identify forest disturbances (Jin & Sader, 2005). Wulder et al. (2006a) detected and mapped pine beetle red attack using the Wetness index, which was included for change detection in the Enhanced Wetness Difference Index (EWDI). On the contrary, Kuzera et al. (2005) applied the Brightness and Greenness indices to assess forest disturbance. Wulder et al. (2004) estimated time since forest harvesting using all three TC components. Healey et al. (2005) combined the full potential of the three TC components into a Disturbance index (DI). This index has been designed to detect stand replacing disturbances (Healey et al., 2005; Masek, 2005; Healey et al., 2006).

The normalized difference moisture index (NDMI) is another index, which has been used to detect forest disturbances (Jin & Sader, 2005). These authors also reported a high correlation of this index with TCW.

The main aims of our study were to (1) compare the sensitivity of different indices to the spectral response of forest disturbances, (2) describe and compare the dynamics of two types of disturbances (DD, GD), and (3) assess the determination of spectral response by field vegetation data in DD and GD.

While a majority of studies is focused on the detection of clear cuts or areas attacked by insects, we compare the spectral response and dynamics of both types of disturbance. We consider the description of forest disturbance dynamics to be proxy information not only for management of natural protected areas, but also for forest product management. Further unique aspects of this study are multitemporal comparisons of satellite and field vegetation data.

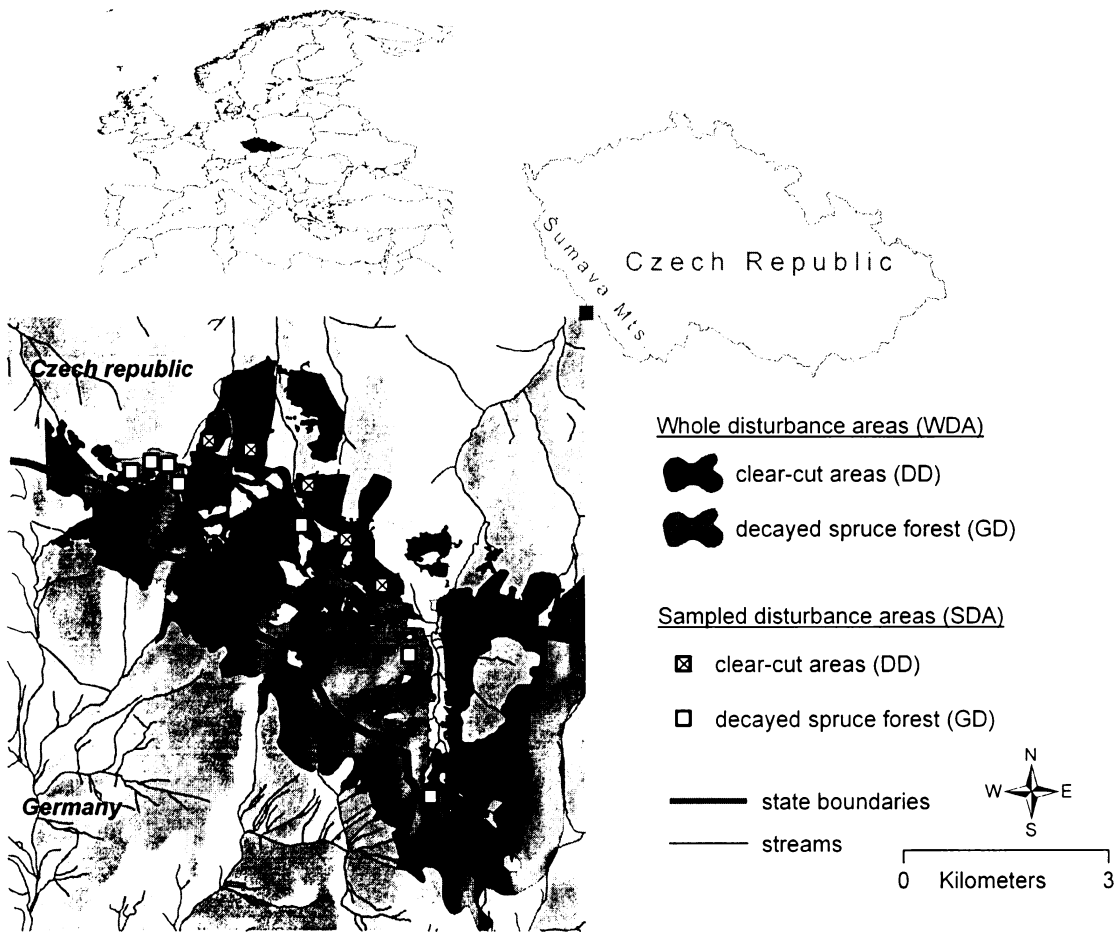

Fig. 1 Study area located in the Sumava Mountains, Czech Republic – Germany border region.

2. Study area

The study area is located in the central part of the Sumava Mountains, in the border region between the Czech Republic and Germany (see Fig. 1). The whole area is included in the Šumava National Park (Czech Republic) and the Bavarian Forest National Park (Germany). Both national parks are part of a UNESCO biosphere reserve.

Norway spruce forest (*Picea abies* [L.] Karst.) is the dominant land cover unit in this locality. During the last 20 years, a bark beetle (*Ips typographus* (L.) outbreak caused spruce forest decay in this area. The bark beetle outbreak had its origin in windfallen trees (173 ha) in 1983 and 1984 after two hurricanes in the western part of the Bavarian Forest NP. In 1984, the managers of the Bavarian Forest NP decided to retain 86 ha of spruce forest without human intervention. These fallen and heavily damaged trees provided the

basis for the start of the outbreak (Heurich et al., 2001, Skuhravý 2002). The main acceleration of bark beetle dispersion took place between 1995 and 1996. In the Šumava NP, two approaches were applied to the attacked forests: (1) a small portion of the stands in the core zone of the national park was left without intervention (gradual disturbance, GD) and (2) clear cut areas (discrete disturbance, DD), which originated due to salvage logging of attacked stands to prevent the propagation of bark beetle. Forest losses in the Šumava and Bavarian Forest NPs reached more than 5000 ha in the form of damaged spruce groves and more than 1420 ha in the form of cuttings (Skuhravý, 2002).

Both disturbance type areas (DD, GD) used for multitemporal comparisons were defined as the maximum extent (whole disturbance areas –WDA) of clear cutting (3.26 km^2) and bark beetle outbreak (20.2 km^2) areas in 2002. Except for the WDA, we defined the sampled disturbance areas (SDA), which are associated with the field research plots.

2. 1 Field research plots

Twelve permanent research plots, 400 m^2 each, were selected in 1997 in representative parts of available stands of clear cut areas (5 plots, DD) and forest decayed by bark beetle (7 plots, GD). All types of plots were more or less equally distributed over the study area. The selection reflected the real situation in the field, i.e. the advance of the bark beetle attack and the creation of clearings by foresters. Both disturbances, bark beetle attack in the case of stands without interventions, or clearcutting in the case of stands with interventions, occurred in 1997. A detailed description of field research plots is given in Jonášová & Prach (2004).

3. Methods

3.1 Satellite data processing

Thirteen Landsat TM/ETM+ scenes were used in our study (Table 1). These scenes were acquired from June to November. The reason of such heterogeneity of acquisition time is the cloudiness in the mountain area, which causes a lack of satellite data with sufficient quality. Nevertheless, data from the period of main disturbance changes were acquired in summer. Because our study area is located in the overlap zone of the Landsat paths, it was possible to use scenes from both the 191 and 192 paths. The scenes covered the whole

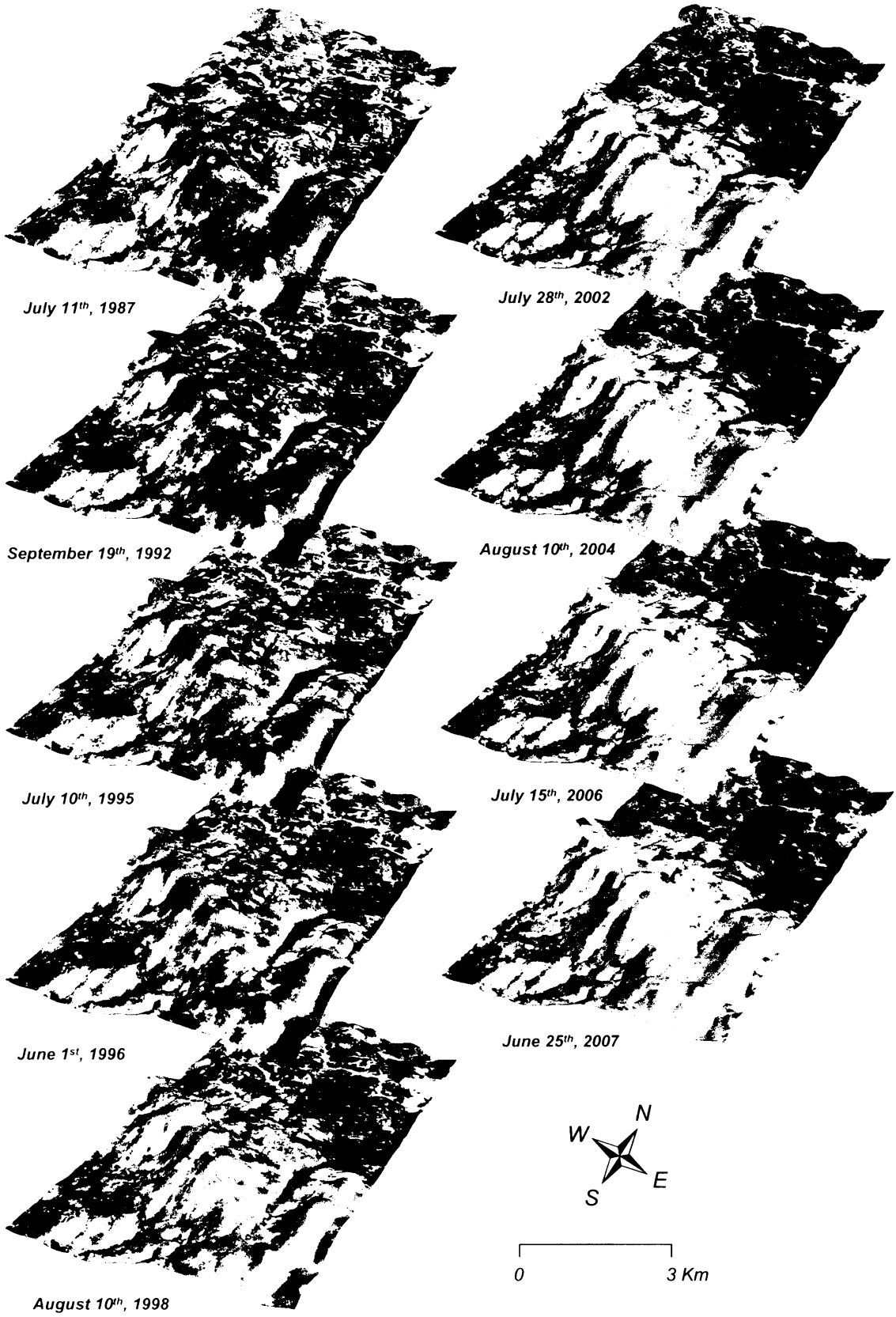

Fig. 2 Selected scenes document the progress of bark beetle outbreak since 1987. The attacked spruce stands are expressed as cyan, the death stands with light blue.

Table 1 Landsat TM and ETM+ imagery.

Acquisition date	Landsat scene	Landsat sensor
Nov. 26, 1985	Path 192, Row 26	TM
Jul. 11, 1987	Path 192, Row 26	TM
Sep. 18, 1989	Path 192, Row 26	TM
Nov. 23, 1990	Path 192, Row 26	TM
Sep. 19, 1992	Path 192, Row 26	TM
Jul. 11, 1995	Path 191, Row 26	TM
Jun. 1, 1996	Path 192, Row 26	TM
Nov. 8, 1998	Path 192, Row 26	TM
Jul. 28, 2002	Path 192, Row 26	ETM+
Aug. 8, 2003	Path 192, Row 26	TM
Aug. 10, 2004	Path 192, Row 26	TM
Jul. 15, 2006	Path 192, Row 26	TM
Jun. 25, 2007	Path 191, Row 26	TM

forest disturbance development: 1) initial stage of spruce forest decay by bark beetle, 2) acceleration of bark beetle outbreak, resulting in clear cutting the surrounding buffer zone and 3) beginning of forest regeneration. The satellite scenes were orthorectified into the S-JTSK coordinate system (Krovak projection, Bessel ellipsoid 1841) according to the Satellite map of the Czech Republic (2002 ArcData Praha, s.r.o.) and a DEM created from contour lines (1:25 000). The ATCOR atmospheric correction model (Geomatica Algorithm Reference, 2003; Richter, 1990) was applied to those images to convert DN values to at sensor radiance.

The following spectral indices were estimated: NDMI, TC (Brightness, Greenness, Wetness) DI and DI′. NDMI is based on the contrast between SWIR and NIR reflectance (Jin & Sader, 2005, Gao, 1996):

$$NDMI = \frac{NIR - SWIR}{NIR + SWIR}$$

The TC was estimated from six (1-5;7) Landsat TM/ETM+ bands. Landsat TM and ETM+ differ in the coefficients for TC estimation (Crist & Cicone, 1984; Huang et al., 2002).

All of the above mentioned indices (NDMI, Brightness, Greenness, Wetness) were normalised using the rescaling (Healey et al., 2005; Masek, 2005):

$$I_r = (I - I_\mu)/I_\sigma$$

Where I_r is a rescaled index value (NDMI, Brightness, Greenness, Wetness), I_μ the mean forest index, and I_σ is the standard deviation of the forest index.
Next, we estimated the Disturbance Index (DI), which emphasizes the contrast between the forest stand and bare soil (Healey et al., 2005; Masek, 2005):

$$DI = Brightness - (Greenness + Wetness)$$

The DI is based on the different spectral response of deforested areas, which have higher reflectance of Brightness and lower reflectance of Greenness and Wetness, than mature forests (Healey et al., 2006). Because of the different Greenness behavior in our study, which was caused by specific vegetation dynamics, we modified the DI equation to:

$$DI' = Wetness - Brightness$$

where the Greenness was excluded and the sign was changed by transposition of the Wetness and Brightness indices. However, it is only a formal modification in order to express the values in the same sign as Wetness and NDMI.

3. 2 Field research plots

Data about natural regeneration and cover of vegetation layers were obtained following Jonášová and Prach (2004). Natural regeneration was measured by recording the numbers of seedlings of spruce and broadleaved species divided into two height-categories: (1) ≤ 50 cm, (2) > 50 cm. Percentage cover of tree canopy, moss, herb, and brush layers were visually estimated in each plot (Kent & Coker, 1992). All of the data were obtained repeatedly in 1998, 2002, and 2007. The geographic coordinates for all 12 field research plots were determined using a GPS.

Every field research plot was associated with the nearest square (60 x 60 m), which included four Landsat pixels. These squares, called sample disturbance areas (SDA), were

selected from the whole disturbance areas (WDA) in order to compare spectral response from the above mentioned indices with data from the field research plots.

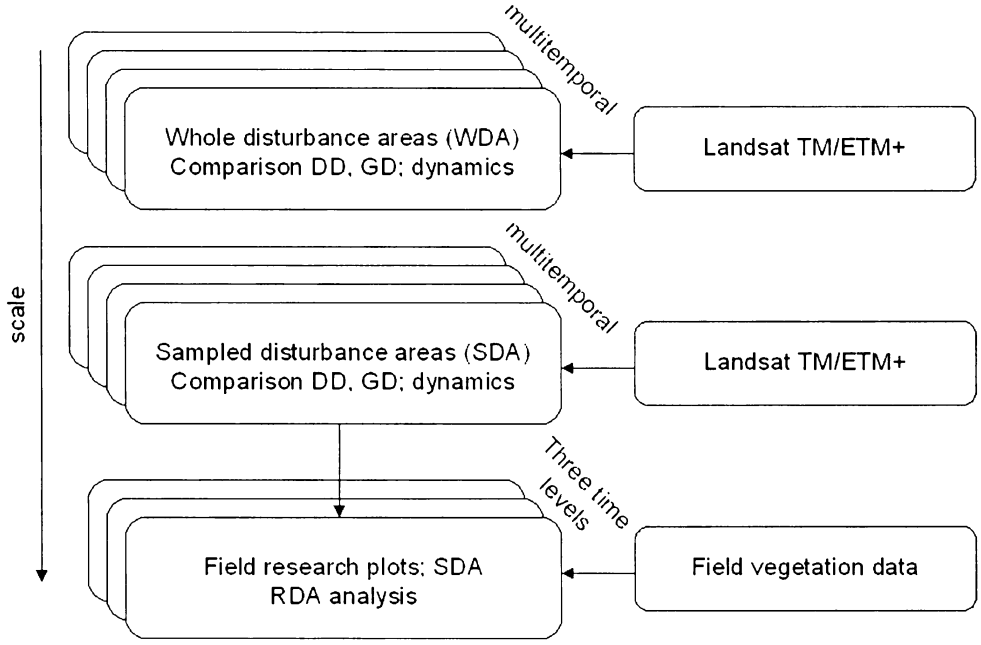

Fig. 3 Scheme of data processing. The two upper levels of analyses were based on the comparison of spectral indices from 13 scenes. The third bottom level represents a combination of both spectral indices and field vegetation data.

3. 3 Data analyses

The spectral responses of DD and GD (from WDA) were compared in given years using repeated measures ANOVA. The Scheffé post hoc test was used in the case of significant differences.

Spectral indices values (from SDA) were related to the field data, i.e. numbers of seedlings and covers of vegetation layers, by Redundancy Analysis (RDA) using Canoco for Windows (Ter Braak & Šmilauer, 1998). The spectral indices were used as dependent variables, while numbers of seedlings and covers of vegetation layers were used as environmental variables. Type of plot (dead stand and clearcut) was used as dummy variables and time was used as a passive environmental variable. The significance of the relationship was tested by the Monte Carlo permutation test. This was followed by two partial analyses, where the influence of seedlings number and vegetation layers were

evaluated separately. The resulting ordination diagram was produced using CanoDraw (Ter Braak & Šmilauer, 1998).

4. Results

4. 1 Multitemporal analysis of disturbance dynamics in whole disturbance areas (WDA)

In the first level we assessed the general ability of indices to describe the forest disturbance dynamics in DD and GD. The temporal development in both disturbance types (DD and GD) can be divided into three main parts according to the spectral response (see Fig 4): (1) a period of relatively stable forest with invariant spectral response (1985 – 1992), (2) acceleration of forest disturbance resulting in a gradation of changes in the normalized spectral values (1992 – 2004), and (3) a period after forest disturbance acceleration, where the normalized values return towards their former state (2004 – 2007).

A common feature of the first period was the small variances between the normalized values of all used spectral indices. In the second period, the normalized values were either increasing (Brightness and Greenness) or decreasing (NDMI, Wetness, DI).

Next, the sensitivity of the spectral indices was assessed. The general criterion was the difference between the rescaled values in the time of disturbance and the state before the beginning of the disturbances. The DI´ had the largest change in values during the disturbance. The lowest change occurred in the NDMI and Greenness indices (see Fig 4).

The results for a majority of the spectral indices indicated that DD and GD had significantly different spectral response during the acceleration of forest disturbance (2004 – 2007). In addition, the Greenness and NDMI indices showed significant differences between DD and GD during the whole time of disturbance, starting from 1995 and 1996, respectively (Table 2).

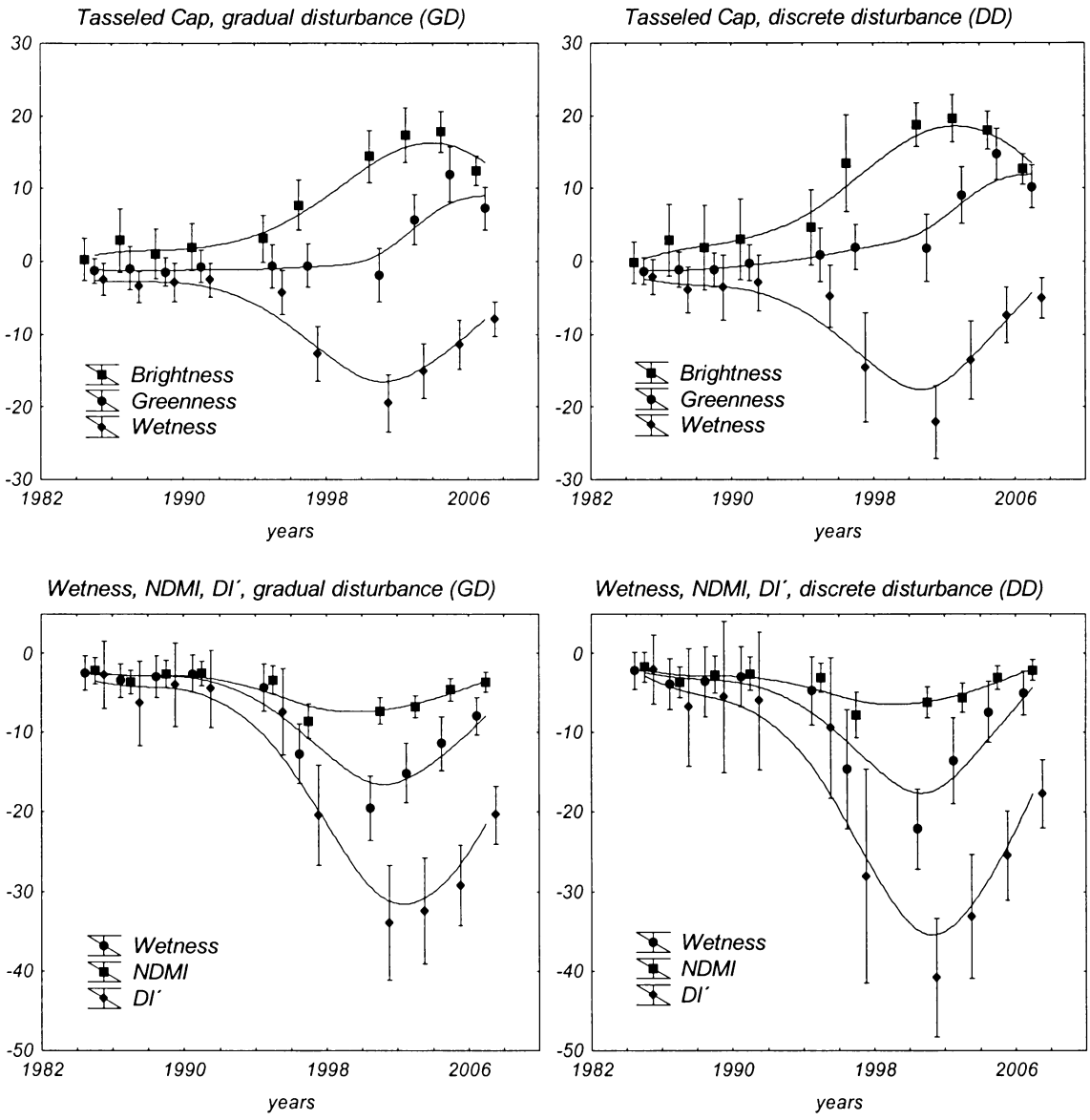

Fig. 4 Comparison of the progress of spectral response of selected indices (mean, standard error of mean and ±1 standard deviation). Both left plots illustrate the dynamics of decayed forest disturbance (GD) and the right ones the clear cut disturbance (DD).

Table 2 Similarity test of two disturbance types (DD, GD), for multiple years, in whole disturbance areas (WDA). The numbers represent p-values of the Scheffé post hoc test from repeated measures ANOVA. The bold marked values express significant values at the 0.05 level.

	Brightness	Greennes	Wetness	DI	DI'	NDMI
1985	1.00	1.00	1.00	1.00	1.00	0.00
1987	1.00	1.00	1.00	1.00	1.00	1.00
1989	0.69	1.00	0.76	1.00	0.42	1.00
1990	0.93	1.00	0.37	1.00	0.47	1.00
1992	0.21	1.00	1.00	0.99	0.50	1.00
1995	**0.00**	**0.00**	0.05	0.97	**0.00**	1.00
1996	**0.01**	**0.00**	1.00	**0.00**	0.59	**0.00**
1998	**0.00**	**0.00**	**0.00**	**0.00**	**0.00**	**0.00**
2002	**0.00**	**0.00**	**0.00**	**0.00**	**0.00**	**0.00**
2003	**0.00**	**0.00**	0.97	1.00	0.19	**0.00**
2004	**0.00**	**0.00**	**0.00**	**0.00**	1.00	**0.00**
2006	1.00	**0.00**	**0.00**	**0.00**	**0.00**	**0.00**
2007	1.00	**0.00**	**0.00**	1.00	**0.00**	**0.00**

4. 2 Multitemporal analysis of sampled disturbance areas (SDA)

Results of the comparison of spectral response of both disturbances (DD, GD) in given years correspond with the general progress of forest disturbance assessed on the larger areas (Fig. 5). However, in this case the differences between the DD and GD are more obvious, unlike for the WDA. The spectral response of DD had larger differences from the original values than GD for all indices. Also, DD showed a considerable increase of spectral indices from 1996 to 1998 in comparison to GD.

4. 3. Canonical analysis

RDA analysis (Fig. 6) showed that natural regeneration (seedling numbers) and vegetation layer covers significantly influenced spectral response. Covers of vegetation layers explained slightly more variability in spectral response data than numbers of seedlings. Both groups of variables, when used together, explained 61.3 % of the

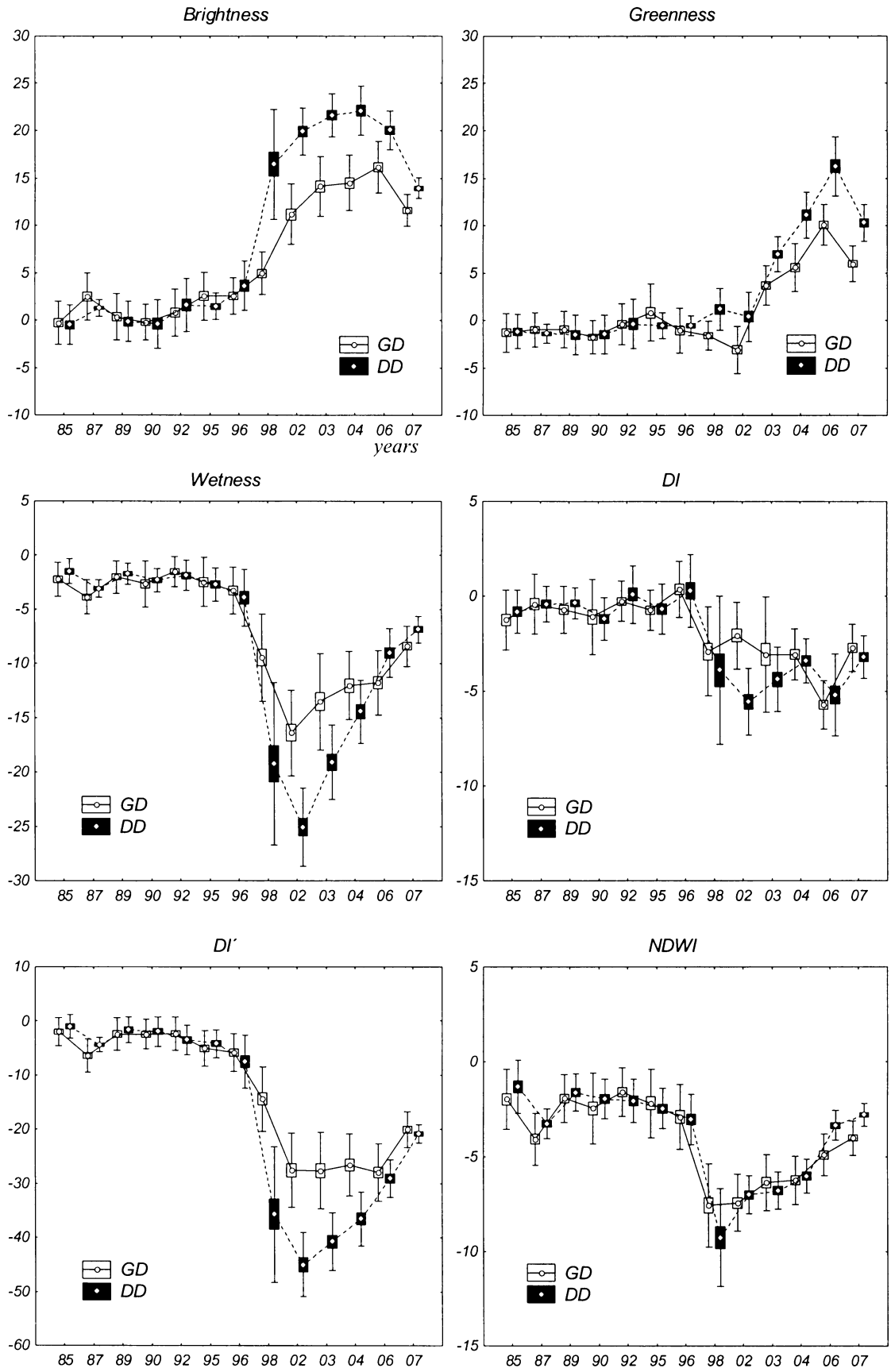

Fig. 5 Comparison between DD and GD using different spectral indices in sampled disturbance areas (SDA) (mean, standard error of mean and ±1 standard deviation).

variability (Tab. 3). Indices Brightness, DI, DI', and Wetness seem to be the most influenced by the type of disturbance (high values of Brightness in clear cut areas, high values of the other indices in the dead stands). Brightness was positively influenced by herb layer cover (E1), DI and DI' were positively influenced especially by the moss layer (E0) and tree canopy (E3), and Wetness mostly by seedlings of broadleaved species taller than 50 cm, but partly also by spruce seedlings taller than 50 cm and brush layer cover. The Greenness Index had increased values during the observed time period in both types of disturbance. Greenness was slightly higher in clear cut areas and was positively influenced by the herb layer cover (E1). NDMI correlated positively with the presence of seedlings taller than 50 cm and brush layer cover.

Table 3 Results of the RDA analysis. Explained variability means the percentage of the total variation in indices data that can be explained by each group of explanatory variables without including the others. The total explained variability is that explained by all explanatory variables.

Explanatory variables	**Explained variability (%)**
Numbers of seedlings	34.7
Covers of vegetation layers	42.9
	Total explained variability (%)
	61.3

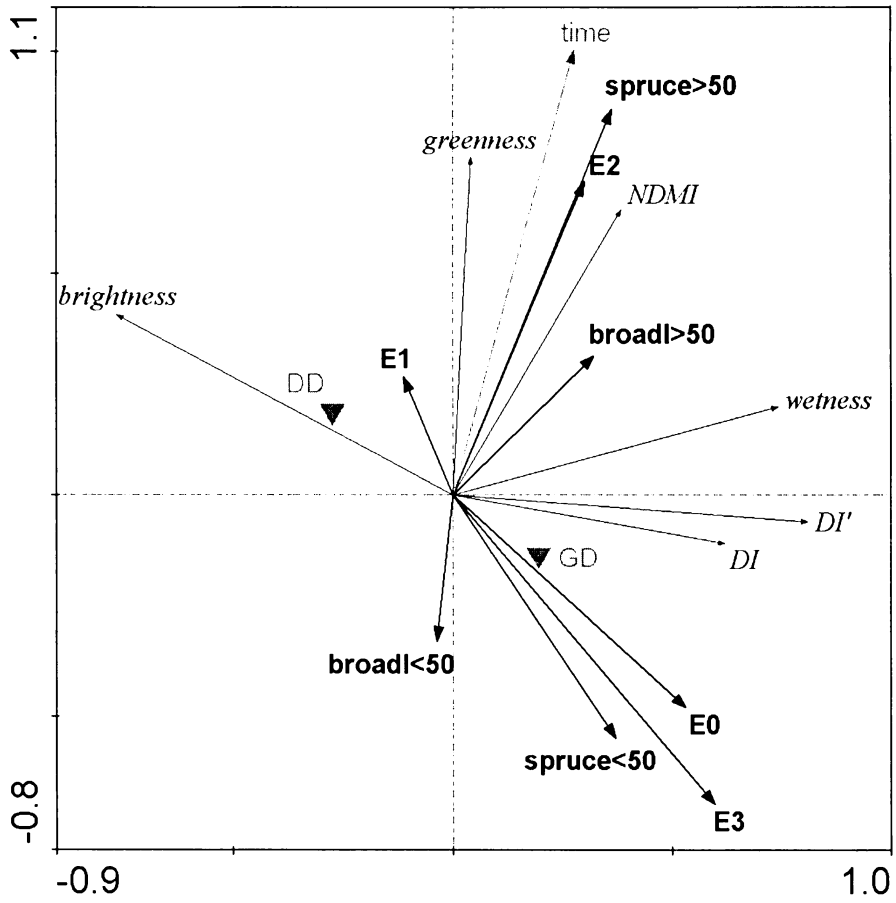

RDA analysis showing indices values (in italics) in relation to the numbers of seedlings of spruce and broadleaved species (smaller and higher than 50 cm), covers of vegetation layers (E0 – moss layer, E1 – herb layer, E2 – brush layer, E3 – tree canopy), disturbance type (DD, GD) and time. Disturbance type and time were used as passive variables.

5. Discussion

5.1 Sensitivity of spectral indices to forest disturbances

Spectral indices based on SWIR are commonly used to assess forest disturbance caused by harvesting (Franklin, 2001; Healey et al., 2006), insect attack (Wulder et al., 2006b), etc. However, according to Healey et al. (2006), the sensitivity of these indices to deforestation is different. Our study also confirms the differences of these spectral indices. Both TC indices, Wetness and Brightness, showed high sensitivity. Their combination in the DI′ index enhanced the disturbance effect. DI′ is generally based on DI (Healey et al., 2005); our modification (DI′) reflects the specific vegetation condition in our study area and is based on excluding Greenness from the original DI. The reason for this was that,

instead of the expected increase in Greenness values during deforestation, which usually represents a decrease in green biomass, the values significantly increased, although with a few years delay. That was caused probably by the fast increase in herb layer cover after tree cutting. Furthermore, the spectral response was influenced by the planting of new trees in the clear cut areas (Jonášová & Prach, 2004). In the decayed forest (GD), the main reason for the increase in the greenness index was probably the growth of herb vegetation (including the seedlings) due to increased forest light levels (Jonášová & Prach, 2004).

NDMI, which is the normalized ratio of NIR and SWIR, had lower sensitivity in identifying the forest disturbance. This may be caused by enhancing the weight of NIR in the NDMI, which corresponds with results of Healey et al. (2006), who reported an inconsistent relationship between NIR and forest structure. On the other hand, Jin and Sader (2005) described a high correlation between NDMI and Wetness.

5.2. Dynamics of forest disturbances (GD, DD)

The similar temporal dynamics in both the WDA and SDA document the satisfactory explanatory value of SDA. The risk of inaccuracies is higher in the SDA because of the lower number of cases (pixels). However, when the individual sampled areas are well defined and have sufficient geometric accuracy (RMSE < 0.5 pixel), the data will be relevant for such an assessment. Furthermore, the data from the sampled areas expressed more precisely the differences between DD and GD, because the smaller sampled areas express one forest state (i.g. either forest or clear cut areas) in the time of data acquisition. The comparison of the temporal dynamics of DD and GD using all spectral indices showed that GD has a more gradual behaviour with fewer differences in values than DD. This is due to slower forest decaying by bark beetle. During this process, trees are drying and the herb vegetation starts to grow due to opening up stand overstory (Waring & Running, 1989). On the contrary, clear cutting (DD) occurs as a discrete event. However, the decision whether to consider clear cut areas as discrete or continual events, will be influenced by the scale and extent of harvesting.

5. 3 Synthesis of spectral indices and field vegetation data

Field vegetation data were needed for a correct interpretation of the temporal dynamics of the disturbances. Temporal changes of the spectral indices in both WDA and SDA could be interpreted so that the return of values, after their acceleration, to their original values is

caused by forest regeneration. However, the data from the field research plots show that the seedlings make up a small part of the vegetation cover, which is composed mostly by herb species in both types of disturbances (Jonášová & Prach, 2004).

Generally, the pixel value of remote sensing data is integral information depending on the proportion and spectral character of the assessed subject (Lillesand et al., 2004). This is supported by the results of the RDA analysis, in which more than 60% of variability of spectral indices data was explained by vegetation layer covers and numbers of seedlings. A detailed study of the RDA results shows that it is possible to divide the spectral indices into two groups. The first group includes indices whose variability is explained by disturbance type (DD, GD) and covers of the moss (E0) and tree canopy layers (E3): Brightness, DI, DI′ and potentially Wetness. These indices emphasize SWIR. On the contrary, the indices in the second group, Greenness and NDMI, emphasize NIR and were positively correlated with the numbers of seedlings taller than 50 cm. Furthermore, these indices showed a higher sensitivity to type of disturbance (DD and GD) during the deforestation. This shows the possible use of different indices for specific issues.

7. Conclussion

The DI′ combining the Wetness and Brightness indices showed the highest sensitivity to identifying the forest disturbance. It is valid for our study areas to exclude the Greenness index from the original DI index, because the increase in Greenness values was due to the survival and/or regeneration of the herb layer. However, the DI seems to be generally valid for the clear cut areas, where the understory vegetation was removed or damaged.

Both compared types of disturbances (DD and GD) resulted in different dynamics, where the GD expressed slower development and lower deviations from original values than DD. These differences are clear particularly when using the samples disturbance areas (SDA), where the forest stand was uniform and well defined. The field vegetation data were used to correctly interpret the temporal dynamics of the disturbances. The RDA analysis confirmed the significant influence of natural regeneration (seedling numbers) and covers of vegetation layers on of indices values. Furthermore, according to the RDA results, the indices were divided into two groups, which correspond with enhancement of either NIR or SWIR.

The uniqueness of this study is the multitemporal comparison of the spectral response of two disturbance types, as well as using field vegetation data in this comparison. Because we assessed the temporal changes on the defined areas, it was possible to describe the disturbance dynamics in the real time and area. The resulting different spectral response of two types of disturbances can be used for disturbance type classification and/or disturbance forecast. However, it is important to consider the disturbance dynamics, because different types of forest disturbances express various spectral response during disturbance development.

Acknowledgements

We are grateful to Keith Edwards for language improvement. This project is funded by two Institutional research projects MSM 6007665806 and AV0Z60870520 and by scientific projects GA AV KJB600870701.

References:

Cohen, W. B., Spies, T. A., Alig, R. J., Oetter, D. R., Maiersperger, T. K., Fiorella, M. (2002): Characterizing 23 years (1972–1995) of stand-replacing disturbance in western Oregon forest with Landsat imagery. *Ecosystems*. 5,122-137.

Crist, E. P. Cicone, R. C. (1984): A physically-based transformation of Thematic Mapper data - the TM Tasseled Cap, *IEEE Trans. on Geosciences and Remote Sensing*. GE-22, 256-263.

Franklin, S. R. (2001): Remote sensing for sustainable forest management. CRC Press (Lewis), Boca Raton, FL, 407.

Gao, B. C. (1996): NDWI – A normalised difference water index for remote sensing of vegetation liquid water from space. *Remote Sensing of Environment*. 58: 257 – 256.

Geomatica Algorithm Reference, (2003): PCI Geomatics.50 West Wilmot Street, Richmond Hill,Ontario, Canada,L4B 1M5

Healey, S. P., Cohen, W. B., Yang, Z., Krankina, O. N. (2005): Comparison of tasseled cap-based Landsat datastructures for use in forest disturbance detection. *Remote Sensing of Environment*. 97, 301-310.

Healey, S.P., Yang, Z., Cohen, W. B., Pierce, D. J. (2006): Application of two regression-based methods to estimate the effects of partial harvest on forest structure using Landsat data. *Remote Sensing of Environment.* 101, 115-126.

Healey, S.P., Cohen, W. B., Yang, Z., Kennedy, R. E. (2007): Remotely sensed data in the mapping of forest harvest patterns. 63-84 In Wulder, M. A., S. E. Franklin, (eds.) Understanding Forest Disturbance and Spatial Pattern: Remote Sensing and GIS Approaches, CRC Press (Taylor and Francis),Boca Raton, FL.

Heurich, M., Reinelt, A., Fahse, L. (2001): Die Buchdruckermassenvermehrung im Nationalpark Bayerischer Wald. 9 – 48. In: Nationalparkverwaltung Bayerischer Wald: Waldentwicklung im Bergwald nach Windwurf und Borkenkäferbefall. Bayerische Staatsforstverwaltung.

Horler, D. N. H., & Ahern, F. J. (1986): Forestry information content of Thematic Mapper data. *International Journal of Remote Sensing.* 7, 405– 428.

Huang, C., Wylie, B., Yang, L., Homer, Zylstra, G. (2002): Derivation of a tasselled cap transformation based on Landsat 7 at-satellite reflectance. *International Journal of Remote Sensing.* 23, 1741-1748.

Iverson, L. R., Graham, R. L., Cook, E. A. (1989): Applications of satellite remote sensing to forested ecosystems. *Landscape Ecology.* 3: 131-143.

Jin, S., Sader, S. A. (2005): Comparison of time series tasseled cap wetness and the normalized difference moisture index in detecting forest disturbances. *Remote Sensing of Environment.* 94, 364-372.

Jonášová, M., Prach, K. (2004): Central-European mountain spruce (Picea abies (L.) Karst.) forests: regeneration of tree species after a bark beetle outbreak. *Ecological Engineering,* 23, 15-27.

Kauth, R. J., Thomas, G. S. (1976): Tasseled Cap – a graphic description of the spectral-temporal development of agricultural crops as seen by Landsat. Proceeding from Remotely Sensed Data Symposium, Purdue University, West Lafayette, Indiana, USA. P. 4b41-4b51.

Kent, M., Coker, P., (1992): Vegetation description and analysis. A practical approach. Belhaven Press, London etc.

Kuzera, K., Rogan, J., Eastman, J. R. (2005): Monitoring vegetation regeneration and deforestation usány change vector analysis: Mt. St. Helens studa area. ASPRS Annual Conference, Baltimore, Maryland.

Lambert, N. J., Ardö, J., Rock, B. N., Vogelmann, J. E. (1995): Spectral characterization and regression-based classification of forest damage in Norway spruce forest stands in the Czech Republic using Landsat Thematic Mapper data. *International Journal of Remote Sensing*. 16, 1261-1287.

Lillesand, T. M., Kiefer, R. W., Chipman, J. W. (2004): Remote Sensing and Image Interpretation. John Wiley and Sons. New York.

Linke, J., Betts, M. G., Lavigne, M. B., Franklin, S. E. (2007): Introduction: Structure, Function, and Change of Forest Landscapes. 1-29. In Wulder, M. A., S. E. Franklin, (eds.) Understanding Forest Disturbance and Spatial Pattern: Remote Sensing and GIS Approaches, CRC Press (Taylor and Francis),Boca Raton, FL.

Masek, G. J. (2005): LEDAPS Disturbance index: Algorithm Description v.1. Algorithm Description for LEDAPS disturbance products. *http://ledaps.nascom.nasa.gov/ledaps/docs1.html*

Muchoney, D. M., Haack, B. N. (1994): Change detection for monitoring forest defoliation. *Photogrametric Engineering and Remote Sensing*. 60, 1243-1251.

Oliver, C. D., Larson, B. C. (1996): Forest Stand Dynamics. John Wiley & Sons, New York.

Pickett, S.T.A., White, P.S., (eds.) (1985): The ecology of natural disturbance and patch dynamics. Academic Press, New York.

Richter, R., (1990): A fast atmospheric correction algorithm applied to Landsat TM images. *International Journal of Remote Sensing*. 11, 159-166.

Rykiel, E. J. Jr., Coulson, R. N., Sharpe, P. J. H., Allen, T. F. H., Flamm, R. O. (1988): Disturbance propagation by bark beetles as an episodic landscape phenomenon. *Landscape ecology*. 3, 129 – 139.

Skuhravý, V. (2002): Lýkožrout smrkový (Ips typographus L.) a jeho kalamity. Der Buchdrucker und seine Kalamitäten. Agrospoj, Praha. (in czech)

Ter Braak, C. J. F., Šmilauer, P. (1998): CANOCO Reference Manual and User's Guide to Canoco for Windows. Microcomputer Power, Ithaca, USA.

Toomey, M., Vierling, L. A. (2005): Multispectral remote sensing of landscape level foliar moisture: techniques and applications for forest ecosystem monitoring. *Canadian Journal of Forest Research*. 35, 1087-1097.

Waring, R.H., Running, S.W. (1998): Forest ecosystems: Concept and management. Academic press, San Diego, CA.

Wilson, E. H., Sader, S. A. (2002): Detection of forest harvest type using multiple dates of Landsat TM imagery. *Remote Sensing of Environment*. 80, 385-396.

Wulder, M. A., Skakun, R. S., Kurz, W. A., White, J. C. (2004): Estimating time since forest harvest using segmented Landsat ETM+ imagery. *Remote Sensing of Environment*. 93, 179–187

Wulder, M. A., White, J. C., Bentz, B., Alvarez, M. F., Coops, N. C. (2006a): Estimating the probability of mountain pine beetle red-attack damage. *Remote Sensing of Environment*. 101, 150-166.

Wulder, M. A., Dymond, C. C., White, J. C., Leckie, D. G., Carroll, A. L. (2006b): Surveying mountain pine beetle damage of forests: A review of remote sensing opportunities. *Forest Ecology and Management*. 221, 27–41.

Wulder, M. A., S. E. Franklin, (2007): Understanding Forest Disturbance and Spatial Pattern: Remote Sensing and GIS Approaches, CRC Press (Taylor and Francis),Boca Raton, FL.

SOUHRNNÁ DISKUSE

Hodnocení lesních disturbancí v optické části spektra

Hodnocení spektrálního projevu disturbancí lesa pomocí dálkového průzkumu Země je široce rozšířenou metodikou, vyvinutou a používanou zejména v zemích s rozsáhlými lesními porosty (Franklin, 2001). K takovému hodnocení jsou využívány zejména spektrální indexy, které byly v počátcích založeny zejména na blízkém IČ spektru (Leckie & Gougeon, 1981). V současné době se ukazuje jako výhodnější dávat ve výpočtech větší váhu středním IČ vlnovým délkám (Healey et al., 2006). Jedním z nejčastěji používaných indexů je třetí komponenta lineární transformace Tasseled cap (TC) označovaná jako Wetness index, neboť do značné míry koreluje s obsahem vody v listech a vlhkostí povrchů (Crist & Cicone, 1984; Kauth & Thomas, 1976). Index Wetness jsem v kapitole 1 (str. 34 - 45) použil k prvotnímu srovnání družicových dat (Landsat TM/ETM+) ze dvou termínů. První z termínů (11. 7. 1987) vyjadřoval podmínky lesních porostů centrální Šumavy ještě před akcelerací rozšíření lýkožrouta smrkového. Druhý termín družicových dat (28. 7. 2002) odráží podmínky po této hlavní fázi rozpadu lesa, která probíhala 1995 – 1998 (Heurich et al., 2001). Toto srovnání je založené na diferenční analýze hodnot Wetness převedených do relativní škály. Výsledek hodnot indexu ukázal pokles hodnot v oblasti odlesněných ploch. Rovněž Jin a Sader (2005) popisují dobrou vypovídací schopnost tohoto indexu pro detekci odlesněných ploch. Wulder et al. (2006) využili také index Wetness pro hodnocení změn lesních porostů tak, že rozdíly hodnot indexu Wetness z dvou termínů jsou vyjádřeny jako index EWDI (Enhanced wetness difference index). Index EWDI poprvé uvádějí Skakun et al. (2003). Srovnatelnost hodnot indexu v čase však autoři zajistili převedením radiometrických hodnot na reflektanci. To je přesnější způsob jak vyjádřit změny tohoto indexu v čase.

Proto byl v následující práci použit podobný způsob, který navíc rozšiřuje srovnání dvou termínů na multitemporální analýzu zahrnující 13 družicových scén (kapitola 6, str. 112 - 133). V tomto případě byly vypočítány kromě indexu Wetness i zbývající komponenty TC transformace (brightness, greenness), disturbanční index DI, který zahrnuje všechny tři komponenty (Healey et al., 2005), navržena vlastní varianta DI´a vypočítaný normalizovaný vlhkostní index NDMI (Gao, 1996; Jin & Sader 2005). Pro správnou interpretaci družicových dat byla využita pozemní data procentuálního pokryvu vegetace a počtu semenáčků smrku, které zpracovali Jonášová & Prach (2004). Výše

zmíněné spektrální indexy ukazují rozdílnou citlivost pro detekci odlesněných ploch, přičemž indexy s vyšší váhou středního IČ (DI′, Wetness a Brightness) vykazovaly citlivost vyšší než indexy zdůrazňující blízké IČ záření (NDMI, Greenness). To je v souladu s výsledky, které uvádějí Healey et al. (2006), kdy rovněž nejvyšší citlivost k odlesněným plochám vykazují indexy zvýrazňující střední IČ pásmo.

Multitemporální srovnání vývoje rozpadlých smrčin a holých sečí ukazuje, že na holinách dochází k větším spektrálním změnám oproti původnímu stavu než u rozpadlých smrčin. Výraznější spektrální projevy holých sečí jsou pravděpodobně způsobeny vlivem přechodného poškození přízemní vegetace včetně nových semenáčků a následným rozvojem travních porostů (např. *Calamagrostis sp.*). V rozpadlých smrčinách k tak výraznému rozvoji trav nedošlo kvůli částečně přetrvávajícím původním druhům bylinného patra (Jonášová & Prach, 2004); rovněž také kvůli tomu, že velký podíl ploch připadá na dřevní hmotu rozpadlých smrčin. Rozvoj travních porostů na holinách má pravděpodobně za následek i tendenci hodnot spektrálních indexů navracet se dříve do původního stavu než je tomu v rozpadlých smrčinách. To by mohlo vést k mylné interpretaci, že na těchto plochách dochází k rychlejší regeneraci smrku nebo jiných dřevin. Rozvoj travních porostů však naopak významně brání přirozené regeneraci lesa (Mansourian et al., 2005) a proto je pozemní průzkum nezbytnou pomůckou pro správnou interpretaci družicových dat.

Hodnocení lesních disturbancí pomocí termálního DPZ

Lesní porosty snižují cirkadiánní amplitudy teplot a působí proto mikroklimaticky, s rostoucí plochou i mezoklimaticky, jako stabilizační prvek v krajině. Principem je fakt, že koruny stromů podle zapojení propouští k zemi jen určité procento energie (Geiger, 1965; Petrík a kol., 1986). Povrch půdy se tak během dne přehřívá méně, přičemž je známo, že teploty kolísají nejvíce na této povrchové vrstvě (Campbell, 1977). Výsledkem jsou během dne nižší teploty vzduchové hmoty v lesním porostu, což způsobuje zpětně i ochlazování patra korun (Petrík a kol., 1986), navíc koruny tvoří větší povrch, který se také lépe ochlazuje. Dalším faktorem, který vede k vyrovnávání teplot v lesních porostech je evapotranspirace, při které se spotřebovává teplo na výpar z půdy i z rostlin. Integrální hodnotou, která může identifikovat míru těchto procesů, jsou teploty krajinného krytu (Quattrochi & Luvall, 1999). Ty mohou být také využity pro detekci změn, které se projeví

jako odchylka v čase na identických plochách nebo v daném okamžiku jako rozdíl oproti okolním porostům.

V této práci byla testována hypotéza, že se odlesnění projeví ve změně teplot krajinného krytu, které bude možné detekovat pomocí termálních družicových dat (Landsat TM/ETM+). Tato hypotéza je založena jednak na výsledcích z terénního měření (Yoshino, 1975), ale také na poznatku diferencovaného termálního projevu různých typů krajinných složek (Quattrochi & Luvall, 2004). V kapitole 1 (str. 34 – 45) jsem k ověření této hypotézy použil diferenční analýzy (Coppin & Bauer, 1996). Využití takového přístupu pro hodnocení změn teplot krajinného krytu v čase popisují Hashimoto & Suzuki (2004), přičemž tato studie má omezenou vypovídací schopnost, protože porovnávané teploty v jednotlivých termínech jsou vyjádřeny v absolutních hodnotách (°C), které jsou závislé na podmínkách počasí. Pro odstranění tohoto problému jsem převedl hodnoty teplot do relativní škály kvantilových tříd. Výsledkem byla na odlesněných plochách změna z nejnižších teplotních tříd na nejvyšší (rozpadlé smrčiny, holé seče). Zůstával zde však problém, že není možné identifikovat malé změny, protože ty byly skryty v kategoriálně se měnících teplotních třídách.

Tento problém se podařilo odstranit standardizací hodnot teplot v následném článku (kapitola 2, str. 46 – 59), což umožnilo porovnat teplotní změny v důsledku rozpadu smrčin a asanací lesa za vzniku holých sečí. Holé seče tak ukázaly významně vyšší změny směrem k nárůstu teplot oproti rozpadlým smrčinám. Důvodů pro to může být několik:

1) rozpadlé smrčiny představují velmi členitý povrch s množstvím zastíněných ploch (Zielonka & Piatek, 2004)

2) velký podíl kmenů odumřelých smrků v rozpadlých smrčinách může zvyšovat reflektanci a tím snižovat emisivitu, což se projeví nižšími teplotami,

3) na holých sečích se může projevit i vyšší vysychání půdního profilu vlivem poškození bylinného patra při asanaci dřevin.

Při použití diferenční analýzy jsou nutným předpokladem pro oba nebo více porovnávaných termínů stejné změny teploty s výškou (termální stupeň) a stejná změna teplot na plochách s různou expozicí vůči dopadajícím slunečním paprskům. Protože tyto předpoklady není možné nikdy zcela zajistit, je výsledek diferenční analýzy vždy zatížen určitou chybou.

Proto jsem se v další části práce zabýval tím, jak takové nedostatky eliminovat. Možným řešením je využití mnohorozměrné regresní analýzy (Coppin & Bauer, 1996) pro identifikaci teplotních změn vycházejících z jednoho termínu. Principem je srovnávání

teplot v rámci jediné jednotky krajinného krytu, v tomto případě lesních porostů. Výběr jediné jednotky je nutný, neboť odlišné jednotky krajinného krytu (les, louka, voda) mají zásadní vliv na distribuci teplot krajinného krytu (Quattrochi & Luvall, 2004). Využití dat z jednoho termínu eliminuje do značné míry vliv počasí (vyjma případů přechodu atmosférických front apod.), naopak proti předchozí diferenční analýze odpadá výhoda srovnání polohově identických hodnot (pixelů). Tím vyvstává problém se srovnáním teplot krajinného krytu na místech s odlišnou nadmořskou výškou, sklonem a orientací svahu.

V metodickém článku (kapitola 3, str. 60 – 80) byl hodnocen vliv parametrů reliéfu na teploty krajinného krytu vypočítaných z termálního pásma družicových dat. První výsledky těchto regresních analýz vykazují poměrně malé procento vysvětlené variability ($R^2 = 0,38$). Důležité zpřesnění výsledků přineslo vyloučení okrajových zón a menších lesních porostů. Důvodem je okrajový efekt (Saunders et al., 1999; Geiger et al., 2003; Klassen et al., 2002), který způsobuje odlišnou energetickou bilanci a následně i termální projev těchto zón. V článku byla také hodnocena šířka zóny, kde se ještě okrajový efekt významně projevuje. Na základě analýz dat s různým prostorovým rozlišením byla určena šířka 90 m. Při odstranění větších šířek se již procento vysvětlené variability ($R^2 = 0,47 – 0,57$) významně nezvyšovalo, naopak prudce klesal počet případů (hodnot teplot) vstupujících do modelu. Pomocí této a řady dalších dílčích analýz byl vytvořen regresní model vlivu parametrů reliéfu na teploty krajinného krytu.

Tento model byl následně použit pro porovnání teplot krajinného krytu rozpadlých smrčin a holých sečí (kapitola 4, str. 81 – 100). Stejně jako v případě diferenčních analýz byly zjištěny vyšší hodnoty teplot krajinného krytu na holých sečích. V tomto případě je však možné teplotní změny vyjádřit v absolutních jednotkách (°C). Je však nutné mít na paměti skutečnost, že takto vyjádřené teplotní rozdíly (mezi živým lesem a odlesněnými plochami a jejich srovnání) odrážejí stav povětrnostních podmínek před (podle extremity změn ne více než několik dní) a v době snímání družicových dat. Například po intenzívní srážkové činnosti se teploty povrchů s různými vlastnostmi (tepelná vodivost, albedo apod.) vyrovnávají (Humes et al., 2004).

Popis multispektrálního vývoje teplotních změn pak přináší kapitola 5 (str. 101-111). Z těchto výsledků je patrné zvyšování teplot krajinného krytu v souvislosti s rozpadem nebo sanací lesních porostů.

Obě metody použité k hodnocení teplotních změn (diferenční analýza, regresní modely) ukázaly, že v letním období dochází na odlesněných plochách k vyššímu nárůstu teplot oproti povrchům korun smrkového porostu. Při srovnání dvou typů disturbancí jsou

významně vyšší teploty krajinného krytu na holých sečích oproti rozpadlým smrčinám vlivem lýkožrouta. Metoda využívající regresní modely je poprvé použitým a mnohem přesnějším přístupem pro hodnocení teplotních změn krajinného krytu oproti diferenční analýze.

ZÁVĚR

Výsledky hodnocení spektrálních projevů lesních porostů centrální Šumavy ukázaly, že v důsledku odlesnění došlo k významným změnám hodnot:
1) spektrálních indexů založených na blízkém a středním IČ,
2) teplot krajinného krytu.

Při srovnání dvou typů disturbancí vykázaly holé seče větší rozdíly od původních hodnot oproti rozpadlým smrčinám. Navíc při srovnání průběhu obou typů disturbancí představují holé seče výrazně dynamickou změnu, na rozdíl od rozpadu smrčin v důsledku lýkožrouta, který má více pozvolný průběh. Podobné výsledky vyplývají i ze srovnání teplot krajinného krytu, kde holé seče nabývají významně vyšších hodnot teplot. Pro hodnocení termálního projevu byla navržena nová metodika, představující normalizaci teplot krajinného krytu v podmínkách komplexního reliéfu. Z výše uvedených výsledků vyplývá, že holé seče představují ve srovnání s rozpadlými smrčinami výraznější změnu, která může mít přímé důsledky pro regeneraci lesních porostů. Tyto důsledky se týkají teplotní extremity ale také změnami bylinného patra holých sečí, které mohou způsobit ztíženou obnovu lesa.

Literatura

Campbell, G. S. (1977): An Introduction to Environmental Biophysics. Springer-Verlag. New York.

Coppin, P. R., Bauer, M. E. (1996): Change detection in forest ecosystems with remote sensing digital imagery. *Remote Sensing Reviews*. 13, 207-234.

Crist, E. P. Cicone, R. C. (1984): A physically-based transformation of Thematic Mapper data - the TM Tasseled Cap, *IEEE Trans. on Geosciences and Remote Sensing*. GE-22, 256-263.

Franklin, S. R. (2001): Remote sensing for sustainable forest management. CRC Press (Lewis), Boca Raton, FL.

Gao, B. C. (1996): NDWI – A normalised difference water index for remote sensing of vegetation liquid water from space. *Remote Sensing of Environment*. 58, 257 – 256.

Geiger, R. (1965): The climate near the ground. Harvard Univ. Press, Harvard.

Geiger, R., Aron, R. H., Todhunter, P. (2003): The climate near the ground. Sixth edition. Rowman & Littlefield Publishers, Inc., Langham etc.

Hashimoto, S., Suzuki, M. (2004): The impact of forest clear-cutting on soil temperature: a comparison between before and after cutting, and between clear-cut and control sites. *Journal of Forest Ressearch*. 9,125–132.

Healey, S. P., Cohen, W. B., Yang, Z., Krankina, O. N. (2005): Comparison of tasseled cap-based Landsat datastructures for use in forest disturbance detection. *Remote Sensing of Environment*. 97, 301-310.

Healey, S.P., Yang, Z., Cohen, W. B., Pierce, D. J. (2006): Application of two regression-based methods to estimate the effects of partial harvest on forest structure using Landsat data. *Remote Sensing of Environment*. 101, 115-126.

Heurich, M., Reinelt, A., Fahse, L. 9 – 48. (2001): Die Buchdruckermassenvermehrung im Nationalpark Bayerischer Wald. In: Nationalparkverwaltung Bayerischer Wald: Waldentwicklung im Bergwald nach Windwurf und Borkenkäferbefall. Bayerische Staatsforstverwaltung.

Humes, K., Hardy, R., Kustas, W, P., Prueger, J., Starks, P. (2004): Estimating environmental variables using thermal remote sensing, in Thermal Remote Sensing in Land Surface Processes, J. Luvall and D. Quattrochi, (Eds) CRC Press, pp. 110 – 132.

Jin, S., Sader, S. A. (2005): Comparison of time series tasseled cap wetness and the normalized difference moisture index in detecting forest disturbances. *Remote Sensing of Environment*. 94, 364-372.

Jonášová, M., Prach, K. (2004): Central-European mountain spruce (Picea abies (L.) Karst.) forests: regeneration of tree species after a bark beetle outbreak. *Ecological Engineering*. 23, 15–27.

Kauth, R. J., Thomas, G.S. (1976): Tasseled Cap – a graphic description of the spectral-temporal development of agricultural crops as seen by Landsat. Proceeding from Remotely Sensed Data Symposium, Purdue University, West Lafayette, Indiana, USA. P. 4b41-4b51.

Klassen, W., van Breugel, P. B., Moors, E. J., Nieveen, J. P. (2002): Increased heat fluxes near a forest edge. *Theoretical and Applied Climatology*. 72, 231 – 243.

Leckie, D. G. Gougeon, F. A. (1981): Assessment of spruce budworm defoliation using digital airborne MSS data. *Proceedings of the Seventh Canadian Symposium on Remote Sensing*. Winipeg, Manitoba. 190-196.

Mansourian, , S., Vallauri, D., Dudley, N. (2005): Forest Restoration in Landscapes; Beyond Planting Trees. Springer. USA, NY.

Petrík, M., Havlíček, V., Uhrecký, I. (1986): Lesnícka bioklimatológia. Príroda. Bratislava.

Quattrochi, D. A., Luvall, J. C. (1999): Thermal infrared remote sensing for analysis of landscape ecological processes: methods and applications. *Landscape Ecology.,* 14, 577–598.

Quattrochi, D. A., Luvall, J. C. (2004): Introduction, in Thermal Remote Sensing in Land Surface Processes, J. Luvall and D. Quattrochi, (Eds) CRC Press, 1-8.

Saunders, S. C., Chen, J., Drummer, T. D. Crow, T. R. (1999): Modeling temperature across edges over time in a managed landscape. *Forest Ecology and Management*. 117, 17–31.

Skakun, R.S., Wulder, M.A., Franklin, S.E. (2003): Sensitivity of the Thematic Mapper Enhanced Wetness Difference Index (EWDI) to detect mountain pine needle red-attack damage. *Remote Sensing of Environment*. 86, 433–443.

Wulder, M. A., White, J. C., Bentz, B., Alvarez, M. F., Coops, N. C. (2006): Estimating the probability of mountain pine beetle red-attack damage. *Remote Sensing of Environment*. 101, 150-166.

Yoshino M. M. (1975): Climate in a small area. An introduction to local meteorology. Univ. Tokyo Press, Tokyo.

Zielonka, T., Piatek, G. (2004): The herb and dwarf shrubs colonization of decaying logs in subalpine forest in the Polish Tatra Mountains. *Plant Ecology*. 172 (1), 63-72.